UNIVERSITA' DEGLI STUDI DI PADOVA

ICEA Department

MSc in Environmental Engineering

Master Thesis

Massimo Trivellato

Geotechnical Slope Stability of the Este MSW Landfill

Supervisor

Prof. Marco Favaretti

Academic Year 2013-2014

Un ringraziamento sincero ai miei genitori,

Gianpietro e Loredana

INDEX

Introduction

During the recent decades a growing production of waste in the industrialized countries due to several factors occurred as the increase of population and improvements of economic conditions that have lead to an increase in goods consumption.

This situation, which in recent years has become a major problem especially for some countries, has developed in the population the concept of environmental sensibility, raising the waste problem as one of the more complex question that today's society needs to solve as an act of responsibility towards the future generations.

The reduction of the production of waste, a more moderate exploitation of the available resources and a better management and treatment of waste are three key elements to adopt to increase sustainability, but also the knowledge of the mechanical behavior of waste can be helpful to a proper landfill design, improving in this way its maintenance and duration.

Of particular interest are the problems of landfill stability located close to urban settlements and road infrastructure; in these cases it's necessary to prepare all the necessary precautions to ensure the safety of people and especially on site workers. The release of odors, dust and greenhouse gases with other problematic consequences can be generated after a situation of landfill instability. In addition, also a seismic event of particular intensity may compromise the activity of a landfill and for this reason it has to be considered as an important element in a stability analysis.

This study focuses its attention on the analysis of slope stability for the Este municipal solid waste landfill, located in the south-western part of the Province of Padua and controlled by the waste treatment company S.E.S.A. S.p.a., considering also the seismic contribution. Two different types of analysis methods are been considered, one related to the limit equilibrium (as specified by Italian legislation) and another one that utilized a finite element approach. Both methods are been implemented by the use of specific computer softwares: SLOPE/W for the limit equilibrium methods and PLAXIS for the finite element method.

1. Italian regulation about landfill slope stability

The Ministerial Decree of 14 January 2008 gives new technical legislation rules for the constructions ("Norme Tecniche per le Costruzioni – NTC08") in Italy. This act was active since July 2009 and defines the basics for project, execution and tests for all types of construction regarding terms as safety, utilization and durability of the structures.

Geotechnical aspects of the constructions are presented in Chapter six of NTC, also including slope stability analysis and seismic contribution: these studies have to be considered in the geological and geotechnical reports of the site. In the geological report all the general and specific geological aspects are examined, while in the geotechnical report the chosen criteria for the geological investigations, interpretation of the obtained results and studies related to the elaboration of the geological model, safety measures and analysis during operating period are presented.

Regarding the slope stability analysis, the study must be conducted with the Limit Equilibrium Methods considering the method of slices.

The analysis of the seismic contribution must be done with the pseudo-static method (that will be discussed later).

2. Site description

This section has been prepared in order to illustrate general and technical aspects about the interested area, located in the municipality of Este (Padua).
The landfill is a property of S.E.S.A. (Società Estense Servizi Ambientali) S.p.a. company, a limited liability company with mixed capital (public and private) that deals with waste collection and treatment.
A briefly description of the site illustrates the activities of the company, while some aspects that can be related to landfill stability as geological, seismic and hydrological properties of the area are provided basing on studies made by local authorities and professional technical reports ([4], [5], [25]).

2.1 Geographical Information

Este is located in the south-western part of the Province of Padua (Fig. 2.1), in the south part of the Euganean hills. Currently the municipality of Este has an area of 32.76 km^2 and a population of about 17,000 inhabitants.
The site of interest is located approximately 3 km west of the city center and 1.5 km east of the neighboring city of Ospedaletto Euganeo (Fig. 2.2).
The coordinates that localize the site are:

Latitude: 45° 13’ 35’’ N

Longitude: 11° 37’ 20’’ E

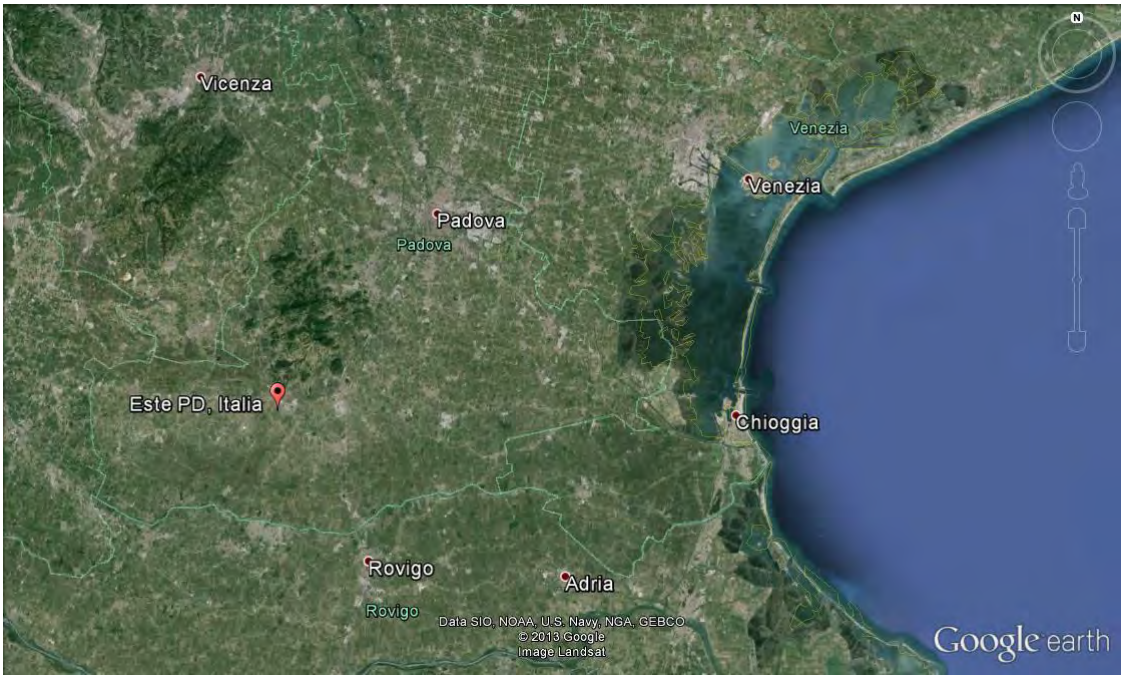

Fig. 2.1 – Este location

Fig. 2.2 – Landfill location

2.2 Stratigraphy and Structure

From the geologic and geomorphologic point of view, the area of interest is located inside the western part of the Po valley, delimitated on the north and on the east by the Pre-Alps, on the west by Lessini mountains, Berici and Euganean Hills and on the south by Adige river and Adriatic coast.

This area is mainly characterized by agricultural activities and consists of a flat morphology, crossed by a dense irrigation network interrupted by the surrounding Euganean Hills.

Po Valley is formed by thick layers of sedimentary materials due to the succession of glacial and interglacial phases; near Este the sedimentary cover goes to about 450 meters deep. These layers are characterized by loose materials of fluvial origin in the area next to the Euganean Hills, while in the medium and lower area of the plain there are fluvial and marine deposits.

The following figure shows the stratigraphy of the site: these information are obtained thanks to stratigraphic data, resulting from geological surveys carried out for the landfill extension project and from an extensive documentation of existing information.

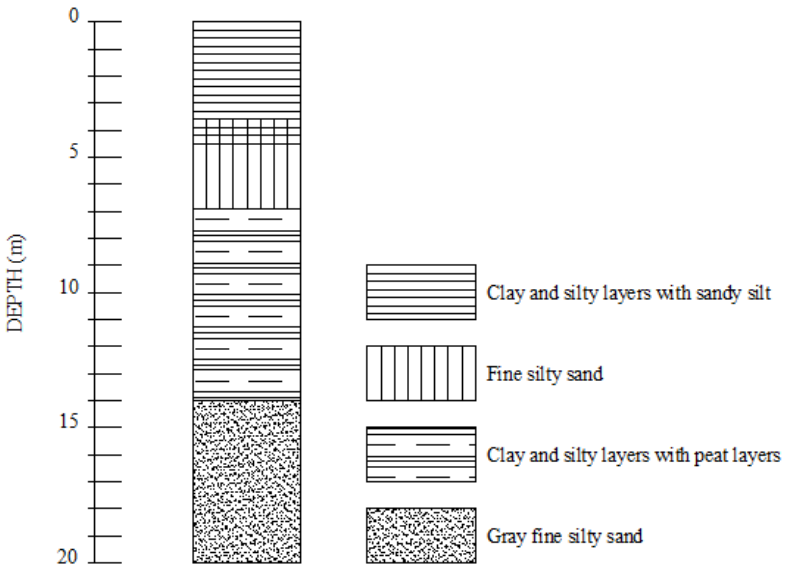

Fig. 2.3 – Stratigraphy of the landfill site

From the ground level to a variable depth between 3.60 and 4.50 m there is an alternation of clay and silty layers. Inside this level there is always a sandy silt layer that starts from 0.30 – 0.80 m from the ground level having a variable thickness between 0.60 and 1.50 m.
From about 3.60 – 4.50 m to a maximum depth of 6.90 m there is a fine silty sand layer, with a variable thickness between 0.25 and 2.40 m.
Below 6.90 m depth until about 14 m from the ground level there is a dense turnover of clay and silty layers along with some peat layers (for a maximum thickness of 20 cm) located between 5.0 and 8.50 m depth. These peat layers are not found in the northern part of the landfill.
Starting from 14 m to about 20 m depth there is a gray fine silty sand layer.
It's important to note that the average depth of the landfill is about 3-4 m depth, and the geotechnical surveys have found a mean permeability of 10^{-10} m/s for the clay and silty samples of the first layer starting from the ground surface, while previous studies have found a permeability of about 2.3×10^{-9} – 1.24×10^{-10} m/s for these materials. These values are conform to the guidelines of the Allegato 1 of the Legislative Decree 36/2003 that indicates a minimum permeability value of 1×10^{-9} m/s for natural materials utilized as substratum for non hazardous waste landfill; the prerogative of a natural barrier system having a thickness higher or equal to 1 m is also respected.

2.3 Hydrological properties

The territory surrounding the plant presents a flat morphology and is crossed by numerous canals and drains (Fig. 2.4) connected to the local irrigation network.
Brancaglia canal flows 800 m to the east of the landfill, but in the immediate proximity are present the following dykes: "Scolo delle Monache" (250 m from the south east side of the landfill), "Scolo Meggiotto" (near to the west side) and "Scolo Maceratoi" (20 m from the previous dyke), all with a thickness not superior to 4 meters and with a depth between 3 and 5 meters from the ground surface. There also small ditches (50 – 80 cm of depth) along the north and south side of the plant.

Fig. 2.4 – Irrigation network in the proximity of the plant.

Regarding the subsoil, samples made by Geodelta company have localized two distinct groundwater aquifers:

- the first is located inside a discontinuous sandy layer that starts from 3.6 – 4.5 m depth until 7 m depth;
- the second is located inside a deeper sandy layer located over 14 m depth.

In order to avoid possible contamination problems, the entire plant is delimited by a bentonite barrier system.

2.4 Climate of the site

The climate of the site belongs to the Mediterranean category with continental characteristics, alternating cold winters to hot humid summers.

The rainfall is not too much elevate and is between 600-800 mm/year. The rainfall distribution is a bimodal type, with an absolute maximum during spring season (May) and a relative maximum during autumn season (October); the absolute minimum is in general in January and the relative minimum in August.

Fig. 2.5 shows the average monthly rainfall for Este during the last 30 years.

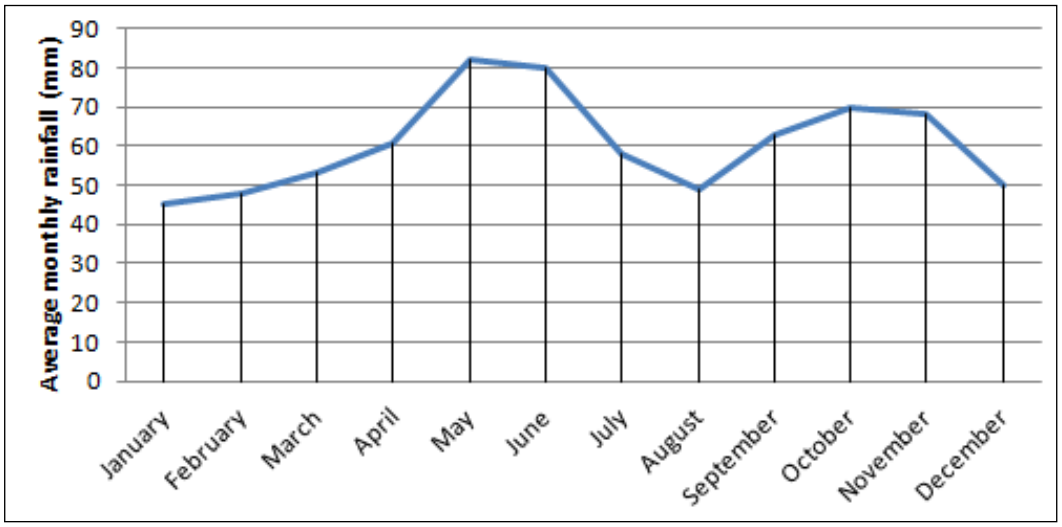

Fig. 2.5 – Este's average monthly rainfall (mm) for the last 30 years (Source: P.A.T.I.)

The trend of the average temperatures presents a peak in July and minimum in January (Fig. 2.6). The maximum temperatures exceed the 29 °C, a situation typical for a continental climate with weak circulation, while the minimum temperatures are around the - 2 °C.

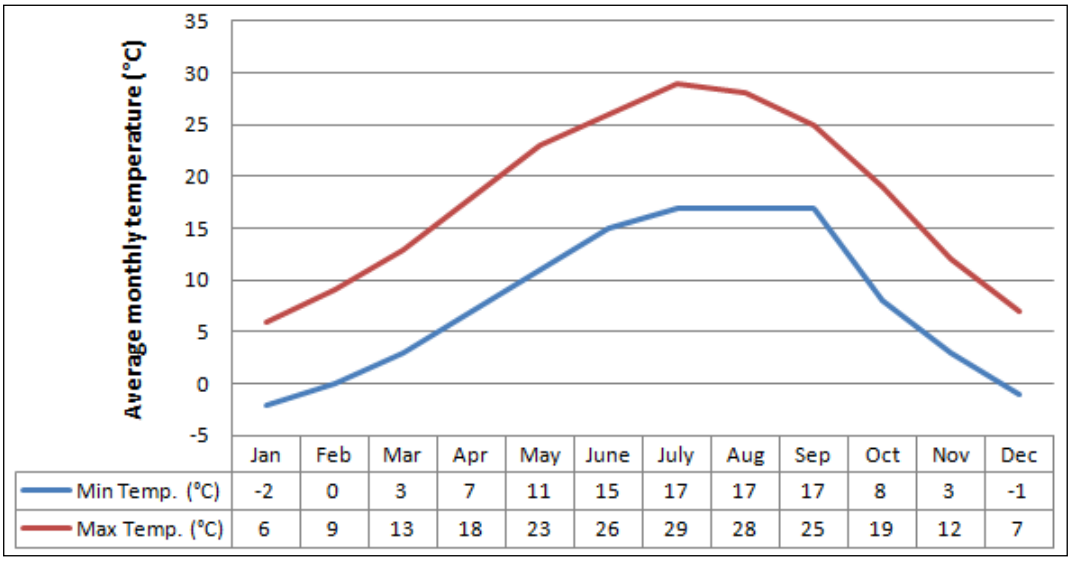

	Jan	Feb	Mar	Apr	May	June	July	Aug	Sep	Oct	Nov	Dec
Min Temp. (°C)	-2	0	3	7	11	15	17	17	17	8	3	-1
Max Temp. (°C)	6	9	13	18	23	26	29	28	25	19	12	7

Fig. 2.6 – Este's average monthly temperature for the last 30 years (Source: Vicenza weather station)

2.5 Seismology

Earthquake hazard can lead to a lot of problematic consequences for the landfill management systems (like damages to barrier and cover systems and to leachate and biogas extraction pipes) but also the stability can results very modified after a seismic event, as happens to Chiquita Canyon landfill in California, where the Northridge earthquake of 17 January 1994 with a magnitude of 6.7 caused a progressive landslide of the lateral sides (Matasovic et al., 1998).

With reference to the P.A.T.I. (Piano di Assetto del Territorio Intercomunale), which is a municipal plan for the disposition of the neighboring municipalities, Este is considered as a part of Veneto region with low seismic risk (class 4). Regarding the Ordinance of the President of the Council of Ministers (O.P.C.M.) 3519/96 and 3519/06, twelve new areas of seismic hazard are been classified (Fig. 2.7): Este is classified with a peak ground acceleration between 0.050 and 0.075 g, a very low range if compared with others belonging to the Veneto region.

In Italy there is a specific legislation relative to the landfill construction criteria and in this study the seismic hazard as be considered as a key factor for the slope stability study of the landfill.

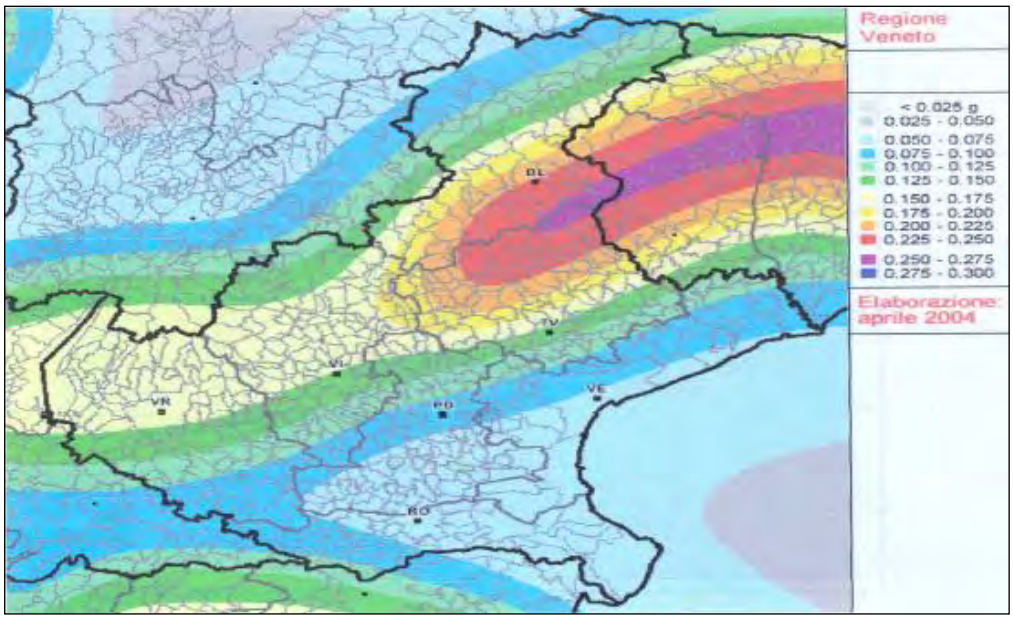

Fig. 2.7 – Veneto seismic risk map (map taken from the P.A.T.I. of Este municipality dated May 2012. The seismic risk is based on the maximum ground acceleration with a probability of exceedance of 10% in 50 years).

2.6 S.E.S.A. waste treatment activities

S.E.S.A. company plays an important role in the waste management and treatment for the province of Padua. The principal activities of the society are:

- collection and transport of urban waste and assimilated;
- collection and transport of hazardous and not hazardous waste;
- landfill management for urban, assimilated and not hazardous waste;
- anaerobic digestion plant and composting plant management;
- management of a power station plant for the production of electrical and thermal energy (for a nominal power respectively of 1,416 MWe and 1,345 MWt) powered by landfill biogas;
- management of four digestors for the residual organic fraction of municipal solid waste that supply six engines for electric and thermal energy production (for a nominal power respectively of 1,416 MWe and 1,345 MWt);
- management of a methane co-generation plant (3,048 MWe and 3,077 MWt) that supports the district heating system;
- management of a mechanical treatment plant for sorted and unsorted residual waste;
- receiving and storage of urban waste and dry goods;

- receiving and storage of hazardous waste;
- remediation of contaminate sites;
- design, construction, installation and maintenance of the plants.

Fig. 2.8 shows an aerial view of the Este S.E.S.A. plant.

Fig. 2.8 – Este S.E.S.A. waste treatment plant

2.7 S.E.S.A. landfill description

2.7.1 General information

The plant is a controlled landfill and was classify as a landfill of first category after provincial legislation of 1984, where it was firstly disposed municipal solid waste (MSW) and waste similar to municipal (RSA); then it was classified as non hazardous waste landfill considering the Legislative Decree n. 36/2003.

The waste come from the municipalities belonging to "Bacino Padova 3", a group of 37 neighboring municipalities of the south-east region of the province of Padua (for a total surface of 704.3 km^2 and almost 142,000 inhabitants) that is responsible for management of separate collection system.

The entire landfill occupies a total area of 130,000 m^2 for a total volume of about 1,520,000 m^3; recently, it was authorized by the Province a new landfilling area ("Lotto Ovest" and "Lotto Nord") of 44,500 m^2 that will occupy a total volume (considering also provisional and final top cover) of about 566,000 m^3.

The total quantity of waste disposed into landfill presents an almost completely decreasing trend during the last years, as shown in Fig. 2.9; the reason for this is due to the improvements made in the separate collection systems of "Bacino Padova 3" in order to recover as much material as possible.

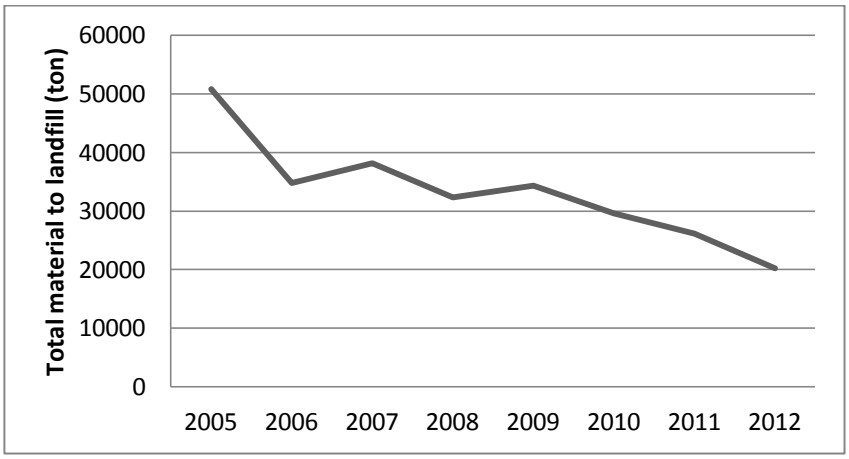

Fig. 2.9 – Material sent to landfill per year since 2005

2.7.2 Principal administrative deeds

This landfill was designed in the 60s and over the years changes to the initial plan have been made in order to increase the available volume for waste disposal maintaining also an adequate level of safety; in this paragraph the principal authorizations and approvals obtained over the years are presented.

The first dumping area was active since the 60s, before that S.E.S.A. company obtained the management of the area in 1995.

Veneto Region with the Decree n.117/AMB dated 16/07/1986 and the Decree n.508 dated 22/02/1991 approved the adjustment and completion of the first dumping area named "Lotto 1". The second dumping area named "Lotto 2" was approved by the municipality of Este with deliberation by the council n. 56 dated 03/06/1991 and authorized by the Regional Committee Resolution n.701 on 12 February 1992. The union of the two landfill bodies was approved on 20 May 1997 according to the Regional Committee Resolution n.1813.

A third dumping area named "Lotto 3" (named also "Ecosistema project") was approved by the Veneto Committee Resolution on 17/03/1998 with deliberation n.791; an update of this project considering also particular safety measures was approved on 16 June 2000 with deliberation n.1696.

The management of a power plant for production of electrical and thermal energy powered by the landfill biogas and the authorization for the installation and exercise of another power plant for production of electrical and thermal energy powered by the biogas produced by the anaerobic digestion plant of the organic fraction of the MSW was authorized by the Regional Committee Resolution n.3032 dated 10/10/2003.

The plan for another enlargement of the dumping area (95,000 m^3) named "Ampliamento Lotto 3" was approved by the Province of Padua with the Measure n.4941/EC/2004 dated 30 December 2004 according to the Legislative Decree n.36/2003; S.E.S.A. company obtained the authorization for the disposal of MSW, waste similar to municipal and non hazardous semi-solid sludge on 8 August 2005 with the Measure of the Padua Province n.4999/EC/2005 according to Leg. Decrees n.36/2003 and n.22/97 Art.28 and to Regional Law n.3/2000 Art.26. Recently some new dumping areas ("Lotto Ovest" and "Lotto Nord") were authorized for the exercise but nowadays have not yet been realized.

S.E.S.A. landfill obtained also the Italian reference for the Integrated Pollution Prevention and Control named "Autorizzazione Integrata Ambientale" (A.I.A.) with the Measure of the Padua Province n.60/IPPC/2008 that was subsequently updated until 2018.
The entire plant received also specific environmental quality certifications like the UNI EN ISO 14001 in the 2004 and the UNI EN ISO 9001 in the 2008.

2.7.3 Sectors and subsectors

The entire existing landfill site occupies a total surface of 130,000 m^2 for a total volume of 1,520,300 m^3. A new dumping area of 44,500 m^2 located in the western and northern part of the landfill has been projected and authorized but not yet realized: Fig. 2.10 shows an aerial view of the landfill site (black line delimits the existing landfill site while red line delimits the designed dumping area).

Fig. 2.10 – Aerial view of the existing (black line) and designed (red line) landfill site

The evolution of the landfill site started from the 60s with the first dumping area now named as "Lotto 1". In the 90s has been authorized and realized the second large landfill zone

named “Lotto 2” and then during the 2000s also “Lotto 3” has been realized. “Lotto Ovest” and “Lotto Nord” are the last two main sites authorized for the landfilling (Fig. 2.11).

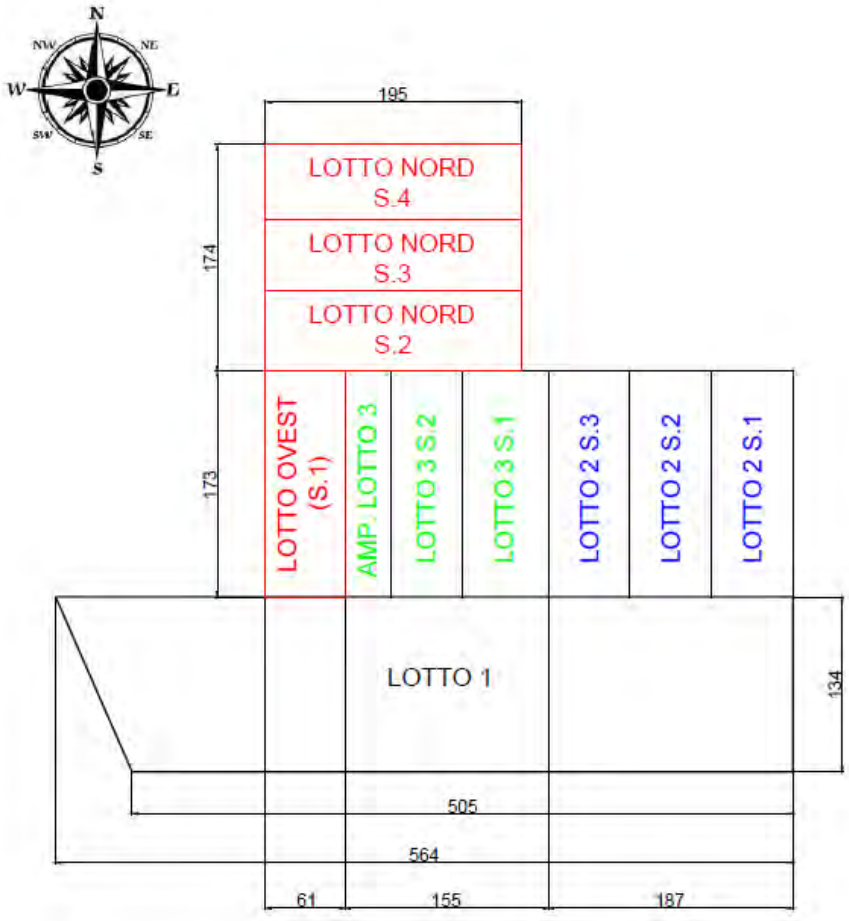

Fig. 2.11 – Scheme of the landfill dumping areas

In this paragraph the principal data of sectors and relative subsectors are described. Table 2.1 reassumes the main data (surfaces and volumes).

LOTTO 1: the first dumping site was active from the ’60 until the 1995, when S.E.S.A. company obtained the control of the zone. This area has a trapezoidal shape for a total surface of 72,000 m^2 for a volume of about 750,000 m^3.

LOTTO 2: the project for the extension of the landfill site was prepared by Este municipality in January 1991 basing on geological and hydro- geological surveys. This site has a rectangular shape for a total surface of about 32,000 m^2 and 251,000 m^3 of volume and is located in the northeastern part of “Lotto 1”; it’s subdivided

in 3 subsectors (S.1, S.2 and S.3), each of them subdivided in 4 basins ("Vasca A, B, C, D") as shown in Fig. 2.12.

The works for the realization of the sectors started in August 1995 and finished in October 1998. The unification of "Lotto 1" with "Lotto 2" was authorized by the Regional Committee Resolution in 1997 with an increase of volume equal to 69,300 m^3.

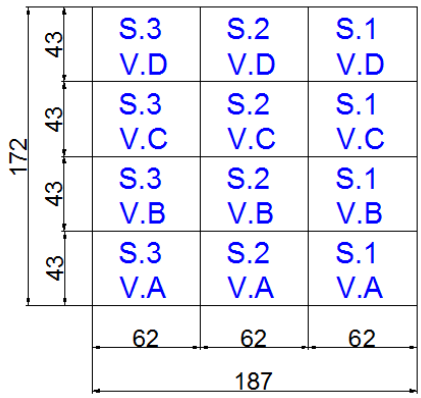

Fig. 2.12 – Scheme of sectors and subsectors of "Lotto 2"

LOTTO 3: the project of this rectangular area placed at the left part of "Lotto 2" was also named "Progetto Ecosistema" and considered a new dumping site of about 20,000 m^3, for a volume of 355,000 m^3 taking into account also the later union of this site with "Lotto 1". In 2004 was design an extension of rectangular shape named "Ampliamento Lotto 3" of about 6,000 m^2 and 95,000 m^3 as volume, considering the waste settlement and the lost of mass due to the biogas production.

"Lotto 3" is subdivided into two main sectors (S.1 and S.2) composed by other two basins ("Vasca A,B"); also "Ampliamento Lotto 3" is formed by two distinct basins named "Vasca A" and "Vasca B" (Fig. 2.13).

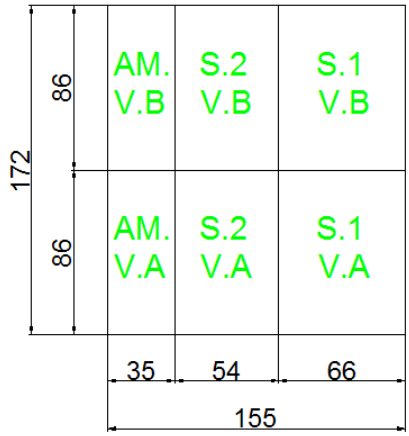

Fig. 2.13 – Scheme of sectors and subsectors of "Lotto 3" and "Ampliamento Lotto 3"

LOTTO OVEST: this rectangular shape site (named also "Settore 1" of the new dumping site) has been projected but not yet realized, it will occupy an area of about 10,500 m^2 located in the north-western part of the landfill (at the left side of "Ampliamento Lotto 3").

LOTTO NORD: this new configuration will include a new rectangular shape area of about 34,000 m^2 as surface, subdivided into three sectors ("Settore 2,3,4") located in the northern part of the existing landfill. The total volume of "Lotto Ovest" and "Lotto Nord" will be equal to about 566,000 m^3, considering also the daily and final top cover materials.

Table 2.1. Principal data of the S.E.S.A. landfill sites (* = authorized but not yet realized).

	SURFACE (m^2)	VOLUME (m^3)
LOTTO 1	72,000	750,000
LOTTO 2	32,000	251,000
Unif. L1 - L2		69,300
LOTTO 3	20,000	355,000
Unif. L1 - L3		
AMPL. L3	6,000	95,000
LOTTO* OVEST	10,500	566,000
LOTTO* NORD	34,000	

2.7.4 Bottom liner systems

S.E.S.A. landfill presents different bottom liner systems because of the development over the years of the legislation regarding this particular aspect. For example "Lotto 1", the part of landfill that was active since the 60s (i.e. when a specific legislation that regulates the entire landfill management was completely absent) doesn't present any type of artificial impermeabilization layer; nonetheless, as specified by the study of the stratigraphy of the site, the natural clay layer at the bottom of the landfill could guarantee a minimum control of leachate.

"Lotto 2", "Lotto 3" were completed under the S.E.S.A. management and present the same type of bottom liner system (Fig. 2.14). "Lotto Ovest" and "Lotto Nord" will have a similar barrier system.

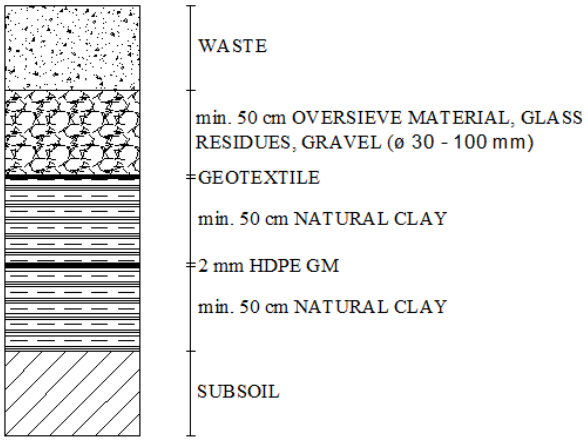

Fig. 2.14 – Scheme of "Lotto 2","Lotto 3" barrier system

2.7.5 Top cover systems

Similar to the various bottom liner systems, also the final top cover systems present some differences relatively to the dumping sites of the landfill due to the different legislation constraints that had to be respected over the years. The following figures show these differences among the distinct landfill zones.

Leveling layer (in Italian "Strato di regolarizzazione") is a particular stratus that permits the correct installation of the overlying strata and can be composed by excavation soil, compost or remediation soil but it has to respect particular concentrations according to CER 170504.

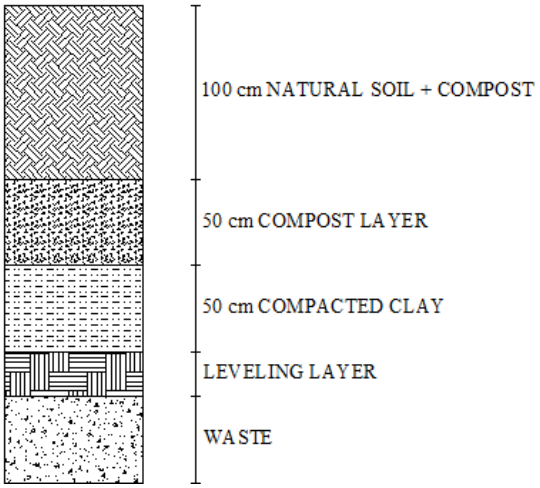

Fig. 2.15 – Scheme of the final top cover of "Lotto 1"

The top cover of "Lotto 2" and "Lotto 3" (also including "Ampliamento Lotto 3") is updated to the regulations of Legislative Decree n.36/2003 that involves more protection layers (Fig. 2.16). As specified by the Veneto Committee Resolution n.1696/2000 that approved this type of final cover, the final configuration of these layers has to respond to the criteria of:

- isolation of waste from the external environment;
- minimization of water infiltration;
- reduction as much as possible of the necessity of maintenance;
- minimization of erosion phenomena;
- resistance to settlement phenomena.

The various compost layers have the function of anti – clogging protection.

The final top cover of "Lotto Ovest" and "Lotto Nord" will be installed in order to respect the guidelines of Legislative Decree n.36/2006, and it will have the same features of the top covers of "Lotto 2" and "Lotto 3".

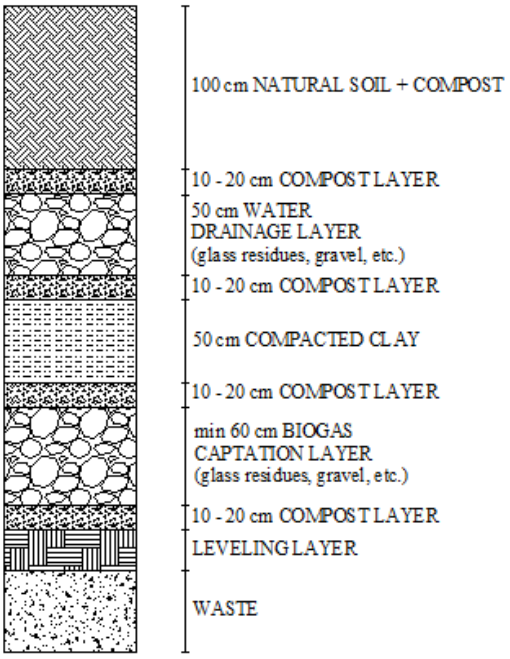

Fig. 2.16 – Final top cover of "Lotto 2" ,"Lotto 3", "Lotto Ovest" and "Lotto Nord"

2.7.6 Biogas management

Starting from the 1997 drilling operations and wells installation were realized in order to extract the biogas from the landfill along with the realization of a co-generation plant for the energy recovery. The gas is constantly sucked by an aspirator and then conveyed to the co-generator. A part of the produced energy is used for the maintenance of the plant while the other remaining quantity is sell to the ENEL company.

The extraction and collection biogas system is a kind of the so-called vertical-horizontal, where the wells are the vertical elements made in HDPE and the HDPE pipes that connect each well to the control station are the horizontal transport elements. The control station monitors all the pipes belonging to a certain landfill area managing the depression with specific control valves.

From the different control stations the main pipe is connected to the co-generation plant (Fig. 2.17) that is formed by an engine that produces electrical and thermal energy with a nominal power of 1.41 kWh.

Fig. 2.17 – Co-generation plant GE Jenbacher supplied by landfill biogas

The thermal energy produced, along with the energy derived from the anaerobic digestion systems, is sent to a district heating network that is able to supply particular public services like the primary and secondary schools, the library and the municipal building of Ospedaletto Euganeo and two schools and the civil hospital of Este.
The quantities of biogas extracted over the last seven years are listed in Table 2.2.

Table 2.2. Quantities of biogas extracted from the landfill per year since 2006.

Year	Extracted biogas (Nm^3)
2006	1,784,501.44
2007	6,573,811.39
2008	4,821,830
2009	4,601,020.5
2010	4,303,262.2
2011	3,172,361.4
2012	1,747,621.1

The constant decreasing quantity of the extracted biogas can be explained as a consequence of the lower discharge of waste into the landfill during time, considering also that the biodegradable quantities are less than in the past due to the improved separate collection system and technologies that utilized this waste fraction (for example the anaerobic digestion for the putrescible organic fraction).

2.7.7 Leachate management

The leachate management system is formed by 35 extraction wells, HDPE pipes that constitute the conveying network, two inox steel storage tanks for a total capacity of 50 m^3 and a control station for the monitoring. Over the years there have been upgrading and adjustment operations were made in order to improve the catchment network.

The blowdown of the wells occurs with submergible pumps connected to the external storage tanks, maintaining always a low hydraulic head inside the wells; leachate is then taken with tankers by the S.E.S.A. operators and sent to the Este's wastewater treatment plant or to the internal physical-chemical plant reducing transportation costs and also environmental impact.

The leachate analysis is made every three months with the samples taken from the adduction pipes of the different landfill sectors connected to the storage tanks; another analysis on the leachate sampled directly from the storage tanks is made once a year.

The drainage network (that will be the same also for the new projected sectors) is formed by HDPE corrugated pipes with saw teeth profile with an external diameter of 200 mm and an internal diameter of 171 mm. The network is placed inside a wasp nest gravel that has a thickness in the higher point equal to 60 cm.

The landfill bottom presents a double inclination of one degree and each sector is divided by anchor trenches of trapezoidal section in order to favor the leachate drainage. The drainage pipes of each sector are connected to two external concrete wells where electrical submergible pumps are installed. The pumps are linked to the storage tanks with HDPE DN 75 pipes.

The quantity of the extracted leachate over the last seven years is shown in Table 2.3.

Table 2.3. Leachate extracted since 2006.

Year	Extracted leachate (ton)
2006	10,779.94
2007	12,549.3
2008	11,294.71
2009	9,990.74
2010	11,076.65
2011	7,095.04
2012	12,968.97

The variation of the quantities of the extracted leachate over the years is partially explained by the yearly rainfall quantity: for example, as shown in Table 2.4 for the year 2012, the trends of the rainfall and leachate quantities are similar.

Table 2.4. Correlation between extracted leachate and rainfall in 2012.

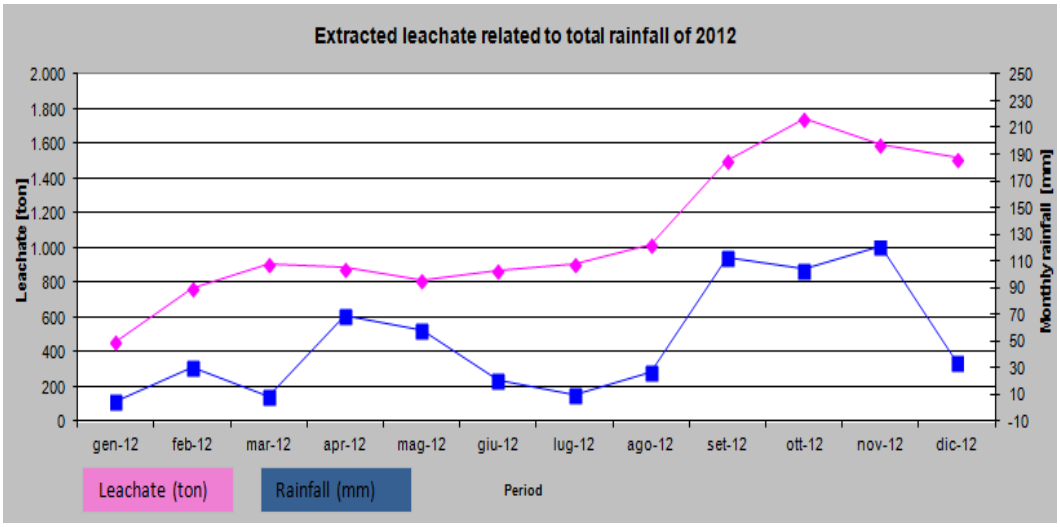

2.7.8 Monitoring and control plan

The entire S.E.S.A. site is monitored by a Plan for Supervision and Control (PSC), an official document that regards different phases of the landfill like construction, management and post-closure. This document was approved by the Province of Padua and indicates rules for the control and monitoring of all activities in the landfill that could have potential impacts on the environment and public health.

In addition it comprehends also the timely measures that have to be taken in case of incidents, the guarantee of a constant training of the management staff and the guarantee to the access to all the principal functioning data and results of the monitoring campaign.

The types of control carried out for the landfill are:

- controls for the input waste and sludge;
- controls during management phase;
- environmental controls.

The environmental controls regards:

- leachate: registration of the quantity of leachate monthly extracted and chemical analyzes performed every three months on particular parameters (pH, temperature, conductibility,

ammonia nitrogen, nitrates, nitrites, chlorides, sulfate, metals, iron and manganese. Every year the analyzes regards also other parameter such as COD and hydrocarbons;

- biogas: monthly evaluation of the parameters of methane, oxygen and carbon dioxide;
- surface water: annual analysis on particular parameters in the surrounding draws. The monitoring regards: temperature, pH, conductivity, COD, BOD_5, ammonia nitrogen, nitrates, nitrites, chlorides, sulfate, metals, organohalogen compounds, pesticides, solvents, hydrocarbons;
- groundwater: ten control wells are installed for the monthly measurement of the levels of the shallow and deep aquifers. Every three months controls are performed to evaluate temperature, pH, conductibility, permanganate oxidability, ammonia nitrogen, nitrates, nitrites, chlorides, sulfate, metals, iron and manganese. Every year the analyzes is extended to other parameters like BOD_5 and PAH;
- air quality: two points for semiannual examination of hydrogen sulfide and ammonia and for annual examination of dusts;
- weather-climate parameters: daily measurements of precipitations, temperature, wind direction and intensity and atmospheric humidity;
- landfill morphology: semiannual examination of volume occupied by waste and available volume for the disposal;
- external noise: annual phonometric investigation on the perimeter of the site.

3. General slope stability concepts

3.1 Introduction

One of the most critical aspects that an engineer must take into account during the design and the management of a landfill is the space saving: this is not only a question of sustainability with ecological footprint consideration, but it's also a delicate issue due to the numerous administrative permits to obtain in order to respect different constraints like the proximity to residential areas or sensitive natural sites.

This aspect can be solved with a reduction of the dimension of the incoming waste to the landfill, for example through compaction of compressible waste, but also diminishing the ratio between horizontal and vertical dimension of the landfill with the result of a higher and inclined structure along the slopes.

To implement this second procedure the elaboration of a stability analysis is fundamental, not only during the project phase, but also during the operational and post operational period because some particular waste can change their properties during time (because of degradation processes and changes of unit weight) leading for example to different shear strength parameters and pore water pressure, i.e. two of the most critical characteristics for the stability.

Moreover, the issue of slope stability is crucial for other reasons: the safety of on-site workers, the protection of investments made in improving the level of engineering of the landfill (like the biogas collection system) and the prevention of large remediation costs (Gharabaghi et al., 2007). Also the introduction of geosynthetic materials through the liner systems has increase the attention to this study due to the carefulness that has to be paid to the integrity of the liners during time.

The study of this problem is very complex due to the heterogeneity of waste and to the ability to obtain geotechnical parameters such as density, moisture content, friction angle and cohesion; laboratory measures present limitations not only for the heterogeneous nature of MSW, but also for the erratically changing of properties within the landfill during time (Vajirkal, 2000).

Usually, literature data indicate the cone penetrometer test as the most accurate procedure to obtain these particular waste parameters, thanks to the high accuracy and minimal efforts and costs of this device that it's able to characterize a large area in a short time period (Vajirkar, 2000).
There are two different types of calculation to study the slope stability analysis: the Limit Equilibrium Methods (LEM) and the Finite Element Methods (FEM); the main difference is that the LEM are based on the static of equilibrium while the FEM are related to the stress – strain relationship.
Both methods will be discussed on this thesis and the Este's S.E.S.A. landfill slope stability will be evaluated using two different calculation softwares that represent these analyses approaches: SLOPE/W for the LEM and PLAXIS for the FEM.

3.2 Factors of influence

Instability of landfills results in most cases as a combination of gravitational forces and water pressures; when gravitational forces are out of balance the failure occurs. Water plays the role of lubricant diminishing the resisting forces causing gradually an increasing of sliding mass velocity that finally leading to the failure. Gravitational forces and water are two of the main causes of the instability. This paragraph presents a briefly description for the factors of influence of the stability ([27],[38],[39],[40]) excluding the seismic contribution that will be discussed further in more detail.

Landfill geometry

The main factors that influence the stability are those which characterize the geometry such as height and angles of side slopes of the landfill. In order to maintain stability is important that bottom, top cover and side slope liners are designed as flat as possible, because instability might occur if the projected slopes were steeper than the friction angle between the materials; the erosion can be limited with a soil vegetation layer in the top cover.

Shear strength

This factor is crucial for the stability because characterizes the interaction between different materials such as geosynthetic liners and soil; moreover, also the strength characteristics of waste are important because moisture content and organic waste (for co-disposal landfill cases) can determine a reduction in the stability.

Unit weight of waste

This parameter is essential because gives an idea of the compressibility of the waste mass; unfortunately, there are significant uncertainties regarding its value. It's very difficult to obtain a certain value, because unit weight values vary significantly not only among different sites but also within the same site.
Compaction effort, layer thickness, overburden stress, moisture content, variations in waste constituents (like size and density), state of decomposition and degree of control during placement (like thickness of daily cover) are the factors that influence unit weight of waste.
A study conducted by Zekkos et al. (2006) proposed an hyperbolic function to describe the relationship between MSW unit weight and depth.

Water content and pore water pressure

Water content of landfill can change due to several factors like waste composition, time of year, rising groundwater accumulation and meteorological conditions. Seepage forces may reduce the resisting forces along the failure surface increasing the driving forces.
Pore pressure can be influenced also by leachate and co-disposal of biosolids. This can lead to an increase of MSW unit weight decreasing the effective stress which eventually lead to shear strength reduction affecting the landfill stability. For the opposite reason a diminishing of the pore water pressure lead to an increase of effective vertical stress making the landfill more stable.

Settlement

Shafer (2000) proposed two different types of settlement that affect landfill stability. One is related to the uniform settlement that, thanks to densification, increase the unit weight of waste favoring the stability; the other one is the localized differential settlement that

promotes surface water to infiltrate within the mass, potentially increasing pore water pressure and piezometric head in the waste mass. This second type of settlement can be related to the presence of biosolids which have high compressibility creating local settlement zones which have a negative consequence for the stability.

External loadings

External loads such as daily top cover, final cover, the movement of vehicles, traffic and stockpiles of materials can affect the landfill stability.

Landfill management

Some particular operations can be done in order to improve landfill stability, such as the mix of biosolids with MSW before landfilling. Also other landfill management systems like biogas and leachate extraction wells should be monitored regularly in order to prevent any damage to the barrier layers.

Vegetation

Vegetation is important not only for aesthetic reasons but also for its property against erosion processes; moreover, vegetation on landfill slopes improves the slope stability because the vegetation roots add cohesion to the top soil acting as a reinforcement.

3.3 Types of landfill's failure

Landfill slope failures are usually due to the loss of shear strength by the multilayer composites, to a change in geometrical properties such as the steepening of an existing slope or to an excessive settlement of waste. The typical geotechnical failure types are also possible depending on site-specific conditions (like the type of cover used) and the placement and geometry of the MSW mass.
In this paragraph potential failure modes are briefly described. Figures are taken from "Geotechnical aspects of landfill design and construction" by X. Quian, R.M. Koerner, D.H. Gray.

Failure of the final cover system

The protection soil that acts as final top cover can slide on the below liner system if the slope is too steep or too long (Fig. 3.1); this can occurs especially during periods of heavy rainfalls.
The solution can be the replace of soil unless the failure surface is placed within the liner system; in this case, the question of long term stability remains and the implications are more complicated.

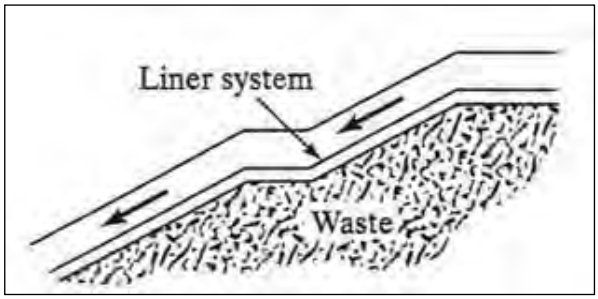

Fig. 3.1 – Failure of the final cover system

Failure of liner system components from anchor trenches

Geomembranes, geotextiles and geonets are components of the geosynthetic liner systems that are fixed into anchor trenches at the slope in order to avoid the tearing and the sliding down of component; the pull out of the liners from the anchor trenches that cause the failure can occur if these components are not properly installed (Fig. 3.2).

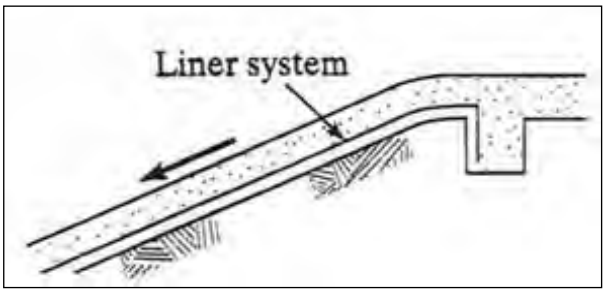

Fig. 3.2 – Failure of liner system components from anchor trenches

Rotational failure within the waste mass

This type of failure is completely independent of the liner system (Fig. 3.3): it involves a movement of a large amount of material from the circular failure surface located within the waste body to the toe of the slope. The reasons of this instability are a too steep waste slope, high liquid content or lack of waste placement control.

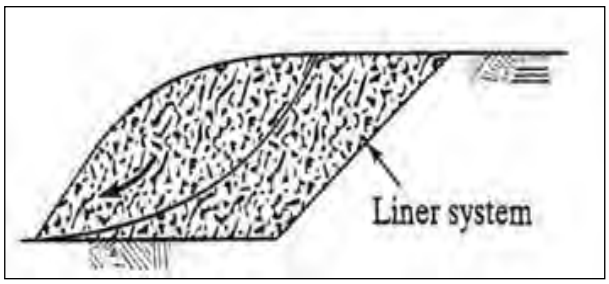

Fig. 3.3 – Rotational failure within the waste mass

Rotational failure through waste mass, liner and foundation soil

Failure can starts from the bottom soft soil propagating until the waste mass; the failure plane may be at or within the liner system, or in the soft subsoil (Fig. 3.4). One reason can be the excessive waste weight. These types of instability have occurred in both unlined and lined sites involving up to 500,000 m^3 of waste.

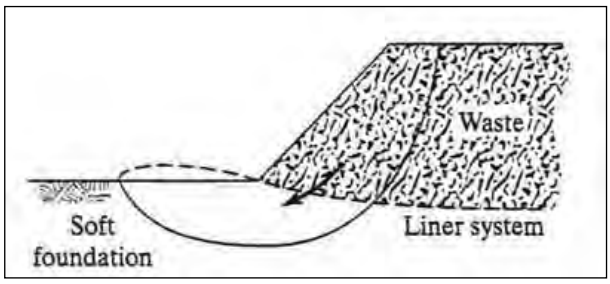

Fig. 3.4 – Rotational failure through waste mass, liner and foundation soil

Rotational failure of soil slope, toe or base

The soil mass behind the waste body or beneath the site could presents instability and then failing. The failure occurs along the slope, at the toe or within the foundation soil (Fig. 3.5).

The reasons can be a too steep slope or the soft foundation soil properties, not involving liner system or waste properties like shear strength or unit weight.

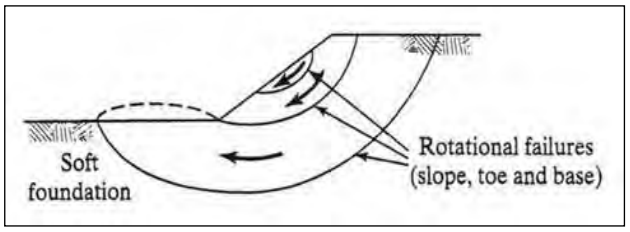

Fig. 3.5 - Rotational failure of soil slope, toe or base

Translational failure by movement along the bottom liner system

This type of instability can occur with the waste mass sliding above, within or beneath the liner system at the base of the waste body (Fig. 3.6). The failure plane is almost linear and can propagate from the toe up through the waste or continue in the liner system along the back slope (Quian et al., 2002). These failures have occurred at both clay-lined sites and geo-synthetically-lined sites. The largest observed volume involved was up to 1,000,000 m^3 of waste.

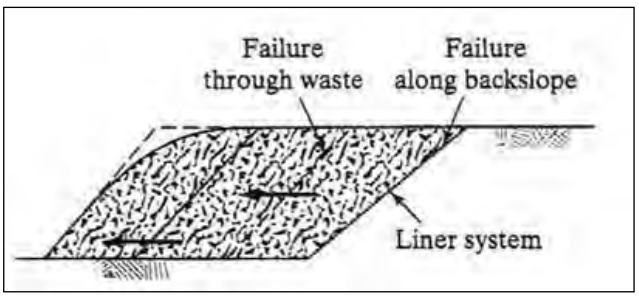

Fig. 3.6 - Translational failure by movement along the bottom liner system

3.4 Seismic contribution

The seismic or dynamic forces are usually oscillatory, multi-directional and act only for moments in time; in order to represent the dynamic loading the static forces are usually involved in this type of study. After the shaking the slope may not completely collapse, but there may be some unacceptable permanent deformations.

As required also by Italian Legislation, a pseudostatic analysis can be performed to consider the dynamic effects, describing the effects of earthquake shaking by accelerations that create inertial forces which act in the horizontal and vertical directions at the centroid of each slice. This type of analysis is a sort of extension of the limit equilibrium method with the addiction of the component of inertia that represents the action of the seismic effect. Seismic contribution is considered introducing static forces applied to the center of gravity of the mass potentially sliding and proportional to the weight W of the interested mass (Fig. 3.7).

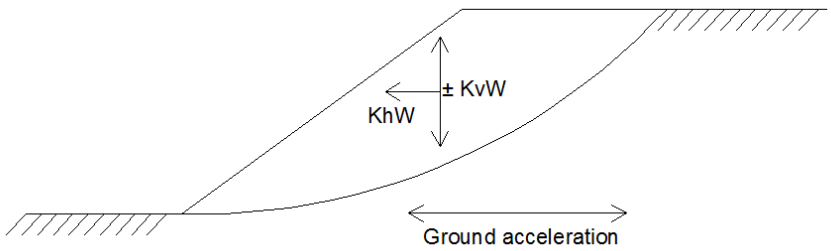

Fig. 3.7 – Inertial forces of the seismic contribution

These forces are defined as:

$$F_H = \frac{\beta_s \cdot a_{max}}{g} \cdot W = K_H \cdot W$$

$$F_V = \pm 0.5 K_H \cdot W = K_V \cdot W$$

where:

- W = slice weight;
- β_s = coefficient of the maximum acceleration reduction;

- a_{max} = maximum seismic acceleration estimated for the site of interest;
- g = gravity acceleration (9.81 m/s^2);

The value of a_{max} is defined basing on the stratigraphic (stratigraphic coefficient S_s) and topographic (topographic coefficient S_T) situation:

$$a_{max} = S \cdot a_g = S_S \cdot S_T \cdot a_g$$

The coefficient a_g represents the maximum horizontal acceleration for the site of interest considering hard ground soil ("A" type for subsoil categories).
Referring to the NTC08 for the Italian legislation, all these coefficients can be found in order to set the values of K_H and K_V to the computer programs.
The value of β_S can be found in the NTC08 (Tabella 7.11.I) as shown in Tab. 3.1.

Table 3.1. Coefficient of maximum acceleration reduction (Tabella 7.11.I, NTC08).

	Categoria di sottosuolo	
	A	**B, C, D, E**
	β_s	β_s
$0.2 < a_g(g) \leq 0.4$	0.30	0.28
$0.1 < a_g(g) \leq 0.2$	0.27	0.24
$a_g(g) \leq 0.1$	0.20	0.20

As shown in Figure 2.7, the value of a_g for the Este's area is between 0.050 and 0.075 g. From Tab. 3.1 results that the value of β_S is equal to 0.20.
The coefficient S_T, referring to the NTC08 (Tabella 3.2.VI), is found in relation to the topographic category (Este is a T1 category, flat territory with isolated peaks and slopes less than 15°) giving a value of S_T = 1.0 (Tab. 3.2).

Table 3.2. Topographic coefficients (Tabella 3.2 VI, NTC08).

Categoria topografica	Ubicazione dell'opera o dell'intervento	S_T
T1	-	1,0
T2	In corrispondenza della sommità del pendio	1,2
T3	In corrispondenza della cresta del rilievo	1,2
T4	In corrispondenza della cresta del rilievo	1,4

To find the value of S_s is firstly necessary to define the value of another coefficient F_0 that from the Appendixes of NTC08 is taken equal to 2.49 (basing on latitude and longitude of the site), and considering a C type ("Tabella 3.2 II" of NTC08) for SESA landfill subsoil category (deposits of coarse grained soils with medium thickness or fine grained soils with a medium consistency), the following formula gives a value for the S_s coefficient:

$$1.0 \leq 1.7 - 0.6 \cdot F_0 \cdot \frac{a_g}{g} \leq 1.5$$

The calculation gives a results higher than 1.5; in this case, the value that has to be considered is $S_S = 1.5$.

Now it's possible to define a_{max}, K_H and K_V:

$$a_{max} = S_S \cdot S_T \cdot a_g = 1.5 \cdot 1.0 \cdot 0.075 = 0.1125 \text{ g}$$

$$K_H = \frac{\beta_s \cdot a_{max}}{g} = 0.002$$

$$K_V = \pm 0.5 K_H = \pm 0.001$$

The two last values will be inserted in the two calculation softwares.

4. Slope Stability Analysis methods

4.1 Introduction

Slope stability analysis is carried out in order to evaluate the safe design of natural (where instability is usually due to the erosion) or artificial slopes (generated by cuttings, excavations or building of embankments) and the conditions for the equilibrium: generally, instability is the result of a combination of gravitational forces and water pressures, usually the main causes of the failure mechanisms.

The main purpose of this type of study is the identification of endangered areas establishing a factor of safety for the potential slip surfaces considering factors as safety, reliability and economics in the long period establishing also potential remedial measures for the most critical cases.

Before the introduction of powerful personal computers, stability analysis was performed graphically or using hand-calculations; simplifying hypothesis had to be taken to find solutions, and the concept of numerically dividing a larger soil body into smaller parts was the most adopted simplification.

Nowadays geotechnical engineers have a lot of possibilities thanks to the use of computer software products that permit to deal with a lot of variables like complex stratigraphy, highly irregular pore-water pressure conditions, almost any type of slip surface shape, concentrated and distributed loads and different linear and nonlinear shear strength models.

The software possibilities ranges from limit equilibrium techniques through finite element limit approaches, and as easily predictable each methods presents its pros and cons: for example, limit equilibrium is the most commonly used and presents simple solution techniques, but it can results unsuitable if the slope fails by complex mechanisms (like internal deformations, progressive creep, etc.).

During the last decade new applications are been developed as the Slope Stability Radar, a system to remotely scan a rock slope to control the spatial deformations of the face, detecting small movements with sub-millimeter accuracy by using interferometry techniques.

4.2 General concepts of Limit Equilibrium Methods

The study of the stability of the earth structures is the oldest type of numerical analysis in geotechnical engineering (SLOPE/W tutorial manual). The first studies were introduced early in the 20th Century: in 1916 Patterson presented a stability analysis of the Stigberg Quay in Gothenberg (Sweden), where the first idea of dividing a potential failure mass into slices was proposed. One of the reasons the limit equilibrium approach was adopted so quickly is that solutions could be founded by hand-calculations.
During the next few decades this study was developed and improved by other engineers like Fellenius and Janbu, until the 1960's when the coming of electronic computers led this technique to more rigorous formulations such as those elaborated by Morgenstern and Price and by Spencer.
All these methods are similar each other but they are also different due to the hypotheses made; nevertheless, there are some general hypotheses that are common to all the limit equilibrium methods (Favaretti):

1 - Mohr-Coulomb failure criterion is satisfied along the hypothetical failure surface, which may be a straight line, circular arc, logarithmic spiral or other irregular surface. The MC failure criterion represents the linear envelope that is obtained from a plot of shear strength of a material versus the applied normal stress (Fig. 4.1). The relation is expressed as:

$$\tau_f = c + \sigma_f \tan\phi$$

where: τ_f is the shear strength at failure on the failure plane, c is the intrinsic cohesion of the material (and the intercept of the failure envelope), σ_f is the normal stress at failure on the failure plane and ϕ is the angle of internal friction (and the slope of the failure envelope). This equation can contain the pore water pressure u in cases of drained conditions (effective stress):

$$\tau_f = c' + (\sigma_n - u)\tan\phi'$$

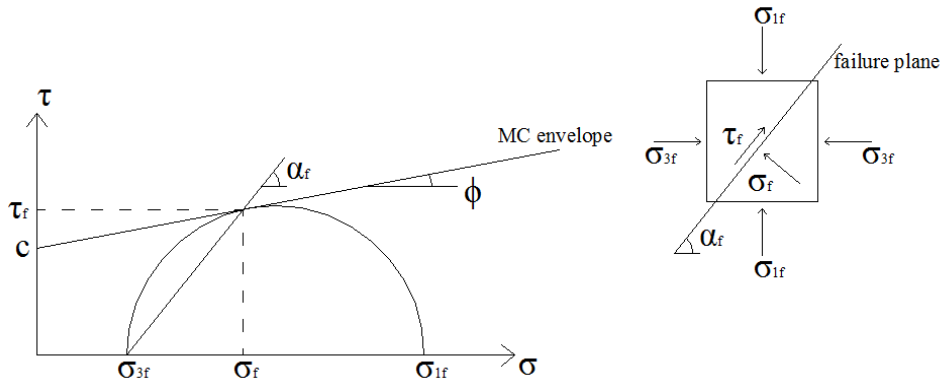

Fig. 4.1 – Representation of the MC failure criterion

2 - Two dimensional sections are analyzed, assuming plain strain conditions.

3 - The actual strength of the soil is compared with the value required for the equilibrium of the soil mass giving a measure of the factor of safety (FOS).

Usually the FOS is defined as the ratio between the ultimate shear strength (τ_f) and the mobilized shear strength (τ) at incipient failure:

$$FOS_\tau = \frac{\tau_f}{\tau}$$

The shear strengths can be studied in two different ways: the first is the so called "total stress approach" while the second is the "effective stress approach".

The first regards short term loading conditions, usually for clayey slopes or slopes with saturated sandy soils with the pore pressure not dissipated; the second approach is used for long term conditions in all kind of soils where drained known conditions prevail. This second way to obtain the shear strength is particularly important for lands where intensive rainfall may occur over a long period, and the water table can rise significantly after a rainstorm (Favaretti).

There also other formulations to define the FOS, as one that assumes the safety factor to be constant along the slip surface, defining it with respect to the moment equilibrium (generally utilized for the analysis of rotational landslides):

$$FOS_m = \frac{\sum M_r}{\sum M_d}$$

where $\sum M_r$ is the sum of the resisting moments and $\sum M_d$ is the sum of the driving moments. The force equilibrium is generally used to translational or rotational failure that can be composed by planar or polygonal slip surfaces:

$$\text{FOS}_\text{f} = \frac{\sum F_r}{\sum F_d}$$

where $\sum F_r$ is the sum of the resisting forces and $\sum F_d$ is the sum of the driving forces.
It's important to note that the simplest slope stability analysis methods cannot fulfill both force and moment equilibrium simultaneously and that these definitions can be very different in the values and the meaning. Nevertheless, most design codes do not present a clear requirement on what FOS they are referring, and only a single safety factor is specified in many of these codes.
The instability of slopes occurs when the FOS $\leq$ 1.0, but in practice this is not completely true because the failure is also caused by the velocity of the sliding soil mass; usually, until F = 1.25 failure doesn't occur (Favaretti, 2010).
4 - Soils are treated as rigid-plastic materials and due to this hypothesis the analysis does not consider deformations.
Limit equilibrium methods can be subdivided in two principal categories:

- methods that consider only the whole soil body (Taylor method, Culmann method);
- methods that subdivide the mass into many slices (that can be vertical or non vertical like for the Sarma's method) considering the equilibrium of each slide (method of slices).

In this study only the methods of slice will be presented because are those used by computer programs and the only types of calculation methods provided for by law; moreover, methods that considers the whole soil body are useful for slopes with homogeneous materials.

4.3 LEM – Method of slices

In order to calculate the mobilized strength for a drained soil, the distribution of the effective normal stresses along the failure surface must be known: this is usually done by subdividing the failure mass of the slope into smaller slices, studying each singular slice as a unique sliding block (Fig. 4.2). The Method of slices (Mos) can study the problem considering complex slope geometries, non homogeneous soil conditions and the influence of external loads.

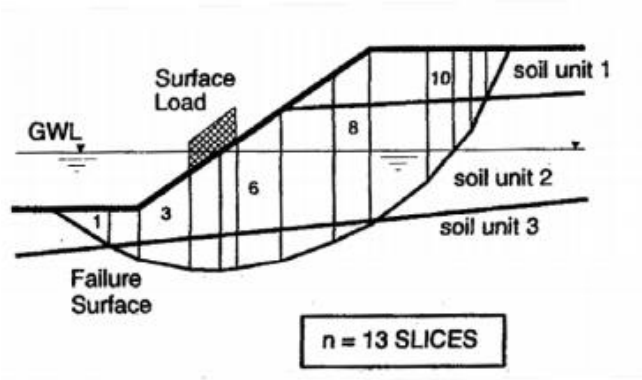

Fig. 4.2 – Non-homogeneous soil mass subdivided into vertical slices along the failure surface

The method of slices has been developed in different terms based on the hypotheses made by the authors. Fellenius (1936) introduced the first method, also known as the Ordinary or the Swedish method, for a circular slip surface. In 1955 Bishop introduced a new relationship for the base normal force, and the equation for the FOS hence became non linear. In the mid-1950s also Janbu advanced a simplified method for non circular failure surfaces, discretizing a potential sliding mass into vertical slices; in 1973 Janbu developed a further development of its previous simplified method. Later, thanks also to the advent of electronic computers, Morgenstern-Price (1965), Spencer (1967), Sarma (1973) and others contributed to the analysis including different assumptions on the interslice forces. In 1986 a procedure of General Equilibrium Method was made by Chugh as a development of the Morgenstern-Price and Spencer methods, satisfying both force and moment equilibrium conditions.

The interslice forces are related to a number of factors linked to the characteristics of materials and their estimation is complicated in the limit element methods; for this reason,

simplified assumptions are made in most approaches either to neglect both or one of them. Nevertheless, the most accurate methods consider these forces in their analysis.
Anyhow, all these methods can be subdivided in three categories basing on the different hypotheses (Favaretti, 2010):

- assumptions on interslice force direction (Bishop, Morgenstern-Price, Spencer);
- assumptions on the thrust line position (Janbu);
- assumptions on the interslice forces distribution (Sarma).

As previously discussed, other suppositions are those that tend to divide a slide mass into *n* smaller slices (and so the irregular base of the slice can be approximated to a chord) and the FOS is considered constant along the failure surface.
Each slice is affected by a general system of forces (Fig. 4.3) and the thrust line is defined as the line that connects the points of application of the interslice forces E_i and $E_{(i+1)}$. Its location can be assumed or determined with a method that satisfies the complete equilibrium, but the simplified methods neglect the location of this force because of the impossibility to satisfy the complete equilibrium for the failure mass.

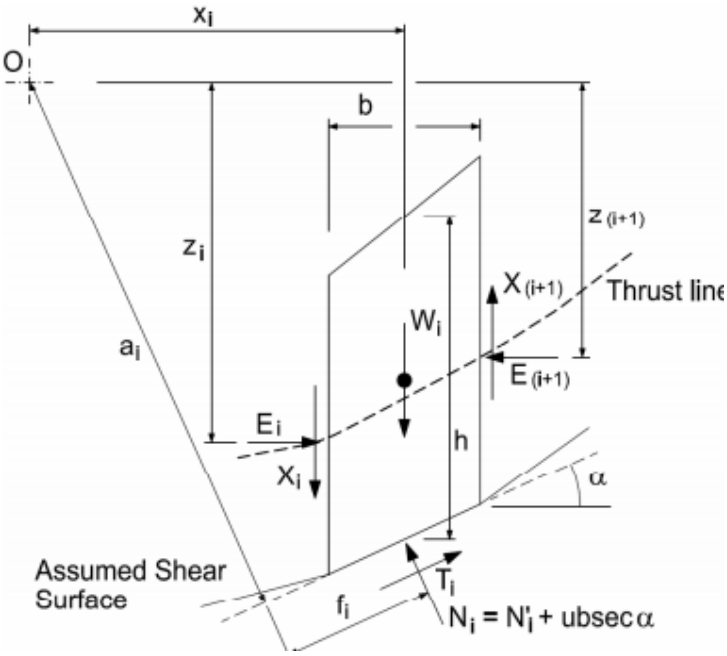

Fig 4.3 – Forces affecting a singular slice (Source: Environmental Geotechnics course)

In fact for this system there are *(6n – 2)* unknowns but only four equations *(4n)* for each slice can be written for the system equilibrium limit (Tab. 4.1); for this reason the solution is statically indeterminate.

Table 4.1. Equations and unknowns of the limit equilibrium of each slice (Source: Environmental Geotechnics course).

Equations	Condition
n	Moment equilibrium for each slice
2n	Force equilibrium in two directions (for each slice)
n	Mohr – Coulomb relationship between shear strength and formal effective stress
4n	Total number of equations
Unknowns	**Variable**
1	FOS
n	Normal force at base of each slice, N'_i
n	Location of normal force, N'_i
n	Shear force at base of each slice, T_i
n - 1	Interslice horizontal force, E_i
n - 1	Location of interslice horizontal force, E_i
n - 1	Interslice vertical force, X_i
6n - 2	Total number of unknowns

Considering Table 4.1, the total unknowns are:

$$6n - 2 - 4n = 2n - 2$$

An assumption to reduce the unknowns number is usually to consider the normal forces on the base of the slices acting at the midpoint; with this hypothesis the number of remaining unknowns becomes:

$$5n - 2 - 4n = n - 2$$

These are the general assumptions that characterized the available methods of analysis that will be discussed in the further subchapter.

4.3.1 General formulation

The assumption is based on a body of soil sliding along a general surface ABCD (Fig. 4.4); the entire soil mass is subdivided into *n* elementary vertical slices separated by *n - 1* vertical boundaries.

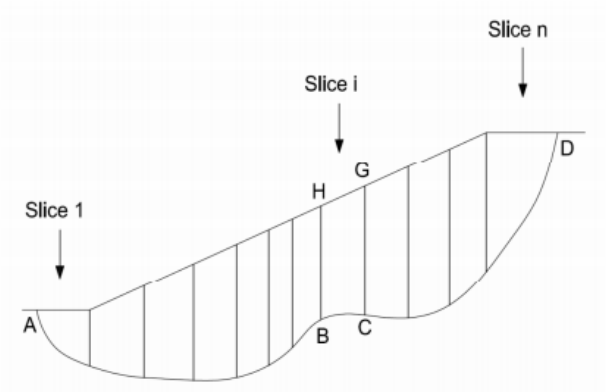

Fig. 4.4 – Soil body subdivided into *n* vertical slices

The stability is satisfy if both force and moment equilibrium conditions are respected for each slide and in case of drained conditions and if $F_c = F_\Phi = F$ along the failure surface, the FOS can be defined as:

$$\tau = \frac{\tau_f}{F} = \frac{c'}{F_c} + \frac{(\sigma_n - u)tan\phi'}{F_\Phi}$$

Considering the equilibrium of the entire soil body, the internal interslice forces (E_i to E_n and X_2 to X_n) must vanish; moreover, with the hypothesis that no external forces are acting on the end of the slices ($E_1 = E_{(n+1)} = X_1 = X_{(N+1)} = 0$), a first value of F can be obtained only referring to the forces equilibrium:

$$\frac{1}{F}\sum_{i=1}^{n}\frac{\sec\alpha_i}{m_{\alpha,i}}\{c'b + [W(1 - r_u) - \Delta X]tan\phi'\}i - \sum_{i=1}^{n}[(W - \Delta X)tan\alpha]i = 0$$

where:

- $m_{\alpha,i} = \frac{1}{FT_i}\{c'b + [W(1 - r_u) - \Delta X]tan\phi'\}i$;

- r_u = coefficient of pore water pressure = $(u \cdot b)/W$

Considering the moment equilibrium of slice *i* around pivot O and that the moments of all internal forces (E_i, X_i) must vanish for the entire body, an expression for the equilibrium of moments can be obtained:

$$F = \frac{\sum_{i=1}^{n} \frac{a_i}{m_{\alpha,i}} \{c'b + [W(1 - r_u) - \Delta X] tan\phi'\} i}{\sum_{i=1}^{n} [Wx]\, i - \sum_{i=1}^{n} \frac{f_i}{m_{\alpha,i}} \left[W \left(1 + r_u tan\alpha \frac{tan\phi'}{F} \right) - \frac{c'b}{F} tan\alpha - \Delta X \right] i}$$

In cases of circular failure surface (a_i = R, f_i = 0 and $x_i = R_i sen\alpha$) the previous equation becomes:

$$F = \frac{\sum_{i=1}^{n} \frac{1}{m_{\alpha,i}} \{c'b + [W(1 - r_u) - \Delta X] tan\phi'\} i}{\sum_{i=1}^{n} [Wsen\alpha]\, i}$$

4.3.2 Fellenius method/OMS

The Ordinary Method of slices (OMS) was made by Fellenius and is one of the simplest method of slices.
The hypotheses are:

- circular failure surfaces;
- only moment equilibrium condition;
- no consideration of the interslice forces E_i and X_i (and so also the location of these forces z_i is equal to 0). There are:

(5n – 2) – (n – 1) – (n – 1) – (n – 1) = 2n + 1 unknowns *< 4n* equations

The FOS is equal to:

$$F = \frac{\sum_{i=1}^{n} [c'bsec\alpha + (N - ubsec\alpha) tan\phi'] i}{\sum_{i=1}^{n} [Wsen\alpha]\, i}$$

The advantage of this method is its simplicity in solving the FOS, since the equation does not require an iteration process.

4.3.3 Bishop's rigorous method

This method is very common in practice of slope stability analysis, and its assumptions are:

- circular failure surfaces;
- both forces and moments equilibrium are satisfied;
- interslice vertical forces X_i (*n – 1* unknowns) defined as: $X_i = \lambda f(x)$ where λ is a constant unknown ("+1") and f(x) a known function. The number of unknowns and equations become:

$$(5n - 2) - (n - 1) + 1 = 4n \text{ unknowns} = 4n \text{ equations}$$

In this way the problem is determinate and the equations of equilibrium are satisfied.
It's important to note that there are several combinations between λ and f(x) that satisfy the problem, but some of these are not possibles because there are two other aspects that have to be respected:

- shear strength along vertical interslice surfaces must be less than the failure strength of soil because these surfaces can't reach the failure condition ($\tau_i = X_i/A_i < \tau_f = c' + \sigma' \tan\phi'$);
- the thrust line must be located inside the sliding body (Fig. 4.5). A solution where the thrust line is located externally to the soil body is not phisically acceptable.

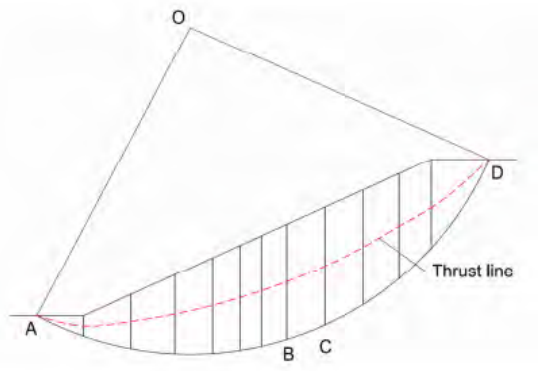

Fig. 4.5 – Thrust line position

4.3.4 Bishop's simplified method

The hypotheses of this method are:

- circular failure surfaces;
- only moments equilibrium condition;
- neglection of the interslice vertical forces X_i. There are:

$$(5n - 2) - (n - 1) = 4n - 1 \text{ unknowns} < 4n \text{ equations}$$

and so the problem is overdeterminated.
Considering that $X_i = 0$, $\lambda = 0$ and $\Delta X_i = 0$ the FOS is equal to:

$$F = \frac{\sum_{i=1}^{n} \frac{1}{m_{\alpha,i}} \{c'b + [W(1 - r_u)]tan\phi'\}i}{\sum_{i=1}^{n} [Wsen\alpha]\, i}$$

The solution of the Bishop's method can be found with an iterative procedure:

- assume an initial value of $F \rightarrow F_0$;
- calculate $m_{\alpha,i}$ with F_0 for each slice;
- determine F using $m_{\alpha,i}$ (if $F = F_0$ the procedure is complete, otherwise the iteration procedure continues).

4.3.5 Janbu's simplified method

The assumptions are:

- any type of failure surface;
- only force equilibrium condition;
- interslice vertical forces $X_i = 0$ (similarly to the Bishop's simplified method) leading to an overdeterminated solution that will not satisfy the conditions of the moment equilibrium.

The FOS is equal to:

$$F = \frac{\sum_{i=1}^{n} \frac{sec\alpha_i}{m_{\alpha,i}} \{c'b + [W(1 - r_u)tan]\phi'\}i}{\sum_{i=1}^{n}[Wtan\alpha]\, i}$$

In order to correct the overestimated value of the FOS, Janbu presented a correction factor f_0 > 1 that has to be multiplied to the previous calculated safety factor to obtain a final value of FOS. This correction factor is a function of the slide geometry and the strength parameters of the soil (Fig. 4.6); in cases of surface intersecting different soil types, the curve $c - \phi$ is generally used to estimate the f_0 value.

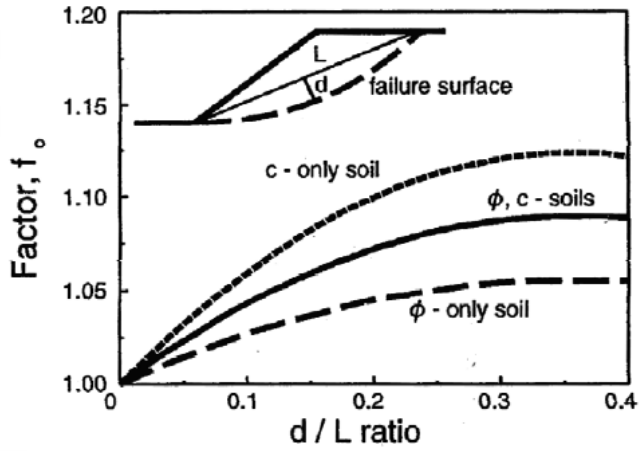

Fig. 4.6 – Estimation of the corrective factor f_0 (Source: Environmental Geotechnics course)

As an alternative, the corrective factor f_0 can also be calculated with the following formula:

$$f_0 = 1 + b_1 \left[\frac{d}{L} - 1.4\left(\frac{d}{L}\right)^2\right]$$

where b_1 depends on the soil type:

- b_1 = 0.69 for c only soils (i.e. for clayey soils);
- b_1 = 0.31 for ϕ only soils (i.e. soils without cohesion);
- b_1 = 0.5 for c and ϕ soils.

4.3.6 Janbu's generalized method

This is an advanced procedure of Janbu's method and the hypotheses are:

- any kind of failure surface;
- both force and moment equilibrium conditions satisfied, since it assumes a location of the thrust line (leading to *4n – 1* unknowns) suggesting also that the actual position of the thrust line is an additional unknown, and thus equilibrium can be respected if the assumption selects the correct thrust line. This line is searched using an iteration procedure until the equilibrium is reached.

4.3.7 Morgenstern – Price method

The assumptions are:

- any kind of failure surface;
- both force and moment equilibrium conditions satisfied;
- the interslice force inclination can vary with an arbitrary function f(x) (leading the number of unknowns equal to *4n*):

$$\frac{X_i}{E_i} = \lambda f(x)$$

where:
- λ = scale factor of the assumed function;
- f(x) = interslice force function that varies continuously along the slip surface.

4.3.8 Spencer's method

This method derives from the previous method and satisfies static equilibrium by assuming that the interslice force inclination can vary with a constant but unknown function f(x) = constant.

4.3.9 Lowe – Karafiath's method

The hypotheses are:

- any kind of failure surface;
- only force equilibrium is satisfied assuming that the interslice forces are inclined at an angle equal to the average of the slope ground surface angle β and slice base angle α; this simplification leads to *4n – 1* unknowns failing to satisfy the moment equilibrium.

Considering θ = inclination of the interslice resultant force the two equations are:

$$\theta = 1/2(\beta + \alpha)$$

$$\frac{X_i}{E_i} = tan\theta$$

4.3.10 Corps of Engineers method

The approach is similar to the previous one, but the assumption on the inclination of the interslice forces θ can be done in two different types: it considers θ parallel to the slope ground surface inclination β (i.e. θ = β) or equal to the average slope inclination between the left and right end points of the failure surface. This hypothesis makes the problem overdetermined and moment equilibrium is not satisfied.

4.3.11 Sarma's method

This method is quite different from the other ones because it was implemented for non-vertical slice or for general blocks (wedge method). It assumes a relationship for the interslice forces similar to the Mohr-Coulomb expression:

$$X = ch + Etan\phi$$

where:

- c and ϕ are the shear strength parameters (cohesive component and material friction angle);

- h is the slice height.

This assumption makes the problem solvable both for force and moment equilibrium (the interslice forces are adjusted until the FOS satisfies the two equilibrium equations).
It's important to note that this method works best when the cohesion is zero or at least very small: if $c = 0$, the interslice shear is directly proportional to the normal as with all the other approaches.

4.3.12 General limit equilibrium formulation

The GLE formulation was studied by Fredlund at the University of Saskatchewan in the 1970s (Fredlund and Krahn 1977; Fredlund et al. 1981). This approach regroups the key elements used by the various methods and can be utilized both for circular and non circular failure surfaces.
This technique is based on two factor of safety expressions and allows for a range of interslice shear-normal force hypotheses. One equation gives the FOS with respect to moment equilibrium (F_m), while the other equation gives the safety factor related to horizontal force equilibrium (F_f).
The relationship between the interslice forces is defined in the same manner of the equation proposed by Morgenstern and Price (1965):

$$\frac{X_i}{E_i} = \lambda f(x)$$

Some important considerations on this method and the others can be done plotting in a diagram as the two FOS vary with λ (Fig. 4.7):

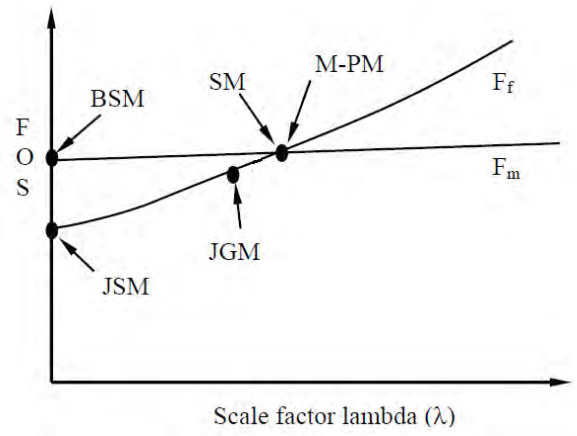

Fig. 4.7 – Presentation of the most common mos methods (Fredlund and Krahn 1977)

The above diagram permits to understand the differences between the FOS from the various methods, and to study the influence of the selected interslice force function.

Two of the assumptions of the Bishop's simplified method (BSM) are the not consideration of the interslice vertical shear forces and the solution only for the moment equilibrium. For the GLE terminology if the shear forces $X_i = 0$ means that $\lambda = 0$, and the FOS for the BSM falls in the moment curve in Figure 4.7 where lambda is zero.

A similar consideration can be done for the Janbu's simplified method (JSM) that also ignores the interslice vertical forces X_i satisfying only the force equilibrium: the FOS for the JSM falls in the vertical axis of the diagram where $\lambda = 0$ on the force curve.

The Morgenstern and Price method (M-PM) and the Spencer method (SM) satisfy both moment and force equilibrium: for this reasons their FOS falls where the two curves cross, and the distinction on which of these methods fall on the crossover point depends on the chosen interslice force function (constant X/E ratio for SM and any general appropriate function for M-PM).

Other methods like the Corps of Engineers and the Lowe-Karafiath have the FOS falling on the force curve, since they only respect the force equilibrium.

4.3.13 Considerations on the interslice force function

The interslice shear force X_i is assumed to be associated to the interslice normal force E_i by the equation $X_i/E_i = \lambda f(x)$. *f(x)* can't be determine for a general problem and the different methods apply different values for the function.

A case where *f(x)* = 1.0 is equivalent to the Spencer method (where *f(x)* is considered a constant value) and can be used for sandy soils. In fact, sandy soils means an effective cohesion *c'* = 0; the MC expression can be applied to the interslice force relation (X_i/E_i = *tanϕ'*) and so the value of λ results equal to *tanϕ*.

f(x) = senx is an alternative very used as the association of the *f(x)* to a trapezoidal or clipped-sine shape (Fig. 4.8, [3]): these types of function are very used for methods like Morgenstern-Price and GLE where both moment and force equilibriums are satisfied simultaneously.

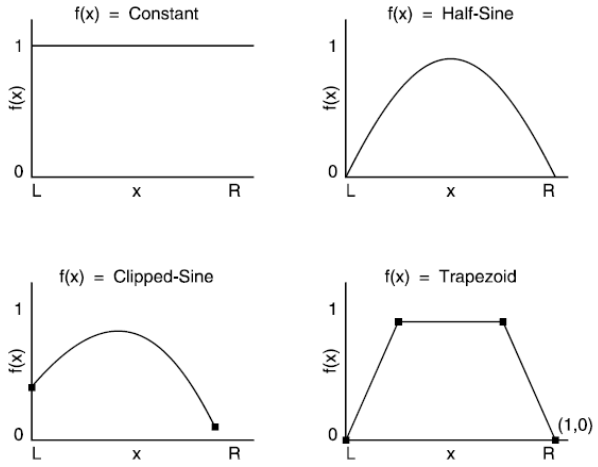

Fig. 4.8 – Shape of interslice force functions

In general, the most commonly used functions are the constant and the half-sine functions. The half sine function is used by default by SLOPE/W program also because this particular function tends to concentrate the interslice shear forces towards the middle of the sliding mass and diminishes the interslice shear in the crest and toe areas (SLOPE/W tutorial manual).

Sarma's method uses an equation similar to the MC expression to relate the interslice shear and normal forces (*X = ch + Etanϕ*): this approach can result interesting due to the correlation between the material properties and the interslice forces, but actually can be

useful only in cases of cohesion equal to zero (as specified before), where the interslice shear becomes directly proportional to the normal force. If a cohesion value is specified, the interslice shear force X starts to become independently of the interslice normal force E, leading to convergence difficulties (SLOPE/W tutorial manual).

4.3.14 Summary of the method of slices approaches

The methods discussed in the previous paragraphs present some similarities and some differences. Table 4.2 reassumes these concepts.

Table 4.2. Summary of LE method of slices.

Method	$\sum F = 0$	$\sum M = 0$	Assumptions
Fellenius/OMS	-	√	Neglects both X_i and E_i
Bishop's rigorous	√	√	$X_i = \lambda f(x)$
Bishop's simplified	√*	√	$X_i = 0$
Janbu's simplified	√	-	$X_i = 0$
Janbu's generalized	√	√**	Considers X_i and E_i acting on the thrust line
Morgenstern and Price	√	√	$\frac{X_i}{E_i} = \lambda f(x)$
Spencer	√	√	Constant inclination (X_i/E_i = const)
Lowe – Karafiath	√	-	Resultant inclination at $\theta = 1/2(\beta + \alpha)$
Corps of Engineers	√	-	Two hypotheses on θ
Sarma	√	√	For general blocks, $X = ch + Etan\phi$

*= force equilibrium only for E_i

** = M equilibrium satisfied if thrust line position correctly selected

Fellenius method is the easier method and its factor of safety can be easily obtained without any iterative calculation and can be solved by hand or spreadsheet calculation; it's well known to be very conservative since sometimes it presents results that can be 20-30 % higher than those obtained with other methods. For this reason it's now rarely used in practice.

The Bishop's method is one of the most worldwide used methods even if its use has been reccomanded only for circular failure surfaces (Abramson et al., 2002), but its analysis is simple for hand calculation and the convergence is fast.

Janbu's simplified method presents only few convergence problems and can be used also for a non circular failure surfaces which is commonly observed in sandy-type soils.

The Janbu's rigorous method consists in the introduction of the correction factor f_0 but the methods to calculate this factor are based on limited case studies and for this reason the use of these factors are questioned for some engineers if applied to complicated non-homogeneous soil slopes.

Morgernstern-Price and Spencer methods consider both force and moment equilibriums and being careful to the thrust line position are two methods suggested by computer softwares like SLOPE/W, since they meet the criteria of fulfillment of all equations of statics considering both shear and normal interslice forces.

The Lowe-Karafiath method and the Corps of Engineers methods are based on hypotheses on the interslice force functions and satisfy only the moment equilibrium; usually the first one gives results close to that obtained with the Janbu's rigorous method even though the moment equilibrium is not satisfied. The Corps of Engineers method in some cases may lead to a high factor of safety, and to account this problem some engineers prefer to adopt a lower inter-slice force angle (Duncan and Wright, 2005).

Sarma's method is particular due to the hyphoteses made on the interslice force function equation, as explained in the previuos paragraph, but in some cases (soils with zero cohesion) it can be very useful.

The General limit equilibrium formulation is usually adopted to provide a framework for discussing, describing and understanding all the other methods, since it can compare the various FOS of the other methods (SLOPE/W tutorial manual). The main difficulty in using the GLE procedure is related to the requirement that the user verify the reliability and reasonableness of the calculated safety factor, preventing its use for automatic search techniques that try to identify the critical failure surface (Favaretti, 2010).

Regarding the factor of safety values, Ambramson et al. (2002) found that for circular failure surfaces the Bishop's simplified method always gives higher FOS values than Janbu's simplified method; this value falls within ± 5% of the safety factor calculated with the more rigorous methods. However, the safety factor can differ by ± 15% as compared with the results calculated by Spencer and Morgenstern-Price methods.

4.4 General concepts of Finite Element Method

Limit element methods are based on the assumptions that results give stresses and forces that satisfy force equilibrium of each slice making also the same safety factor for each of them. These concepts lead to some limitations related to the impossibility to obtain realistic stress distributions along the slip plane or within the potential sliding mass. In order to consider also this question, the finite element approach establishes the stress distribution in the ground surface and then applies these stresses in a stability analysis.

Finite Element Method (FEM) is a numerical analysis based on differential equations to solve problems of engineering and mathematical physics useful for cases with complicated geometries, loadings and material properties. This method was originated from the need to solve complex elasticity and structural analysis problems in civil and aeronautical engineering and then developed also to other branches of the engineering.

FEM is based on a simplified physical model that wants to represent the real object characteristics under investigation by using mathematical models based on a discretization procedure.

The discretization consists in dividing the model body into an equivalent system of many smaller bodies or units (finite elements) interconnected at points common to two or more elements (nodes) and or boundary lines and/or surfaces.

Reassuming, the key factors of the geometry of a FEM (Fig. 4.9) are:

- points: determine the start and end of lines and can be used also to define concentrated loads;
- lines: are used to define physical boundaries of the geometry, the model boundaries and discontinuities in the geometry (for example walls or separation of distinct soil layers);
- clusters: are areas that are fully enclosed by lines and defines zones where the soil properties are homogeneous.

When the geometry model is complete a finite element model can be formed, basing on the composition of clusters and lines of the geometry model.

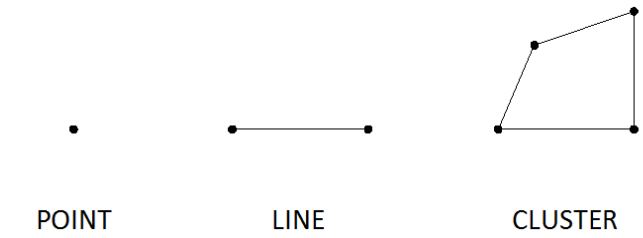

Fig. 4.9 – Components of the geometry model of a FE analysis

The three key components of a finite element mesh are (Fig. 4.10):

- finite elements: smaller (usually triangular) units in which cluster is divided;
- nodes: points that define the elements and usually there are 15-node elements or 6-node elements. Adjacent elements are connected through their common nodes. The displacement are calculated at the nodes during the FE analysis.
- stress points: points where stress and strain are calculated. A 15-node triangular element contains 12 stress points and 6-node triangular elements has 3 stress points.

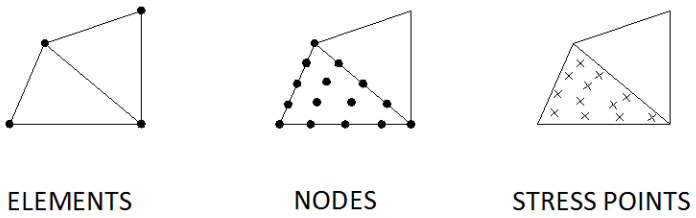

Fig. 4.10 – Components of a finite element mesh

In this thesis the study with the FEM of the slope stability of Este's landfill is done using the PLAXIS program, a finite element software that has been developed specifically for the analysis of deformation and stability in geotechnical engineering projects.

5. Definition of the input sections and parameters

5.1 Chosen landfill sections for the calculation

Shafer (2000) suggested that landfill sections for the study of slope stability are to be selected where both the liner and waste grades are sloping downward at the steepest combination of grades.

S.E.S.A. company provided a series of sections (Fig. 5.1) relating both to the old landfill ("Lotto 1") and to the latest sectors ("Lotto 2" and "Lotto 3"): referring to these sections (1-1, 2-2, 3-3, 4-4, A-A, B-B, C-C) the three steepest ones are chosen in order to start the calculation procedure through the two computer softwares SLOPE/W for the Limit Equilibrium methodology and PLAXIS for the Finite Element approach.

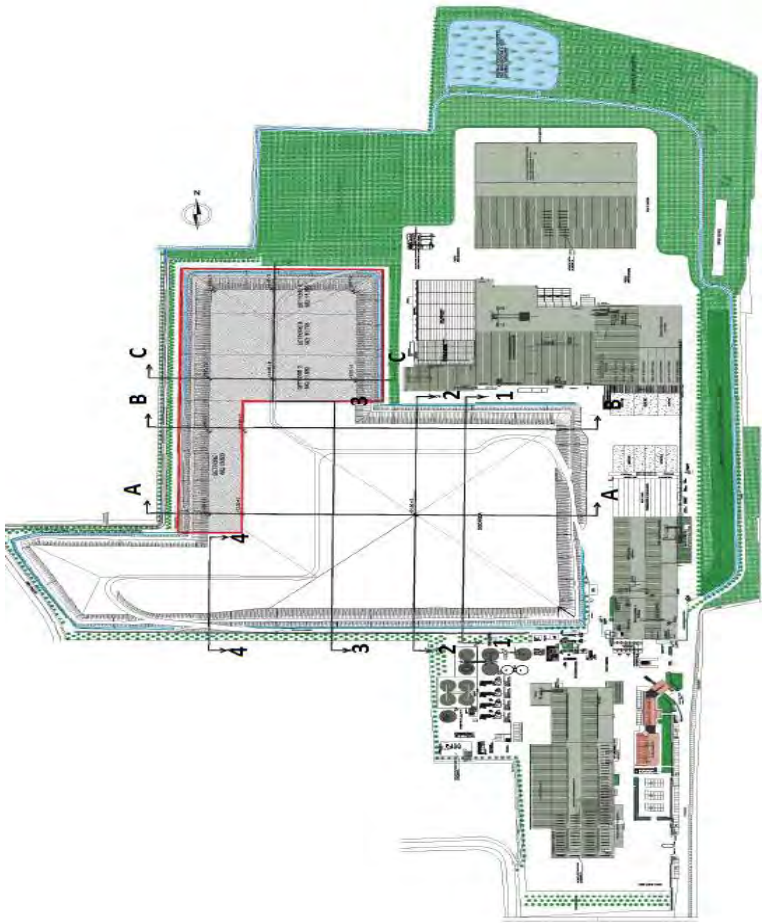

Fig. 5.1 – Planimetry and sections of SESA landfill

The cross sections studied are:

- 4-4: it's located in the south – western part of the site and refers only to the oldest landfill named "Lotto 1"; its study is important to evaluate the stability of the oldest part of S.E.S.A. landfill. Another reason is because in the northwest part of "Lotto 1" a new dumping area has been designed ("Lotto Ovest") leading the evaluation of the stability of the near old site as an issue of particular importance. Moreover, older waste presents a higher organic fraction content than those dumped after an appropriate separate collection system (that started with the fill of "Lotto 2"): this condition can lead to a higher instability if compared to the other situations due to the higher water content into the waste mass. In addition, old landfill presents a final top cover very different if related to the other protection types of the landfill without any type of bottom liner systems. The analysis (as also for the other chosen sections) has been performed considering only an half of the section (Fig. 5.2); indeed the two halves are almost equals both in shape as also for the top and bottom liner systems. This section has the highest point at about 15 meters from the ground surface and presents a long part of the section (about 36 m) practically linear and two steepest slopes (the first of 12 m of horizontal length, the second of 6 m) of 31 degrees, divided by a berm of 8 meters. The landfill bottom (about 3 m below the ground surface) doesn't present any type of protection but is placed inside a natural clay barrier with some silty layers.

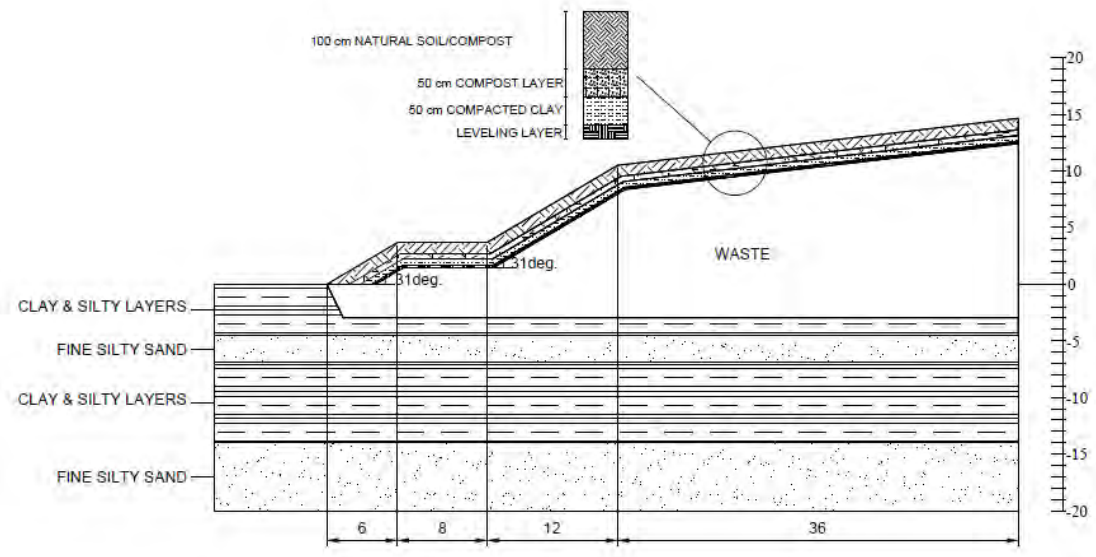

Fig. 5.2 – Left half part of section 4-4

- 2-2: it presents a steepest inclination if compared to section 1-1 and is near to other S.E.S.A. waste treatment activities like the composting and anaerobic digestion plant. This part is composed by "Lotto 1" and "Lotto 3" dumping zones; the study of the slope stability of this section is important because in the northern part of "Lotto 3" there are other S.E.S.A. waste treatment activities (such as the composting treatment plant, Fig. 2.8) and the verification that the landfill slope is stable is fundamental primarily to guarantee the safety of the onsite workers and to not cause any damage to other neighboring activities.

The analysis is performed considering the left half section (Fig. 5.3), even if the two half sections are not completely equal. The right section presents the union between the old landfill and "Lotto 3", and, as previously said, the bottom barrier system of the old landfill part doesn't present any type of protection; anyway, the stability of "Lotto 1" has been already analyzed with section 4-4. This section has the maximum height at about 20 m from the ground surface and presents a long (124 m) and almost flat surface followed by a 31 degrees slope with a horizontal length of 13 m, a berm and another 31 degrees slope (horizontal length = 7 m). The slope has natural soil/compost and clay as protection.

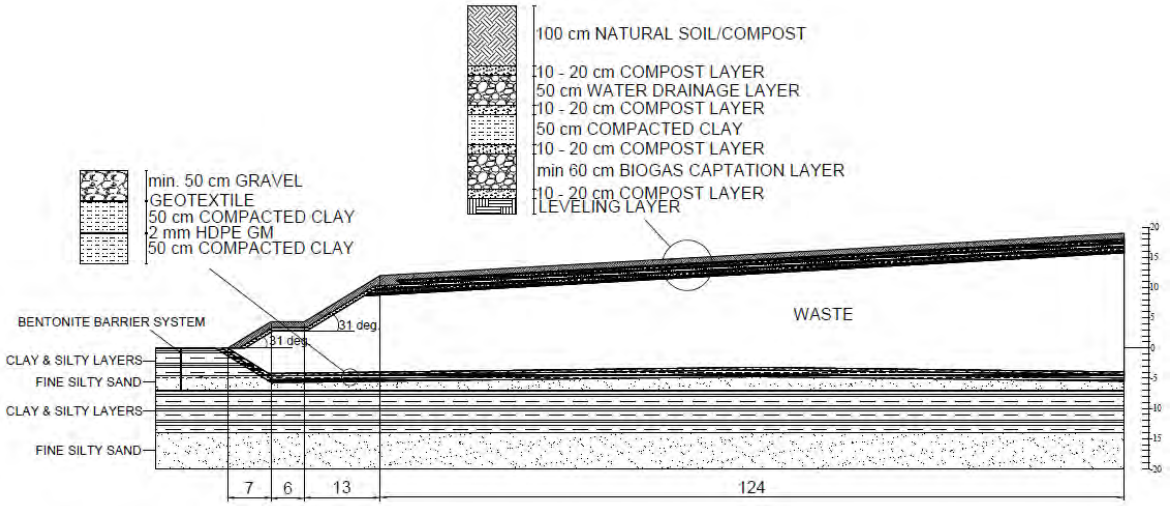

Fig. 5.3 - Left half part of section 2-2

- A-A: it has a steepest inclination if compared to section B-B. Its study is done without considering the future landfill extension ("Lotto Ovest" in this case) because no waste has been dumped in this new area (delimitated by the red line) that it's only been designed for future landfilling operations. Section A-A (Fig. 5.4) is formed by "Lotto 2" and "Lotto 3" dumping zones and, as described in the landfill description chapter, on the left side there will

be installed a new dumping area called “Lotto Ovest” and on the right side of section A-A there is the composting plant of S.E.S.A. activities. These considerations are the critical aspects that leads to evaluate the stability of this landfill section.

Also for this case, the study has been done considering only an half of the entire section due to the nearly symmetry between the two parts, and the left one will confine with the future landfill sector.

The section, similarly to section 2-2, has a long (140 m) and almost flat surface, two steepest slopes (with horizontal length respectively of 7 and 14 m) separated by a berm; at the ground water level a clayey trapezoidal shape berm (h = 5 m, major base = 6.5 m, minor base = 3.5 m) is placed. Soil and clay are the materials that cover the slope.

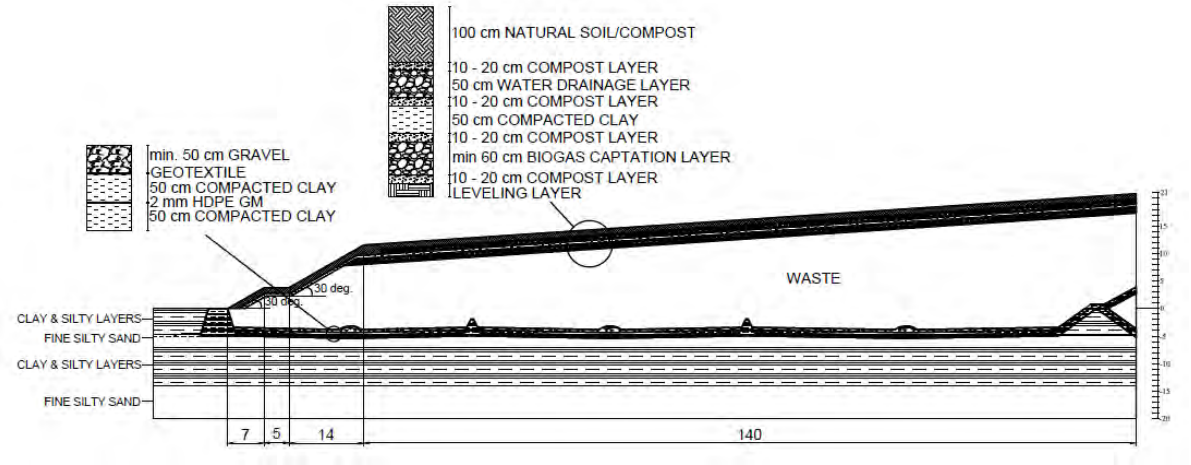

Fig. 5.4 - Left half part of section A-A

These sections will be considered also for the FEM analysis with PLAXIS.

5.2 Geotechnical input data

5.2.1 Material properties

The material properties data present some critical aspects for this study: the impossibility to obtain direct values coming from soil samples of the site is one of the limit of the evaluation of slope stability for this site. For this reason, literature data have been assumed as material properties of Este’s S.E.S.A. landfill (Tab. 5.1). This problem has been partially overcame thanks to the possibility (only for SLOPE/W software) to assign a probability distribution to

all input parameters. In this way, a variability of the input parameters is considered. Moreover, most of the materials are naturally formed materials and their physical properties vary from point to point even if parts of an apparently homogeneous soil. Laboratory results found that most soil properties can be considered as random variables corresponding to a normal distribution function (SLOPE/W tutorial manual). For these reasons, the input parameters for SLOPE/W software (i.e. cohesion, friction angle and unit weight) are been assumed to be normally distributed.

In addition, once that the calculation procedure is completed, a Monte Carlo scheme (with 2000 Monte Carlo trials) is used to compute a probability distribution of the resulting safety factors.

Data regarding the subsoil are taken from data regarding investigations on soils with similar characteristics located in the proximity of the site of interests and typical literature values.

The values of cohesion and angle of internal friction are been diminished by some corrective-precautionary factors (1.25 both for c and $\tan\phi$) as required by the Italian normative NTC 08. The corrective factor relating to the unit weight is 1.0.

Table 5.1. Material properties for Este's S.E.S.A. landfill (MC model).

MATERIAL	Dry unit weight (kN/m^3)	Saturated unit weight (kN/m^3)	Cohesion (kPa)	Internal friction angle (°)	Young's modulus (kN/m^2)	Poisson's ratio (-)	Reference
Natural soil	11.0	16.0	8.0	19.6	2000	0.2	Pistolato (2013)
Compost	6.8	16.4	0	14.8	5000	0.25	Omari et al. (2012)
Compacted clay	16.0	18.0	24.0	29.2	20000	0.4	Look (2007)
Leveling layer	18.2	21.2	0	33.8	100000	0.35	Omari et al. (2012)
Gravel	18.0	20.0	0	28.3	75000	0.3	Look (2007)
Clay with silty layers	17.0	18.0	4.0	20.4	12000	0.4	Soil investigations and literature data
Fine silty sand	16.0	19.0	0	24.7	15000	0.3	Soil investigations and literature data
Clay with silty layers and peat	16.0	18.0	4.0	20.4	12000	0.35	Soil investigations and literature data
Gray fine silty sand	16.0	20.0	0	33.8	20000	0.3	Soil investigations and literature data

5.2.2 Waste properties considerations

The issue relating to the waste properties is very delicate. In fact, MSW have some constitutive similarities in common with natural soils, but they present also particular characteristics as the great deformability for some elements present in the MSW, a physical

and mechanical instability of the organic components and the presence of pore fluids, i.e. leachate and biogas (Favaretti, 2010).
Although waste is heterogeneous, many studies show that municipal solid waste has mechanical properties that vary in a consistent and predictable way (Dixon et al., 2004).

Shear strength parameters

Regarding the shear strength parameters, the factors that affect their behavior are: compressibility, organic and fiber content of waste and degradation extent (Dixon et al., 2004). Tests carried out at the University of Rome (1995) were part of a research program aimed at the mechanical characterization of waste based on in situ and laboratory tests and on the systematic observation of the behavior of Italian landfills (Grisolia et al., 1995). Triaxial tests were conducted on artificially reconstructed waste samples in order to simulate the waste characteristics. The composition of the waste studied was: cloth and wood 6%, paper 32%, plastic 8%, rubble 32% and organic matter 22%, with a water content w = 40%. Preliminary tests, like some compressibility measurements, were carried out in order to verify that the behavior and characteristics of the reconstructed material matches the undisturbed waste samples taken from the landfill.
The results indicated that adopting a level of deformations similar to that commonly found for soils at the scale of laboratory samples (named 15-20%), the shear strength values that could be adopted for waste landfill are a cohesion values c = 5 - 10 kPa and a friction angle of about ϕ = 24°- 30°. Other studies (Dixon et al., 2004) conducted with direct shear tests, shown a cohesion between 0 and 24 kPa and an angle of internal friction varying between 22 and 42 degrees. For design situations, a cohesion value in the range of 0-30 kPa and an internal friction angle of 20-35° would seem reasonable values (Omari, Boddula, 2010).

Unit weight

Factors that govern the unit weight are principally waste composition and landfill operational practices (compaction effort, cover soil placement and liquid management) during waste placement and the effective confining stress currently acting on the waste; although the scarcity of literature data about MSW unit weights, internally consistent waste composition and waste handling practices and predictable confining stress effects suggest

the existence of a characteristic profile of unit weight versus depth for many landfills. Based upon analysis of available laboratory and field data, a characteristic MSW unit weight profile represented by a hyperbolic function was found to exist for individual landfills (Zekkos et al., 2006). Figure 5.5 shows this trend for tests carried out for some landfills. Another study (Fassett et al., 1994) indicated some statistical values for MSW unit weight considering different literature data: for good compaction conditions, a value of around 10.0 kN/m^3 is normally accepted for design conditions.

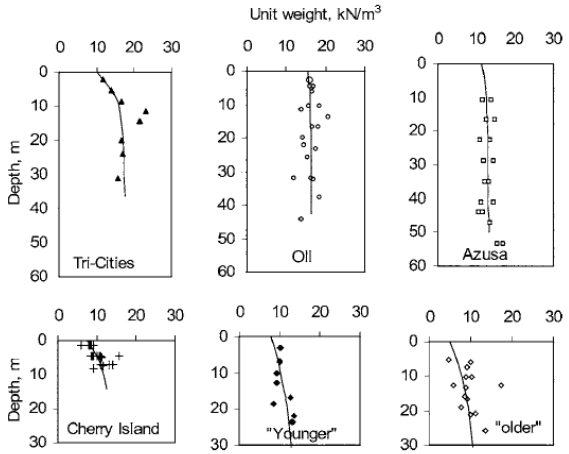

Fig. 5.5 – MSW unit weight trends from in situ tests for individual landfills (Zekkos et al., 2006)

Compressibility

Mechanisms related to waste compression have been summarized by Manassero et al. (1996) as listed in Table 5.2.

Table 5.2. Mechanisms of waste compression and factors controlling magnitude of settlement (Manassero et al., 1996).

Mechanisms resulting in settlement	Factors controlling magnitude of settlement
• Physical compression and creep (mechanical distortion, bending, crushing and re-orientation of particles) • Raveling settlement (migration of small particles into voids between large particles) • Collapse of containers and bridging components (physical/chemical changes such as corrosion oxidation) • Decomposition settlement (biodegradation of organic components) • Settlement of subgrade under applied waste loading	• Initial composition of waste (grading, particle shape, material properties of components, e.g. metal, paper) • Initial density and voids ratio • Layer thickness • Type, thickness and number of cover soil layers • Stress history (pre- and post-filling mechanical treatment) • Leachate levels and fluctuations • Environmental controlled factors (moisture content, temperature, gas generation) • Compressibility of subgrade

It can be assumed that the total settlement is composed by two main components: a primary and a secondary compression. Primary compression consists in the physical compression of particles (distortion, bending, crushing and particle orientation) and consolidation (especially for saturated waste bodies). Usually, this type of compression occurs in a short period of time (few days or few weeks) and incrementally linear compression models can be used to calculate primary settlements. Secondary compression includes creep effects (mechanical compression under constant stress) and degradation processes (chemical and biological); biodegradation is the main component for the secondary compression, and can be influenced by a wide range of interrelated factors (moisture content, temperature and stress level) varying spatially and timing within the landfill.

Lateral stiffness

Stiffness parameters like shear modulus G, Young's modulus E and Poisson's ratio υ are used to quantify the response of a material to a change in stress. These parameters are related by the equation:

$$G = \frac{E}{2(1 + \nu)}$$

Tests conducted by Dixon and Jones (1998) and Dixon et al. (2000) on MSW samples observed a general trend of increasing stiffness with stress (and hence also with depth) level, with the older waste (12-15 years old and partly degraded) that appears to be less stiff than fresh waste (1-5 years old).

Horizontal in situ stress

The difficulty to measure in situ vertical stress of MSW is related to the act of introducing a measuring instrument that alter the stress being measured (Dixon et al., 2004). For a body at rest, horizontal stress σ_h can be related to vertical stresses σ_v by the coefficient of each pressure at rest K_0:

$$K_0 = \frac{\sigma_h}{\sigma_v}$$

A laboratory study made by Landva et al. (2000) concluded that K_0 for fresh waste would be equal to about 0.35-0.4, while for MSW with less reinforcing material than the sample analyzed would have a K_0 value around to 0.5.

Hydraulic properties

Hydraulic conductivity of waste is important due to the influence on the leachate pressure distribution and hence on the magnitude and distribution of effective stresses and therefore on shear strength. The heterogeneity nature of MSW varying point to point the waste permeability but field and laboratory studies provided some important considerations.
Waste structure, the use of low permeability daily cover layers and stress levels play the major role to determine hydraulic waste conductivity (Dixon et al., 2004). A study conducted by Powrie and Beaven (1999) found that the permeability of non-degraded MSW could diminish by over three orders of magnitude to approximately 10^{-8} m/s between placement and burial to a depth of 60 m due to compression.

5.2.3 Waste properties for Este's landfill

MSW properties for Este's landfill are been selected considering the different landfill sectors analyzed. "Lotto 1" (studied with section 4-4) is the old landfill of Este that was active since the 60s until the 1995 when a separate collection system was completely absent. Due to the impossibility to establish waste values directly for this old site, literature data ([15], [28]) are been implemented, considering top and bottom waste data obtained from old MSW landfills (Tab. 5.3).

Table 5.3. Waste properties for "Lotto 1".

MATERIAL	Dry unit weight (kN/m^3)	Saturated unit weight (kN/m^3)	Cohesion (kPa)	Internal friction angle (°)	Young's modulus (kN/m^2)	Poisson's ratio (-)
Top waste (5 m)	9.4	10.8	10.0	30.0	1000	0.25
Bottom waste	11.0	15.4	30.0	20.0	2500	0.45

These values seems reasonable: older and deeper waste present a high cohesion and a low friction angle due to the increased fineness of the waste thanks to degradation processes, while for more recently dumped waste a low cohesion and a high friction angle can be

considered for the characteristics of the waste similar to a granular material; the unit weight is higher for bottom waste due to advanced compression and degradation processes that provided to a voids reduction increasing the waste mass per unit volume (Omari, Boddula, 2010).

"Lotto 2" and "Lotto 3" were active since the end of the 90s until nowadays. For the sections that represented these sectors (2-2 and A-A), data estimated for the Ca' Rossa (VE) landfill (Tab. 5.4) have been used (even if there isn't a distinction between top and bottom waste properties); this landfill presents some similarities with the new part of S.E.S.A. landfill because it was active from the early 90s until 2009 and was designed for the dump of MSW coming from municipalities of the Venetian province.

Table 5.4. Waste properties for "Lotto 2" and "Lotto 3".

Dry unit weight (kN/m^3)	Saturated unit weight (kN/m^3)	Cohesion (kPa)	Internal friction angle (°)	Young's modulus (kN/m^2)	Poisson's ratio (-)
9.0	10.0	20.0	22.0	300	0.33

In order to take into account the variability of the input data, also for each of the waste input parameters a normal distribution function has been considered.

5.2.4 Pore water pressure

From the data of Este's geological data, the shallow groundwater table is located inside a discontinuous sandy layer (4-5 m from the ground surface), while the second is placed inside the deeper sandy layer (starting from about 14 m depth) and is not considered in the calculation because has no influence on the analysis.

The entire landfill site, except for a part of the old landfill, is delimitated by a bentonite barrier system installed until 7 m depth inside the second clay layer in order to avoid possible contamination to the groundwater aquifers, but due to precautionary reasons its influence has not been considered in the analysis.

5.2.5 Reinforcement of soil – structure interaction

Section 4-4 doesn't present any type of geosynthetic material: "Lotto 1" represents the landfill active from the 60s until 1995 and any type of particular cover was provided. The

other two sections presents a geotextile and a 2 mm HDPE geomembrane as parts of the bottom barrier system.

In order to consider the geosynthetics contribution, the SLOPE/W program considers some reinforcement parameters. The first is the factored pullout resistance (*FPR*) per unit length of geosynthetic (kN/m/m) that is intended as the applied bond resistance of the fabric to the soil. Considering a factor of safety (*FS*) dependency, this factor is calculated as:

$$FPR = \frac{PR}{RRF(FS)} = \frac{(S_{IA} + \sigma_v' \tan\delta)SAF}{RRF(FS)}$$

where:

- *PR* = calculated pullout resistance (kPa), the skin friction of the reinforcement bond;
- S_{IA} = interface adhesion (kPa), the cohesion at the contact point between material and geosynthetic;
- σ'_v = the effective overburden stress (kPa), directly calculated by the program according to the position of the geosynthetic;
- δ = interface shear angle (°), the contact angle between material and geosynthetic;
- *SAF* = surface area factor (interface factor, between 0 and 2), used at the contact point between the fabric and the soil;
- *RRF* = resistance reduction factor (-) to account for nonlinear distribution stress reduction over the embedded length.

The second reinforcement parameter is the factored tensile capacity (*FTC*), i.e. the maximum pullout force that has not to be exceed. It's defined as:

$$FTC = \frac{TC}{RF(FS)}$$

where:

- TC = tensile capacity (kN), the maximum capacity that the reinforcement can bear without breaking;
- RF = reduction factor (-) to take into account installation damage, creep and durability.

Parameters considered for 2 mm HDPE geomembrane:

S_{IA} = 0 kPa (cautionary value), δ = 25°, SAF = 1, RRF = 1.5, TC = 249 N, RF = 1.

Parameters considered for the non woven PP geotextile:
S_{IA} = 0 kPa, δ = 30°, SAF = 1, RRF = 1.5, TC = 725 N, RF = 1.

5.2.6 Imposed loading

The loading imposed to the system is the seismic contribution, inputting the two seismic coefficients previously found (Paragraph 3.4): $K_H = 0.002$ and $K_V = 0.001$.

6. Calculation procedure using LEM software: SLOPE/W

6.1 Introduction

SLOPE/W is a component of a complete suite of geotechnical products named GeoStudio and it has been designed and developed to be a general software tool for the stability analysis of earth structures. This software, as the FEM program PLAXIS, implements a two-dimensional analysis: this hypothesis is considered as appropriate for slope design and yields a conservative estimate for the factor of safety because the end effects (resisting forces along the lateral sides of the sliding mass) are not included (Duncan, 1996; Stark and Eid, 1998).
The geotechnical problem can be solved after an input procedure that involves the following five components:

- analysis definition: basic and geometric assumptions to define the problem;
- soil properties: parameters used to describe the soil materials;
- pore-water pressure: definition of the pore water pressure condition;
- reinforcement of soil - structure interaction: nails, anchor, geosynthetic and others;
- imposed loading: surcharges or dynamic earthquake loads.

Characteristics such as soil properties, pore-water pressure conditions, reinforcement of geosynthetic and seismic loadings are already been discussed in the previous paragraph.
Regarding the analysis definition, the Morgenstern-Price method (i.e. one of the approaches that satisfies both moment and force equilibrium) and half-sine function method are been selected for the analysis.
The direction of the slip surface was chosen to follow a right-left path for all of the sections. The methods for the selection of the slip surfaces are decided according to the focus of the study (evaluation of the stability of the top cover system along the steepest slopes and evaluation of the stability of the entire landfill section).

The slip surface has been considered to have 30 slices, each with a minimum depth of 0.1 m and a minimum slice width of 0.1 m.
One of the basic assumptions which has to be made to solve the problem (i.e. to find the minimum factor of safety for the critical failure surface) is the definition of the method to find the failure surfaces.

6.2 Slip surface shapes

One of the key argument in a slope stability analysis is the determination of the position of the critical slip surface with the lowest factor of safety. This procedure is done with a trial operation, creating possible slip surfaces and computing the associated FOS. Once that the procedure is complete, the trial slip surface with the lowest safety factor is considered as the critical slip surface.
There are many different methods to define the shape and positions of trial slip surfaces; in this chapter the two most used methods are presented, considering examples provided by SLOPE/W tutorial manual.

6.2.1 Grid and radius method

The trial slip surface is an arc of circle that is a portion of a circle that cuts through the slope; the circle can be defined specifying the centre and the radius. Many slip surfaces can be specified defining a grid of circle centers and a range of defined radii.
An example taken from the SLOPE/W tutorial manual is shown is Fig. 6.1.

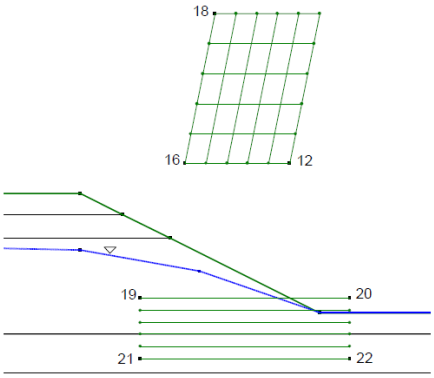

Fig. 6.1 – Grid and radius method

The grid above the slope represents a grid of rotation centers and each point of the grid is a circle center for the trial slips. This example has 36 grid points.

The trial circle radii are specified with radius or tangent lines, and in case of lines these are defined by four corners of a box, specifying also the number of increments between the upper and lower corners (in the above example, there are five increments in the box for a total number of radius lines equal to six).

Once that the grid and the box are defined, the program starts the calculation finding the trial slip surfaces formed by circles (Fig. 6.2), generated from the grid points (i.e. rotation centers), that are tangent to the lines of the box (that define the radii of the circles).

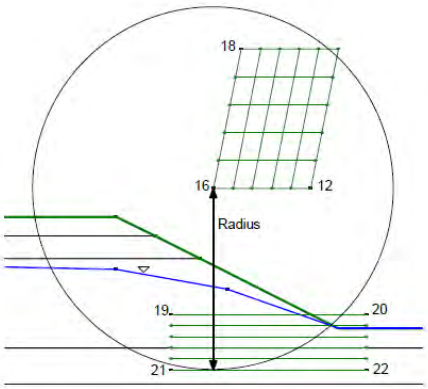

Fig. 6.2 – Example of trial slip surface

The trial slip surface is located where the circle cuts the soil section. In the example the program will compute FOS for 216 (36 centers of rotation multiplied by the six tangent lines) trial slip surfaces. The box of the tangent lines can be located at any convenient position forming any quadrilateral shape (Fig. 6.3).

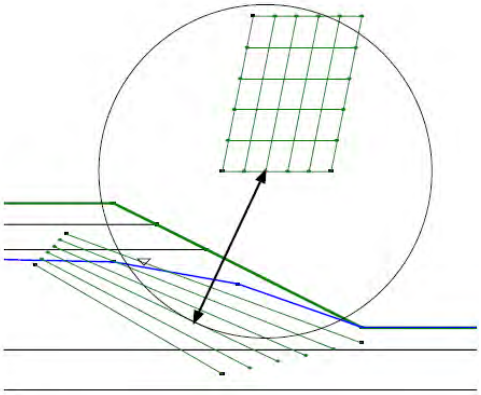

Fig. 6.3 – Specification of radius lines

There are also other possibilities to find trial slip surfaces using grid and radius method, as one that provide the radius line box collapsing to a point or to a single line, a possibility useful for the case to evaluate possible failure surfaces passing through the toe of the slope.

6.2.2 Entry and exit method

One of the problem relating to the previous method is the difficulty to visualize the extents and/or range of trial slip surfaces; this limitation can be solved by specifying the location where the trial slip surfaces will enter the ground surface and where they will exit. The entry and exit method is a variation of the grid and radius method.
Fig. 6.4 presents two red lines along the ground surface and represent the entry and the exit of the trial slip surfaces. The number of entries and exits can be defined as the number of increments along these two lines.

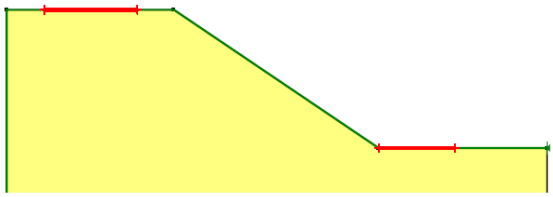

Fig. 6.4 – Entry and exit lines for trial slip surfaces

In order to form the various trial slip surfaces, the software connects a point along the entry line (A, in Fig. 6.5) with a point of the exit line A'. At the mid-point of line AA', a perpendicular line is created by the program and radius points A", B", C" along the perpendicular line are created to form the required third point of a circle with center G. This radius point together with the entry and exit points are used to form the equation of a circle and then the procedure is repeated finding different slip surfaces. In Figure 6.6 the critical slip surface is the darker shaded area.
Finally, SLOPE/W controls also that some physical impossibilities are not taken into account.

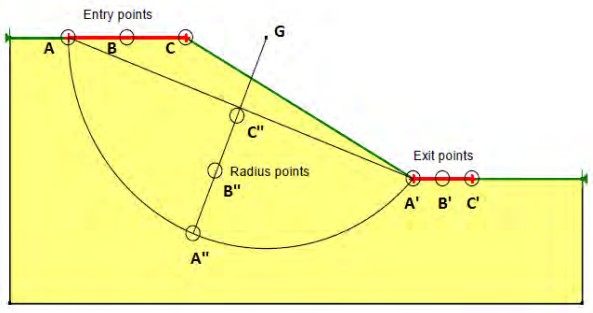

Fig. 6.5 – Scheme of the entry and exit method

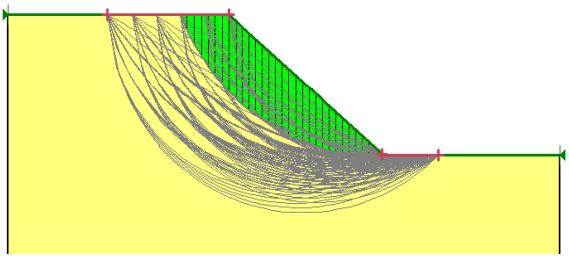

Fig. 6.6 – Critical slip surfaces

6.3 Analysis of section 4-4

The section can be directly imported from the AUTOCAD program to the SLOPE/W software and the different steps for the analysis can be initialized (Fig. 6.7).

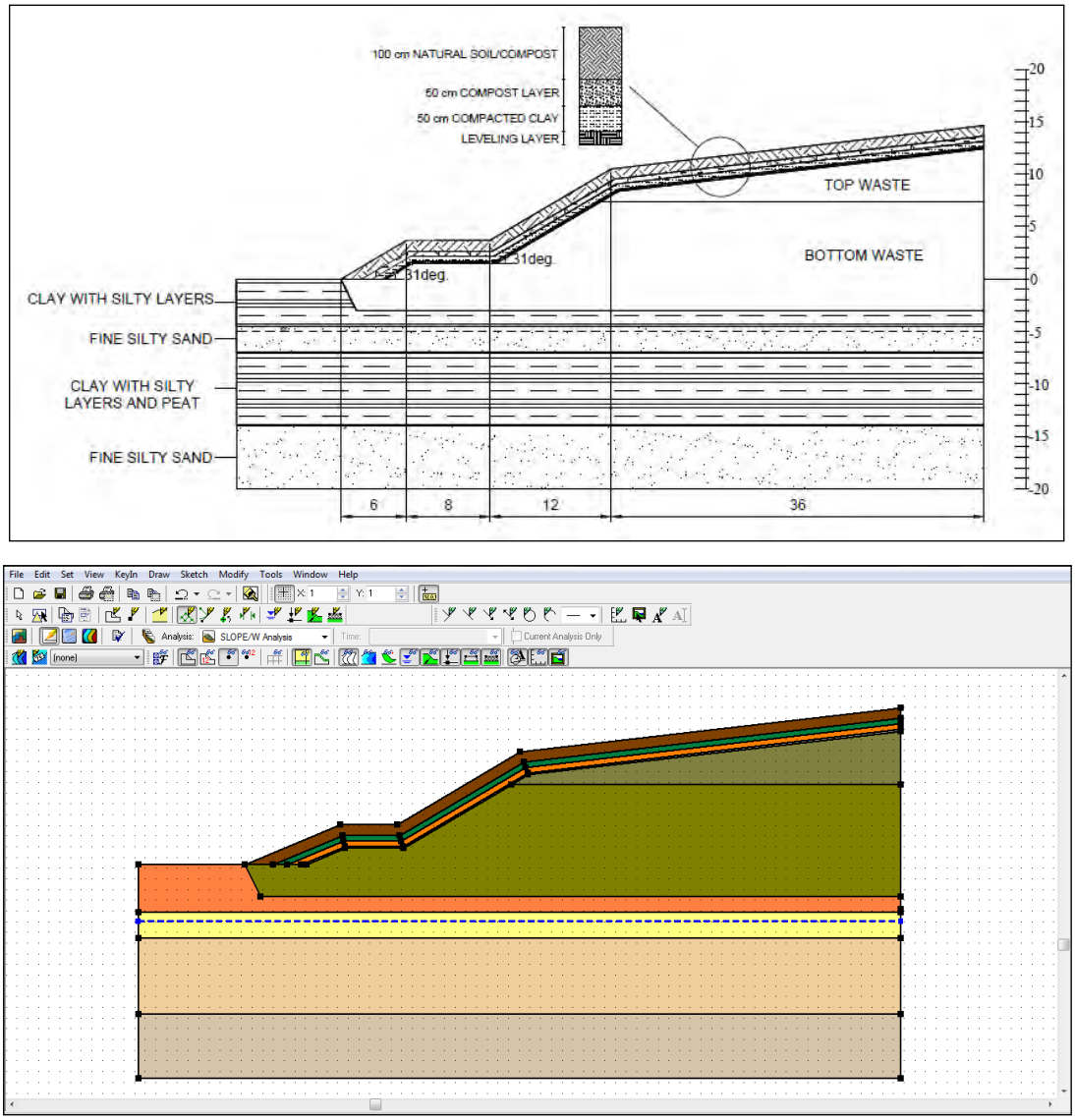

Fig. 6.7 – Section 4-4 imported into SLOPE/W software

6.3.1 Stability Analysis of the top cover system along the steepest slopes

This section presents three different inclinations: one has an horizontal length of 36 m and is almost linear, while the other two (12 and 8 m of horizontal length respectively) have an inclination of 31 degrees. The assessment of the stability of the top cover system has been done for these two parts of the section, with the hypothesis that focus the research of the minimum FOS involving the movement of all the different layers (natural soil, compost, clay and leveling layer). The research of the critical slip surface that meets this requirement has been done applying the grid and radius method, inserting the "radius line box" inside the

top cover system (Fig. 6.8): the grid has 36 centers of rotation with six tangent lines, with the possibility to obtain 216 factors of safety.

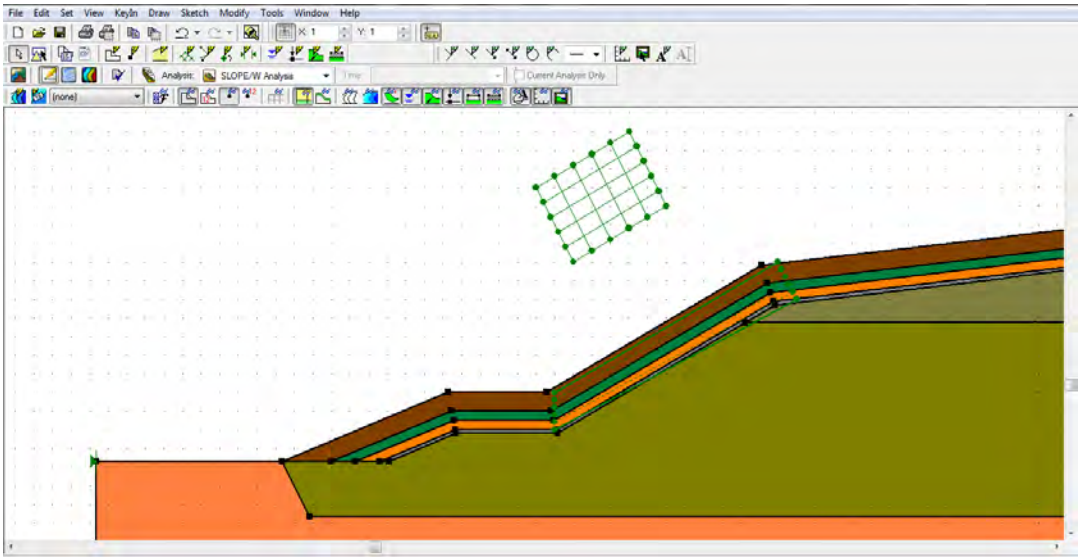

Fig. 6.8 – Application of the grid and radius method to find the critical slip surface for the first slope of section 4-4

The minimum calculated factor of safety, that is the only one of the entire study minor than 1.0 (FOS = 0.99) involves a movement only for soil and compost layers (Fig. 6.9a), while a higher safety factor (FOS = 2.00) regards the instability of the first slope considering the entire top barrier system (Fig. 6.9b).

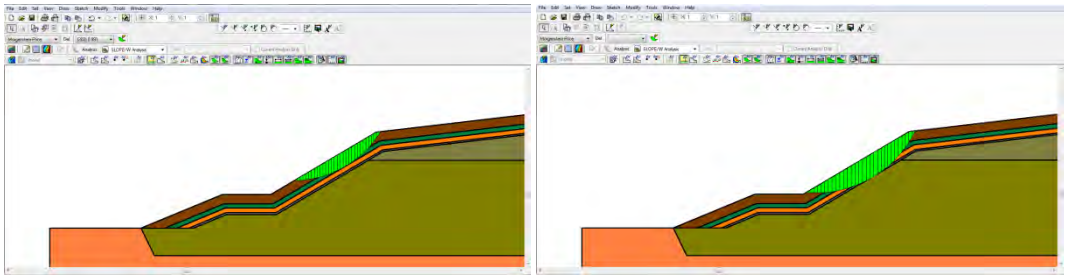

Fig. 6.9 a,b – Critical slip surfaces that involves the top barrier system for the first slope of section 4-4

The analysis on the second steepest slope of the 4-4 section (the nearest one to the ground surface) has been done with the same hypothesis of the previous slope, implementing a grid and radius method for searching the critical failure surface and inserting the radius box inside the cover system (Fig. 6.10). Similarly to the previous slope, the minimum critical

slip surface involves a movement only for the soil and compost layers (FOS = 1.48, Fig. 6.11a), while the most critical surface that involves a displacement for all the top cover layers (Fig. 6.11b) present a FOS = 3.25, indicating a very good stability for the entire barrier system in this part of the landfill.

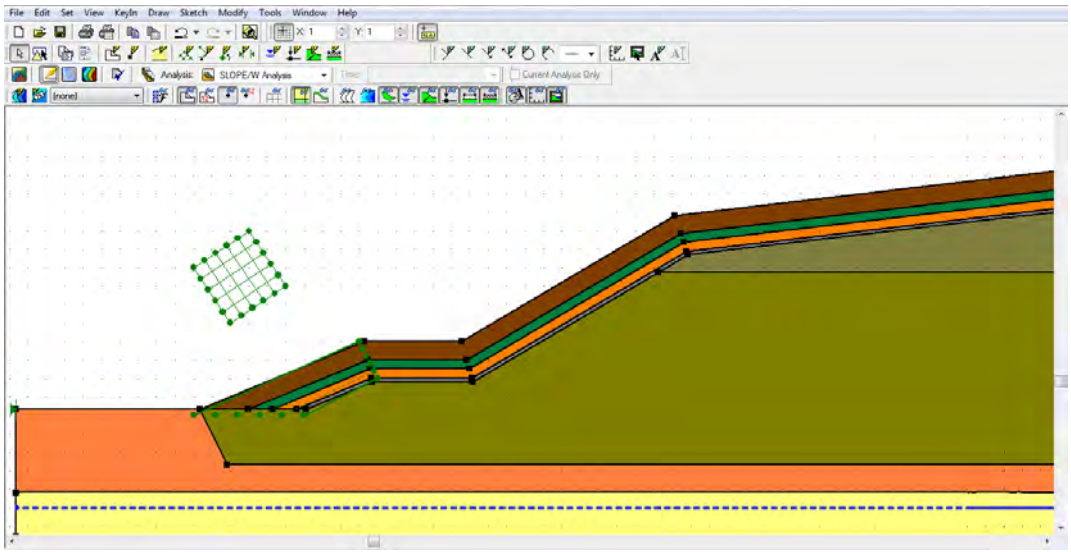

Fig. 6.10 - Application of the grid and radius method to find the critical slip surface for the second slope of section 4-4

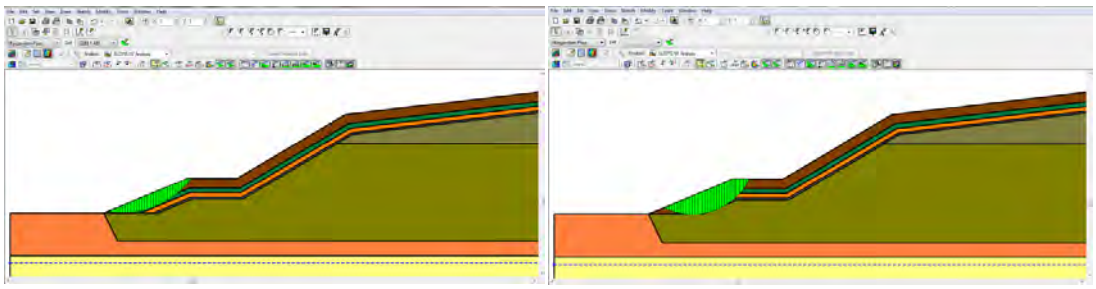

Fig. 6.11 a,b - Critical slip surfaces that involves the top barrier system for the second slope of section 4-4

6.3.2 Stability Analysis of the entire landfill section

The stability of the entire landfill body is firstly evaluated finding the critical slip surface with the Entry and Exit method in order to find the surface passing across the toe of the entire slope (Fig. 6.12).

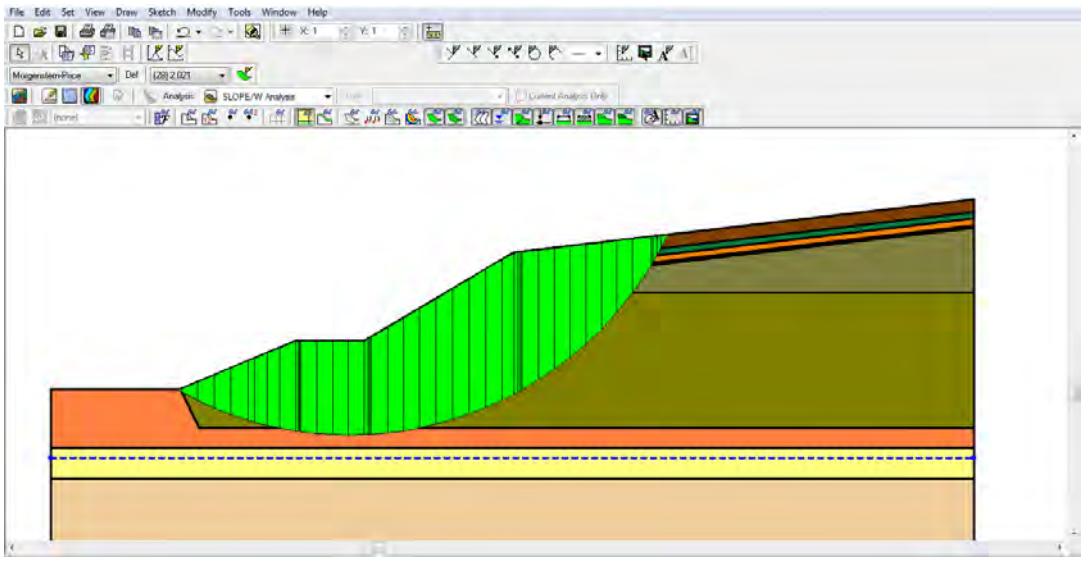

Fig. 6.12 – Slope stability analysis of the entire section 4-4 (failure surface passing through the toe)

The slope results to be very stable: FOS = 2.02, showing a critical failure surface passing through the toe of the slope passing also through the landfill bottom (that doesn't present any type of barrier for this old landfill part).

It has been evaluated also the stability where the critical slip surface could pass through the ground surface (Fig. 6.13); this part of soil will be interested by the future designed landfill enlargement ("Lotto Ovest", Fig. 5.1). The FOS = 1.88 indicates a good stability also for this case.

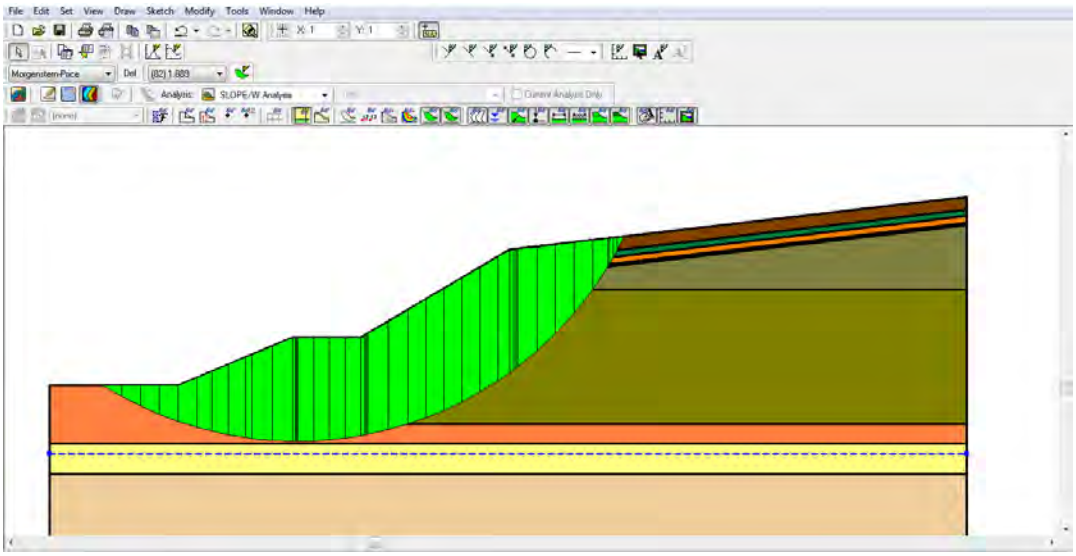

Fig. 6.13 - Slope stability analysis of the entire section 4-4 (failure surface passing through the base)

Another possible critical failure surface could be the one passing through the bottom of the landfill body; this possible failure case has been considered with the application of the grid and radius method, applying the radius box inside the location of the landfill bottom (about 3 m depth. The calculation (Fig. 6.14) gives results indicating a very high stability also for this case: FOS = 2.24 for Morgenstern-Price method.

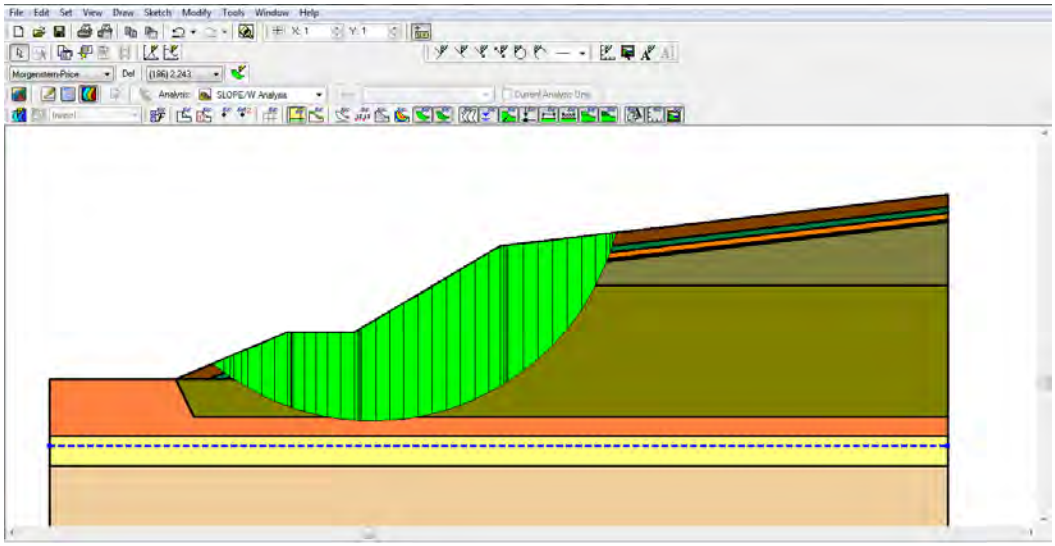

Fig. 6.14 – Slope stability analysis of the entire section 4-4 (failure surface passing through landfill bottom)

6.3.3 Stability Analysis of the entire landfill section varying waste parameters

All the calculated FOS for the stability of the entire landfill body present very safety conditions, but as previously discussed the waste parameters are very variables and obtained from literature data; for these reasons, a study has been conducted in order to establish how the FOS can vary using different waste characteristics to find which might be the worst situations.

It has been calculated the safety factor using Morgenstern-Price method, analyzing nine possible combinations for different waste input parameters: as suggested by some studies ([9], [42]) a value of about 10.0 kN/m^3 as unit weight can be normally accepted for all of the waste strata, and as suggested by a study conducted on MSW Italian landfills (Grisolia et al., 1995), shear strength parameters are been varied between 0 and 10 kPa for the cohesion and 20 and 30 degrees for the internal friction angle (these trial and precautionary parameters are considered as already reduced by the corrective factor of NTC). The study has been conducted for failure surfaces passing both at the toe of slope and on the base of ground

surface, and for slip surfaces passing through the landfill bottom, always considering a Monte Carlo scheme with 2000 trials and a normal probability density functions for the input parameters. Results are listed in Tables 6.1.

Table 6.1. Stability analysis for section 4-4 varying waste characteristics.

	Unit weight (kN/m^3)	**Cohesion (kPa)**	**Internal friction angle (°)**	**FOS for circular failure surface passing…**		
				at the slope toe	**through the base**	**through the landfill bottom**
Type 1	10	0	20	1.14	1.16	1.71
Type 2	10	0	25	1.43	1.45	2.14
Type 3	10	0	30	1.76	1.77	2.51
Type 4	10	5	20	1.49	1.49	1.97
Type 5	10	5	25	1.79	1.79	2.35
Type 6	10	5	30	2.11	2.10	2.72
Type 7	10	10	20	1.80	1.79	2.22
Type 8	10	10	25	2.11	2.05	2.56
Type 9	10	10	30	2.45	2.24	2.93

The worst cases are, as expected, those related to the lower shear strength values; however, the stability is respected also in these cases. In Chapter 8 a sensitivity analysis on the parameters and considerations on the calculated factors of safety are presented.

6.4 Analysis of section 2-2

As for section 4-4, the section is directly imported from the AUTOCAD program to the SLOPE/W software and the different steps for the analysis can be initialized (Fig. 6.15).

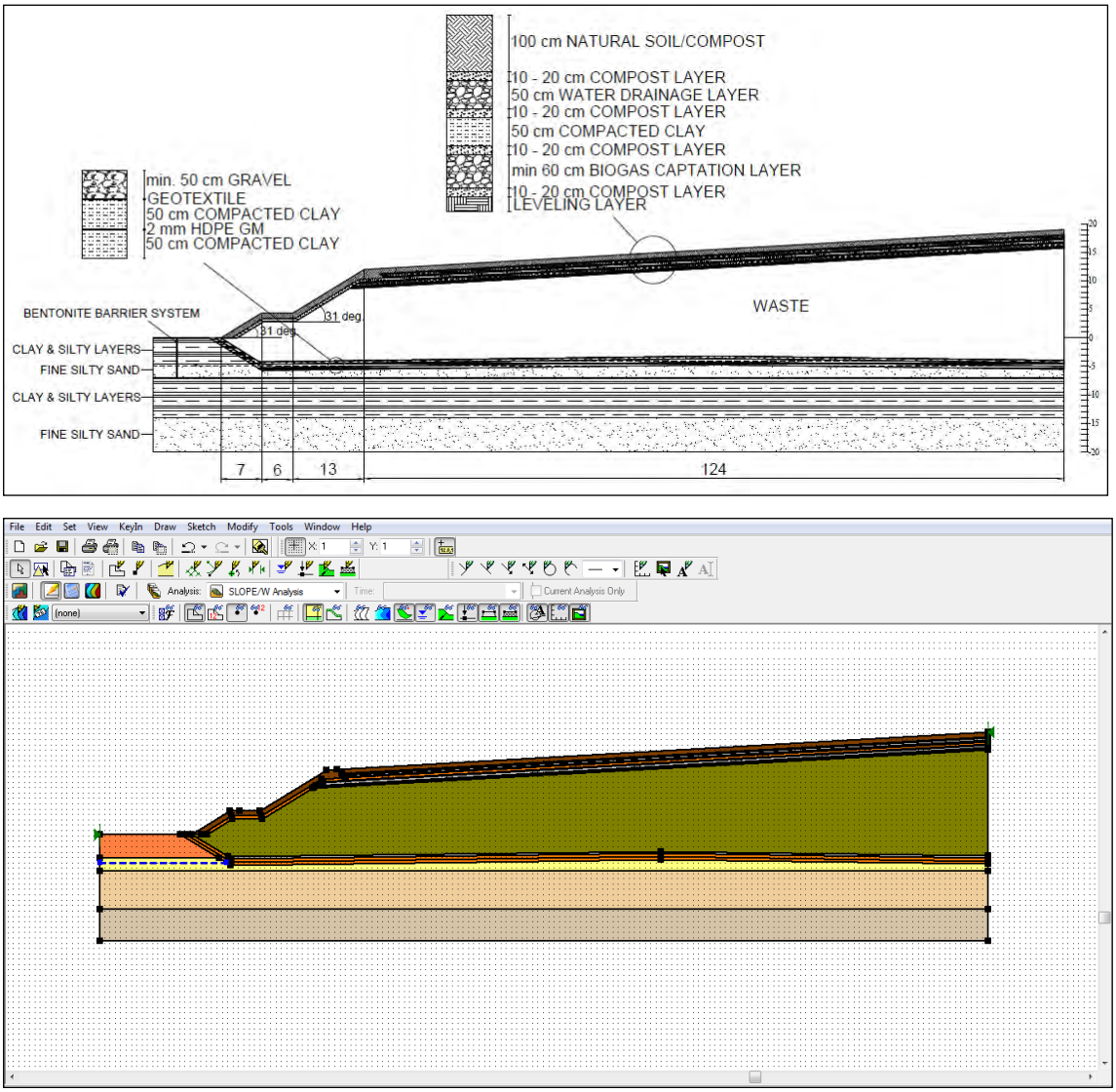

Fig. 6.15 – Section 2-2 imported into SLOPE/W software

6.4.1 Stability Analysis of the top cover system along the steepest slopes

As section 4-4, also this section presents three different inclinations: one very long (124 m) and practically linear, while the other two have an inclination of 31 degrees. The assessment of the stability of the top cover system has been done for these two parts of the section, assuming that the focus of the study is the research of the minimum FOS involving the movement of all the different layers (natural soil, compost, gravel, clay and leveling layers). The research of the critical slip surface that meets this requirement has been done applying the grid and radius method, inserting the "radius line box" inside the top cover barrier system. The minimum calculated safety factor (FOS = 2.64) regards the movement only for

a small part of soil, while the lower FOS regarding the movement of the entire top cover barrier of the first slope (Fig. 6.16) is equal to 3.29, indicating a very good stability for this part of top cover.

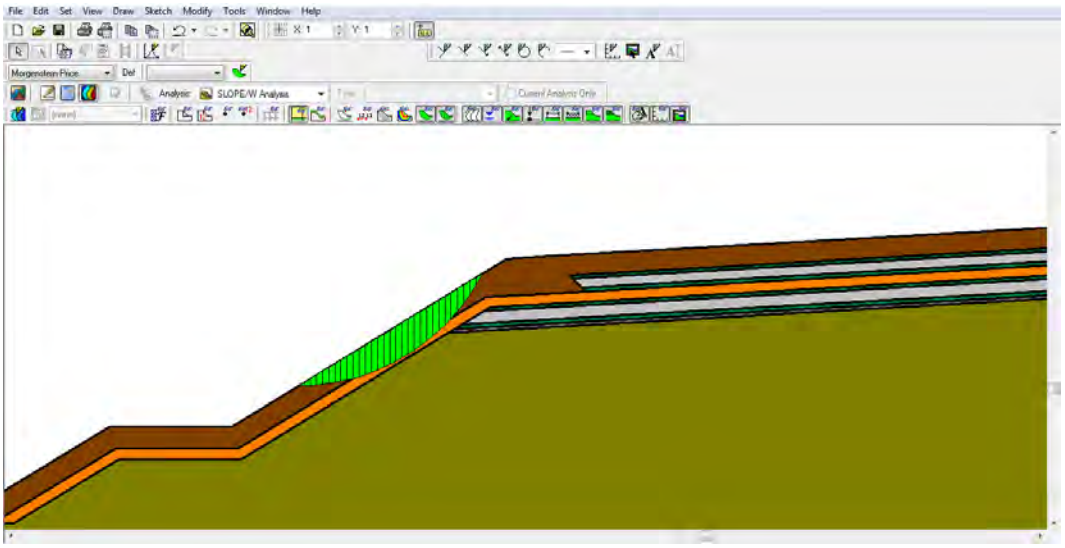

Fig. 6.16 - Critical slip surface that involves the entire barrier system for the first slope of section 2-2

The second steepest slope of section 2-2 (the nearest one to the ground surface) has been analyzed considering the same hypothesis of the previous slope, implementing a grid and radius method for searching the critical failure surface and inserting the radius box inside the cover system. The most critical slip surface that involves all layers is shown in Fig. 6.17.

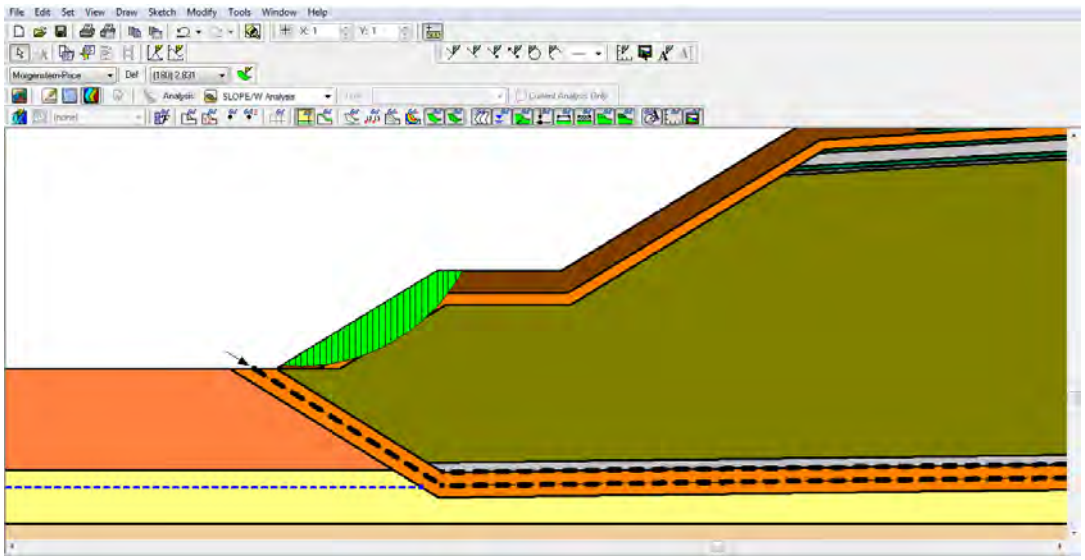

Fig. 6.17 - Critical slip surface that involves the entire barrier system for the second slope of section 2-2

The result for the M-P method indicates that the slope is very stable (FOS = 2.83) also for the slope near the base of the 2-2 section; moreover, this value is also the minimum calculated safety factor and involves all the top cover layers.

6.4.2 Stability Analysis of the entire landfill section

The entire landfill body stability is evaluated finding the critical slip surface with the Entry and Exit method in order to find the surface passing across the toe of the entire slope (Fig. 6.18). The calculated safety factor is equal to 1.75. As for section 4-4, it has been studied also the stability for cases where the critical slip surface could pass through the ground surface (Fig. 6.19). For this case, FOS = 1.81.

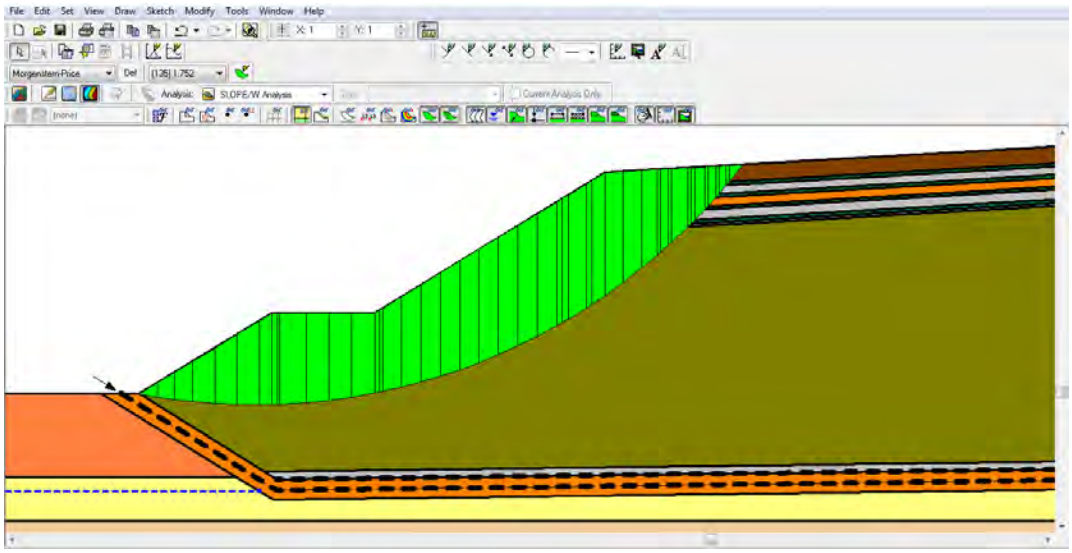

Fig. 6.18 – Slope stability analysis of the entire section 2-2 (failure surface passing through the toe)

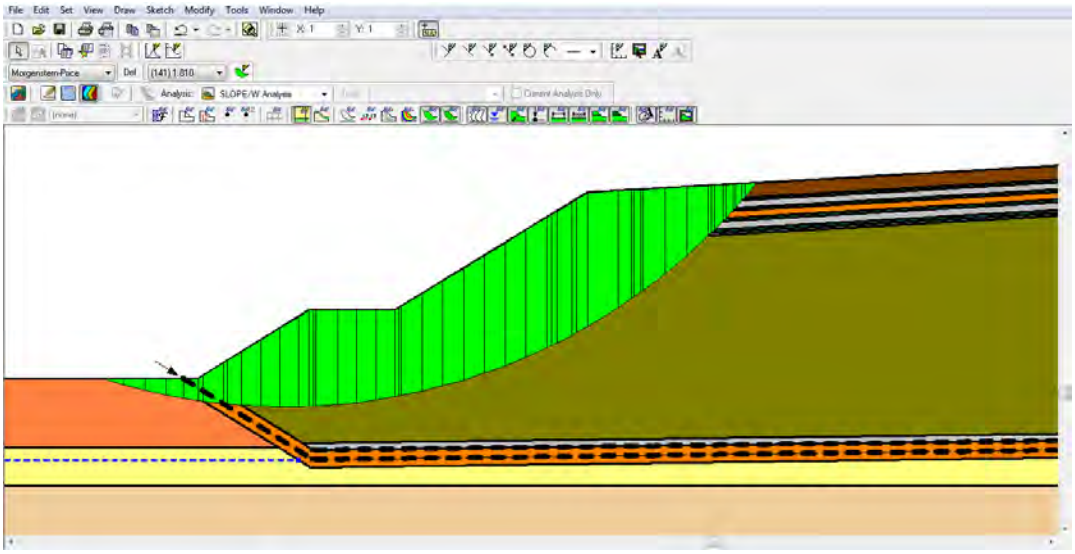

Fig. 6.19 - Slope stability analysis of the entire section 2-2 (failure surface passing through the base)

The grid and radius method has been applied in order to find the critical slip surface passing through the landfill bottom barrier, which is formed by a leachate drainage layer (min. 50 cm), geotextile, clay (50 cm), 2 mm HDPE geomembrane and 50 cm of clay (Fig. 6.20). The safety factor results equal to 3.05 indicating a very good stability, with a circular failure surface passing through the geosynthetics and bottom layers (leachate captation layer and clay) without involving the natural fine silty sand layer.

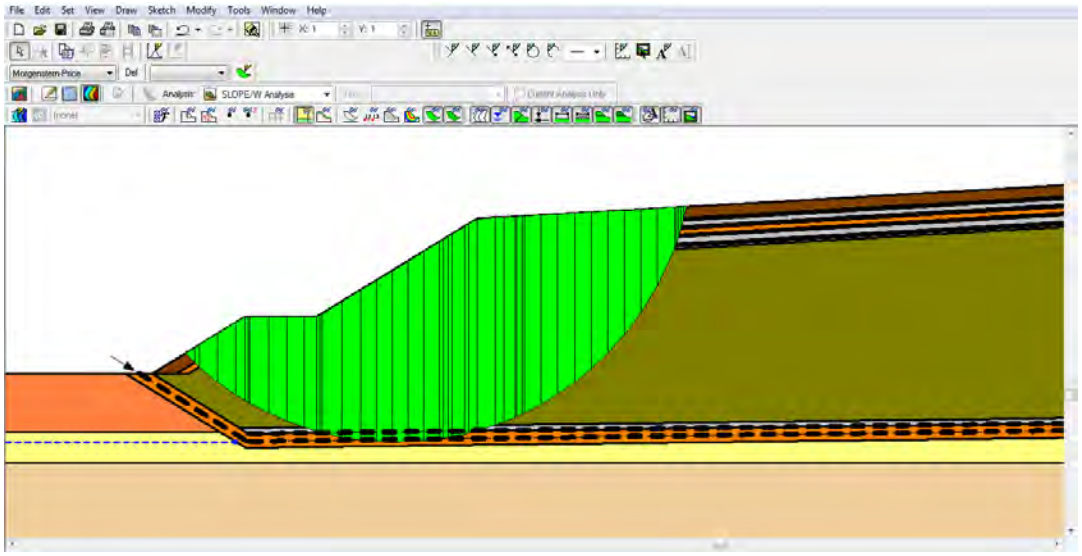

Fig. 6.20 – Slope stability analysis of the entire section 2-2 (failure surface passing through landfill bottom)

For this section has been evaluated also the sliding stability of bottom materials on the two geosynthetic liners (a geotextile is placed between the drainage layer and the shallow clay

layer, while a 2 mm HDPE geomembrane subdivides the two clay layers). The analysis is made with the grid and radius method, considering the material just below the geosynthetic as impenetrable; in this way the impenetrable layer causes the trial slip surface to follow the liner. The thin region just above the impenetrable material presents properties representative of the frictional sliding resistance between the cover material and the liner, i.e. the shear strength along that portion of the sliding surface that follows the material considered as impenetrable. The critical slip surface tangent (Fig. 6.21) to the geotextile liner presents a safety factor equal to 2.24, while for sliding surfaces tangent to the geomembrane (Fig. 6.22) the FOS results equal to 2.74.

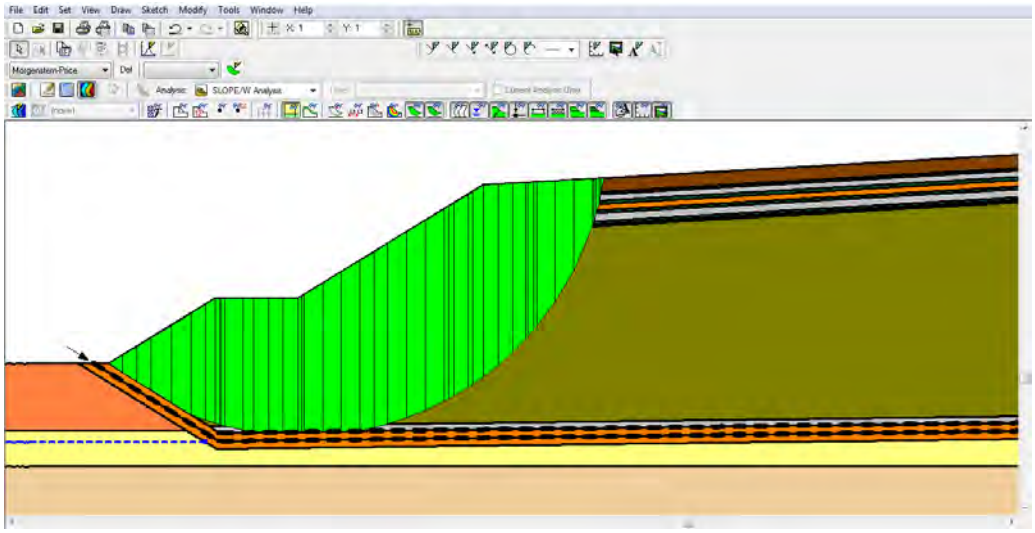

Fig. 6.21 – Sliding stability for failure surfaces tangent to the geotextile liner of section 2-2

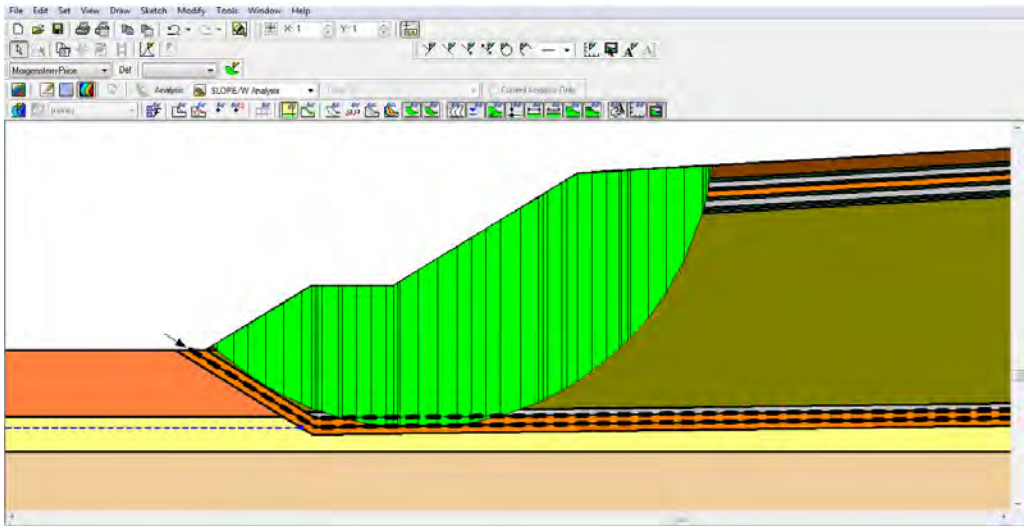

Fig. 6.22 – Sliding stability for failure surfaces tangent to the geomembrane liner of section 2-2

6.4.3 Stability Analysis of the entire landfill section varying waste parameters

As for the previous analyzed section, also the stability of section 2-2 has been studied considering different waste input parameters (Tab. 5.2) due to the high uncertainty of these waste values.

The study has been done considering the first three analyzed possible failure mechanisms (Tab. 6.2), while possible effects of the change of waste input parameters on the geosynthetic liners are discussed in Chapter 8.

Table 6.2. Stability analysis for section 2-2 varying waste characteristics.

	Unit weight (kN/m^3)	**Cohesion (kPa)**	**Internal friction angle (°)**	**FOS for circular failure surface passing…**		
				at the slope toe	**through the base**	**through the landfill bottom**
Type 1	10	0	20	1.02	1.24	1.95
Type 2	10	0	25	1.28	1.48	2.33
Type 3	10	0	30	1.56	1.74	2.74
Type 4	10	5	20	1.31	1.46	2.13
Type 5	10	5	25	1.57	1.72	2.51
Type 6	10	5	30	1.85	1.99	2.92
Type 7	10	10	20	1.56	1.67	2.31
Type 8	10	10	25	1.84	1.93	2.69
Type 9	10	10	30	2.14	2.21	3.09

6.5 Analysis of section A-A

The section is firstly drawn with AUTOCAD program and then imported into SLOPE/W software (Fig. 6.23), considering the three subsectors of "Lotto 3".

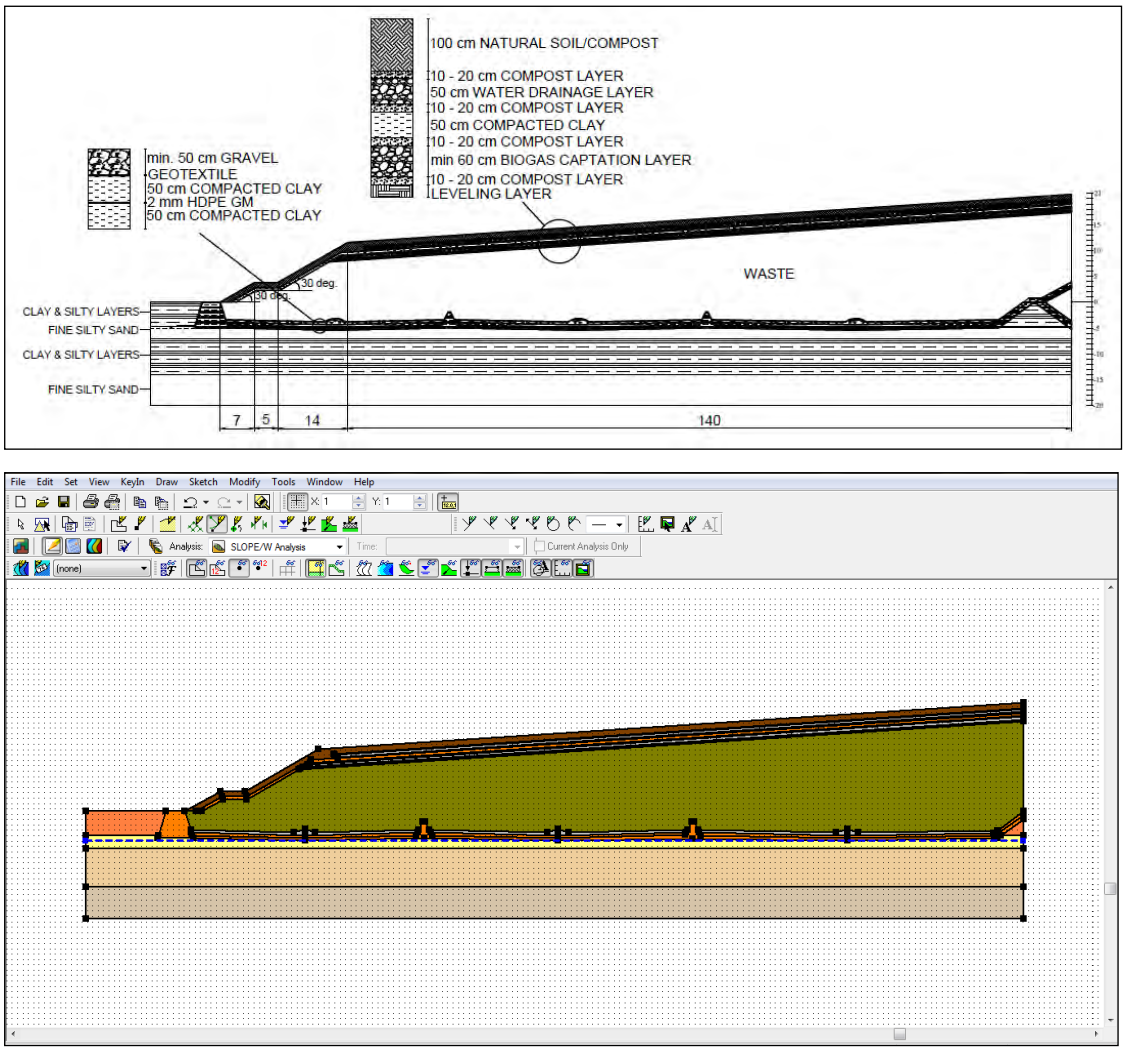

Fig. 6.23 – Section A-A imported into SLOPE/W software

6.5.1 Stability Analysis of the top cover system along the steepest slopes

The slope profile is similar to the other two sections, presenting a long slope almost linear and two other slopes more inclined (30 degrees instead of 31 degrees of the other sections studied). The top barrier system is the same of section 2-2 and the hypotheses to evaluate the two steepest slopes of the profile are the same of the two previous sections.

The FOS of the first slope for the entire top barrier system that involves a large part of soil and clay (Fig. 6.24) is equal to 3.35, indicating a very good stability for this part of top cover. The second steepest slope of the section has a factor of safety equal to 2.97, evidencing a high stability also for this part of the slope profile. The most critical slip surface that involves all layers is shown in Figure 6.25.

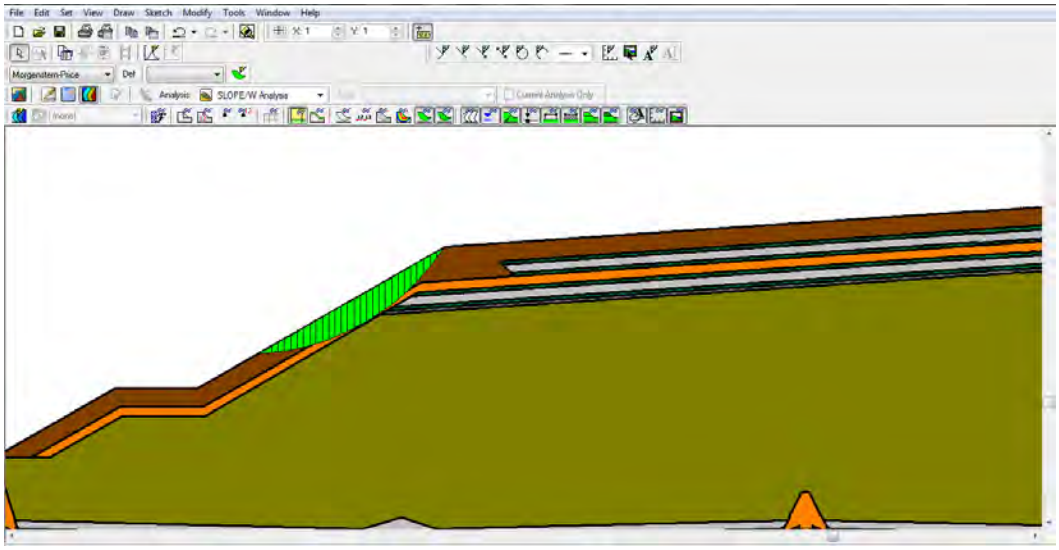

Fig. 6.24 - Critical slip surface that involves the entire barrier system for the first slope of section A-A

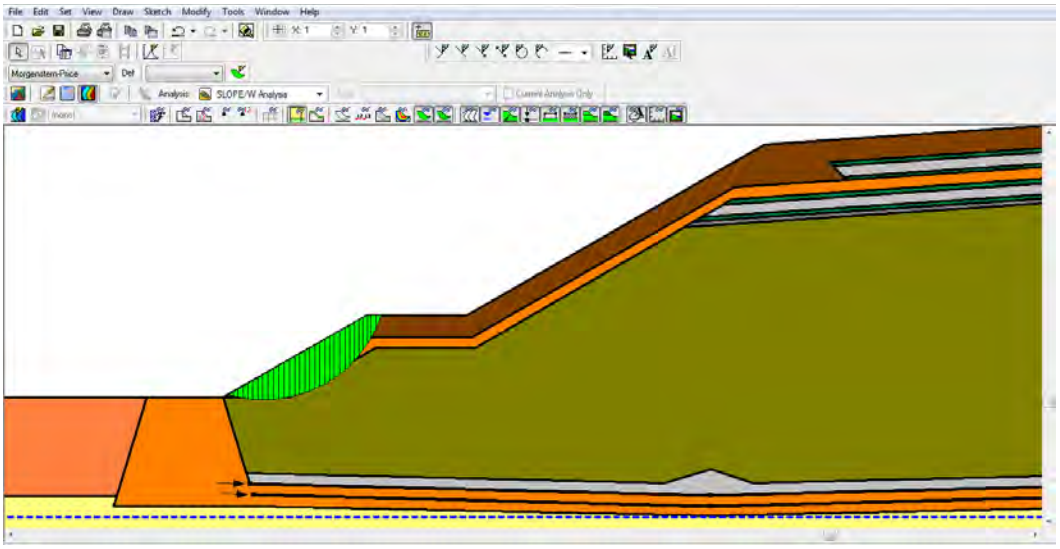

Fig. 6.25 - Critical slip surface that involves the entire barrier system for the first slope of section A-A

6.5.2 Stability Analysis of the entire landfill section

As for the other two sections, the entire landfill body stability has been studied finding the critical slip surface with the Entry and Exit method in order to find the safety factor associated to the critical surface passing across the toe of the entire slope (FOS = 1.75, Fig. 6.26) and through the ground surface, where a clay berm is present to separate this sector from the future designed sector named "Lotto Ovest" (FOS = 1.81, Fig. 6.27). To evaluate the stability for a critical failure surface passing through the landfill bottom (Fig. 6.28), the grid and radius methodology has been applied as for the other two cases, finding a safety

factor equal to 2.54 and a circular failure surface that involves the damage of the fabric liners and a possible groundwater contamination. For all of these possible failure mechanisms the safety is well respected.

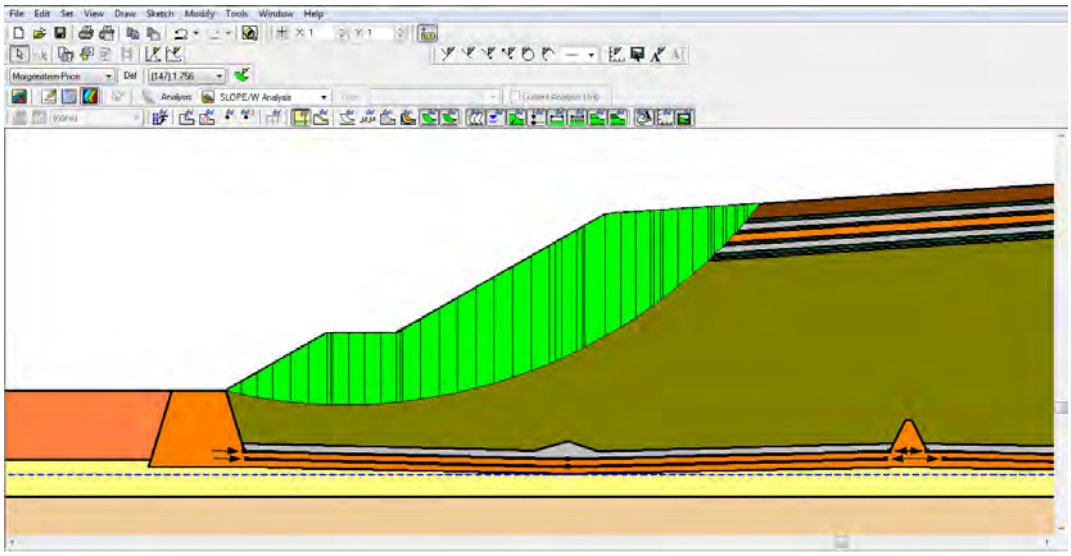

Fig. 6.26 – Slope stability analysis of the entire section A-A (failure surface passing through the toe)

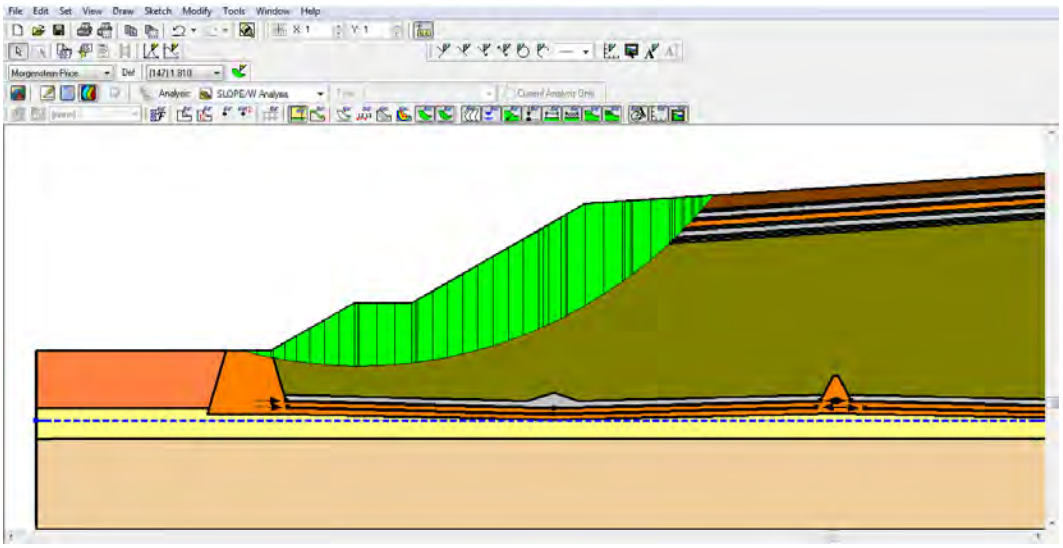

Fig. 6.27 – Slope stability analysis of the entire section A-A (failure surface passing through the base)

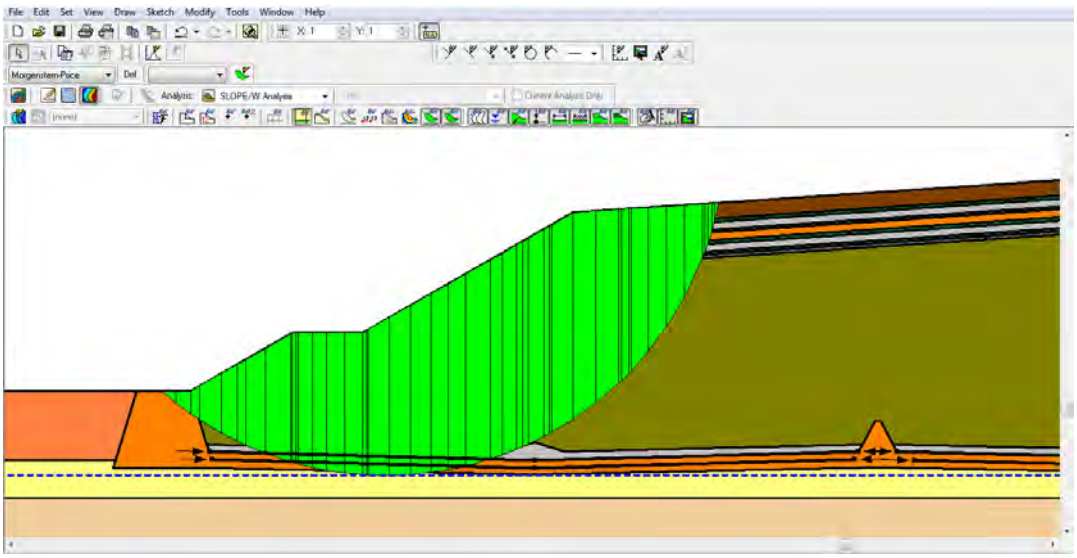

Fig. 6.28 – Slope stability analysis of the entire section A-A (failure surface passing through the bottom)

Similarly to section 2-2, also for this case has been evaluated the stability for possible sliding surfaces along the two geosynthetic liners (geotextile and HDPE geomembrane).
The lower FOS involving a movement of a circular failure surface tangent to geotextile (Fig. 6.29) is equal to 2.12, while in the case of sliding along the geomembrane (Fig. 6.30) the FOS results equal to 2.45, with a sliding mass causing a damage to the upper geotextile.

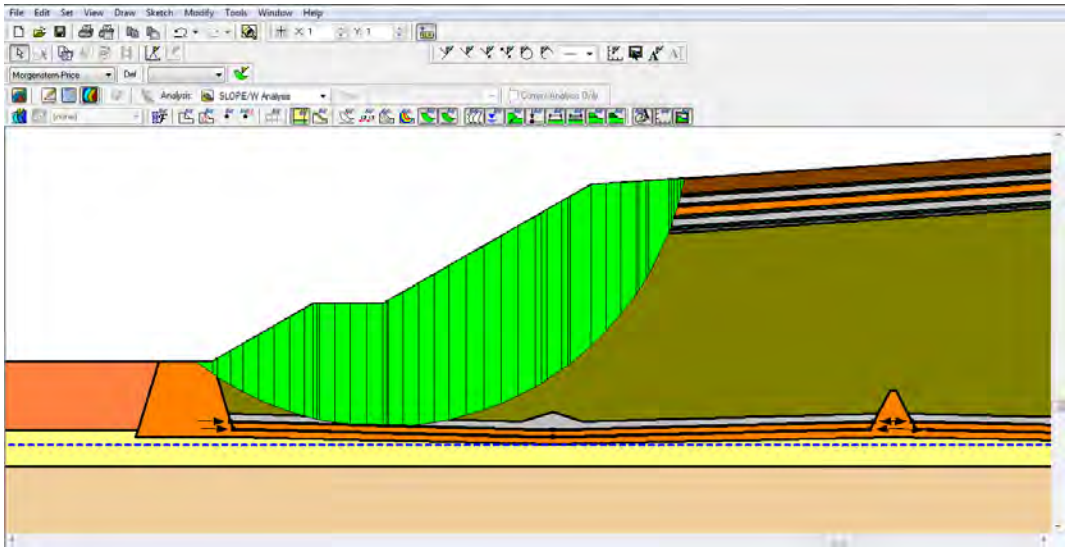

Fig. 6.29 – Sliding stability for failure surfaces tangent to the geotextile liner of section A-A

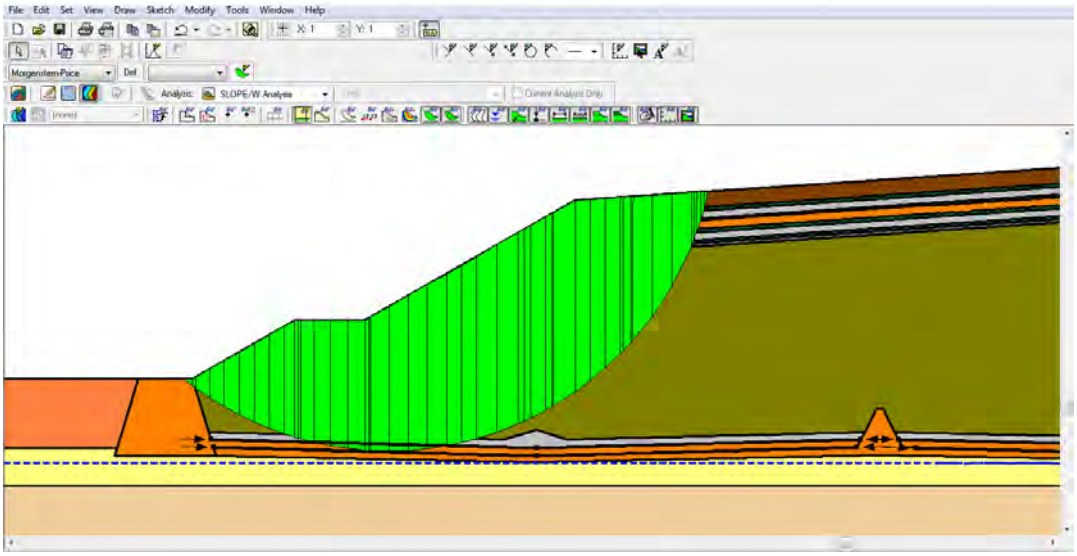

Fig. 6.30 – Sliding stability for failure surfaces tangent to the geomembrane liner of section A-A

6.5.3 Stability Analysis of the entire landfill section varying waste parameters

Results listed in Table 6.3 illustrates the FOS for the various failure mechanisms of section A-A varying the waste input parameters.

Table 6.3. Stability analysis for section A-A varying waste characteristics.

	Unit weight (kN/m^3)	**Cohesion (kPa)**	**Internal friction angle (°)**	**FOS for circular failure surface passing…**		
				at the slope toe	**through the base**	**through the landfill bottom**
Type 1	10	0	20	1.03	1.16	1.34
Type 2	10	0	25	1.28	1.42	1.71
Type 3	10	0	30	1.55	1.68	2.11
Type 4	10	5	20	1.31	1.41	1.57
Type 5	10	5	25	1.57	1.68	1.94
Type 6	10	5	30	1.86	1.95	2.33
Type 7	10	10	20	1.57	1.65	1.80
Type 8	10	10	25	1.84	1.92	2.16
Type 9	10	10	30	2.12	2.21	2.51

7. Calculation procedure using FEM software: PLAXIS

7.1 Introduction

The finite element analysis has been performed using PLAXIS 2D software, drawing the three sections of the landfill directly into the program. The analysis has been done considering initial material and waste characteristics and waste characteristics related to the worst cases among the different case studies examined with SLOPE/W software (i.e. lower FOS and higher probability of failure, with "Type 1" waste parameters).

For section 2-2 and A-A the top cover barrier has been considered as a single block having a density of 2000 Kg/m^3, as indicated by a previous study (Mandato et al., 2003) conducted on this part of S.E.S.A. landfill.

Regarding the general settings of the model, a 15 nodes per elements model with a plane strain type of model has been chosen, because the geometry of the landfill is more or less a uniform cross section with a corresponding stress state and loading scheme over a certain length perpendicular to the cross section, and seismic coefficients are been inserted to consider the earthquake effect. Standard fixities (full fixity at the base and roller condition at the vertical sides) are been chosen as boundary conditions. An elastic-plastic model (Mohr-Coulomb model) is selected to simulate the behavior of the materials and the input parameters are those listed in Table 5.1; due to the impossibility to import a probability density function into PLAXIS for these materials, some parameters are been modified in order to not consider too restrictive conditions.

After the definition of the model geometry and material parameters the entire section is divided into triangular elements in order to perform the finite element analysis; the entire composition of the finite elements is called mesh. For this calculation a very fine mesh has been chosen as definition of the global coarseness of the geometry.

Initial conditions provide initial pore water pressure (piezometric line at 5 m depth placed inside the fine silty sand layer) configuration, paying particular attention to the boundary conditions; all the analyzed sections must to have the right vertical boundary closed due to

the symmetry of the configurations which consider only an half of the section. Once that the pore water conditions are been defined, the initial geometry has been changed to consider the initial situations when the waste were not present.

Initial stresses are been defined by the K_0-procedure: this methodology determines the initial vertical stress σ_{v0}' and the initial horizontal stress σ_{h0}'. These values are related by the coefficient of lateral earth pressure K_0 (σ_{h0}' = K_0 σ_{v0}') that is defined as $K_0 = 1 - sen\varphi$ (Jaky's formula) where φ is the friction angle of each material.

The calculation is done inserting a simulation of the loading of waste and top cover barrier system into the entire landfill section, while the global safety factor has been computed by the phi-c reduction methodology. Discussions about the obtained results are reported in the next Chapter.

7.2 Phi-c reduction safety analysis

Phi-c reduction is the method used by PLAXIS to calculate a global factor of safety. The program defines the FOS as a ratio between the true shear strength and the computed minimum strength required for the equilibrium:

$$FOS = \frac{c - \sigma_n tan\varphi}{c_r - \sigma_n tan\varphi_r}$$

where c and φ are the input strength parameters and σ_n is the actual normal stress component, while parameters c_r and φ_r are reduced strength parameters that are just large enough to maintain equilibrium. This consideration is the basis of the Phi-c reduction method where the cohesion and the tangent of the friction angle are reduced in the same proportion:

$$\frac{c}{c_r} = \frac{tan\varphi}{tan\varphi_r} = \sum M_{sf}$$

The reduction of the shear strength parameters in controlled by the total multiplier $\sum M_{sf}$ which is increased in a step-by-step procedure (usually 100 steps are sufficient to arrive at a state of failure) until failure occurs; the factor of safety is defined as the value of $\sum M_{sf}$ at

failure, provided that at failure a more or less constant value is obtained for a number of successive load step procedures.

7.3 Analysis of section 4-4

The old landfill sector represented by section 4-4 is directly drawing into the PLAXIS program (Fig. 7.1) with the general settings and conditions discussed in paragraph 7.1 and waste properties of Table 5.3. The generated mesh is shown in Fig. 7.2.

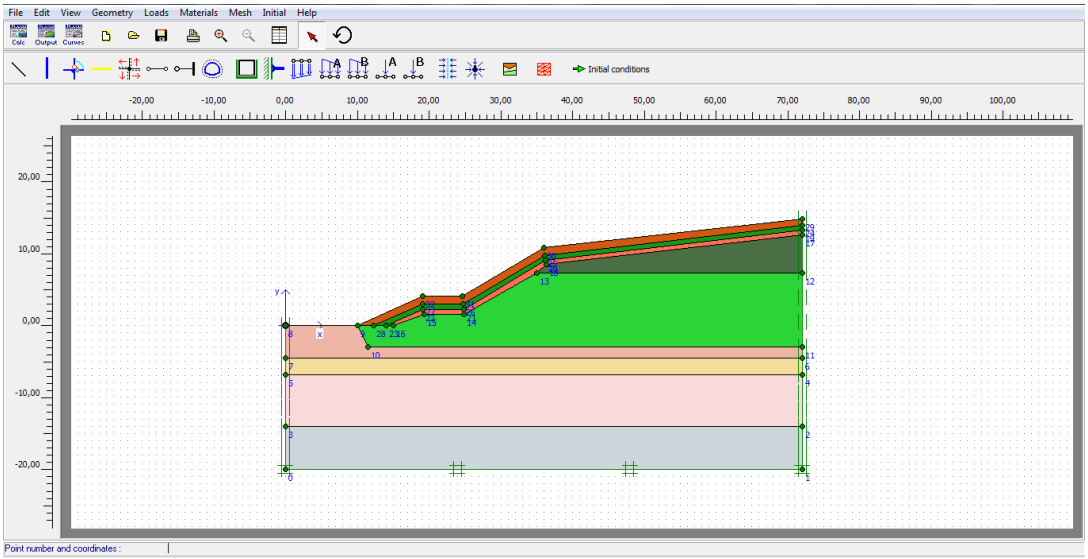

Fig. 7.1 – Section 4-4

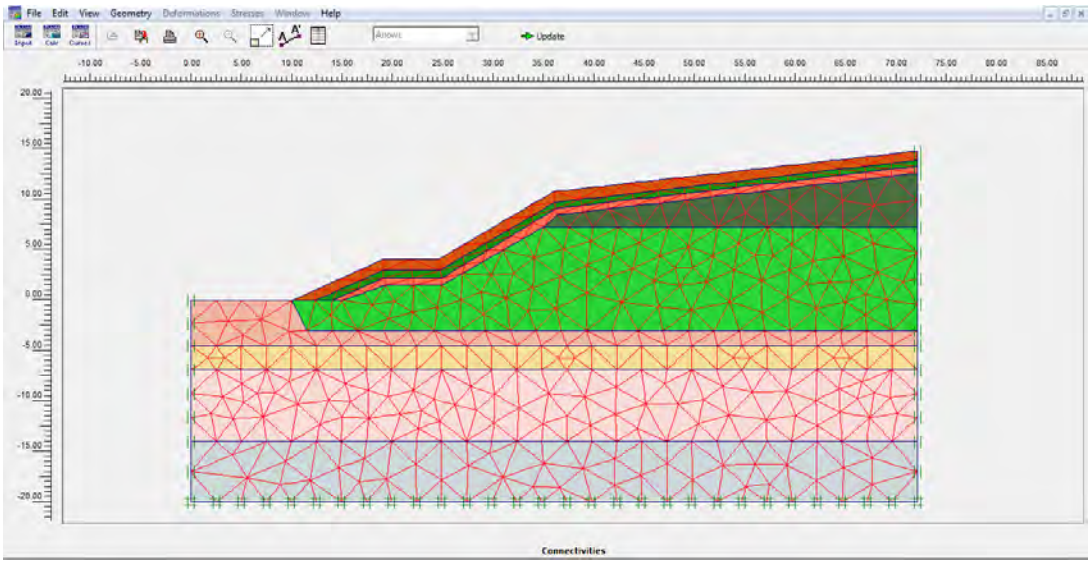

Fig. 7.2 – Generated mesh of section 4-4

The calculated FOS results equal to 1.27; it has been evaluated also the case of different waste input parameters ("Type 1" condition: $\gamma = 10$ kN/m^3, c' = 0 kPa, $\varphi' = 20°$): in this case the FOS results equal to 1.11.

7.4 Analysis of section 2-2

Left half of section 2-2 is drawn directly into the PLAXIS program (Fig. 7.3). As previously said, top cover barrier systems of sections 2-2 and A-A are been assumed as constant loads of 2000 Kg/m^3 (same hypothesis made by a previous slope stability analysis of the site, [20]) for the longest and almost linear part of the cover (including natural soil, compost layer, water drainage layer, compost, compacted clay, compost, biogas captation layer, compost and leveling layer) and 800 Kg/m^3 for the part of the slope covered only by natural soil and compost. Generated mesh with very fine coarseness is illustrated in Fig. 7.4.

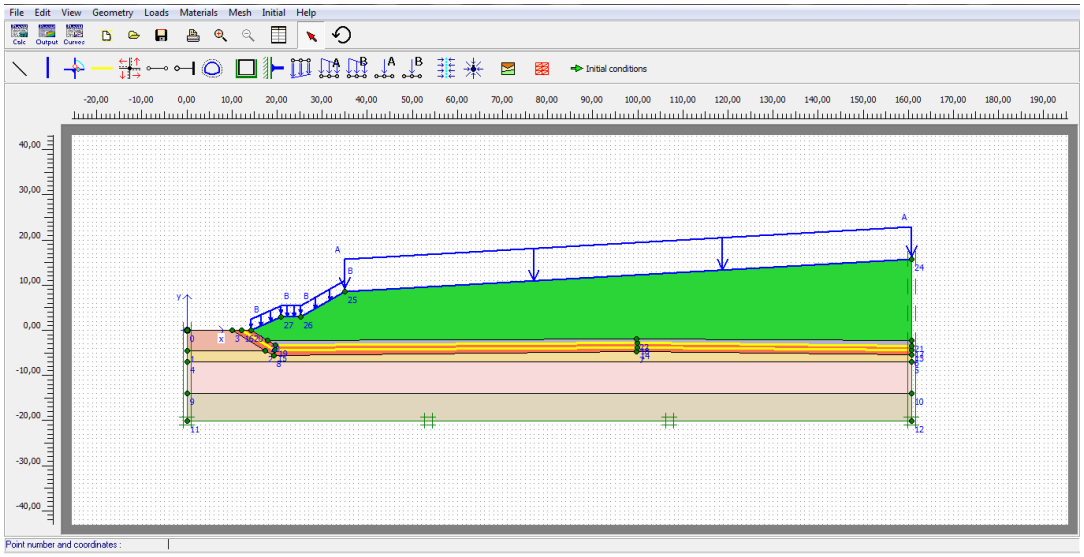

Fig. 7.3 – Section 2-2

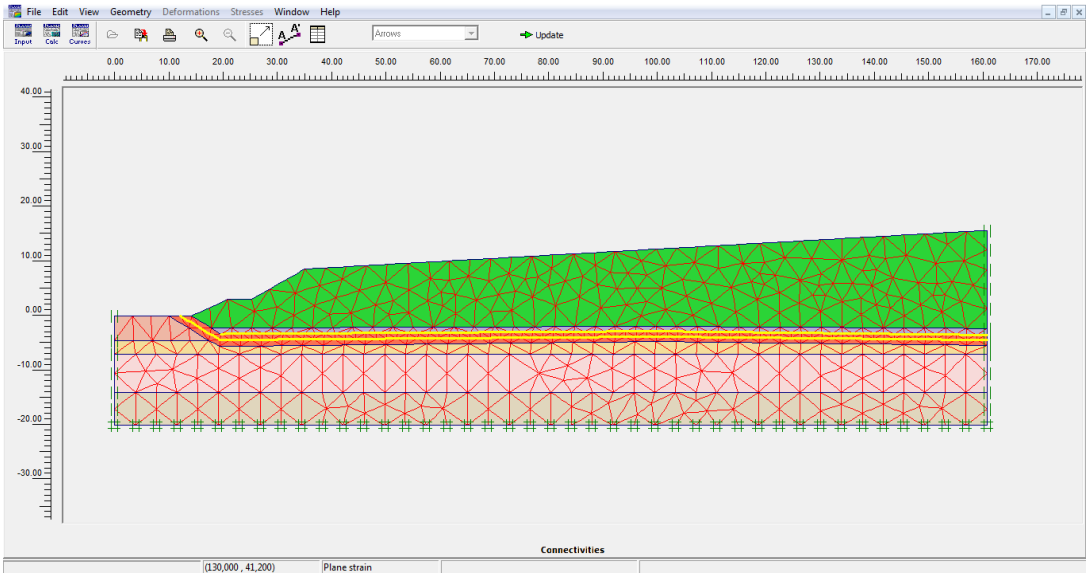

Fig. 7.4 – Generated mesh of section 2-2

The calculated safety factor results equal to 2.57, indicating a very good stability; using the "Type 1" waste characteristics, FOS is reduced to 1.6.

7.5 Analysis of section A-A

Section A-A presents the same hypotheses of section 2-2. The section and the relative generated mesh with PLAXIS are shown in Figures 7.5 and 7.6. Considering the initial waste parameters, FOS results equal to 2.38, while inserting modified waste parameters FOS = 1.35.

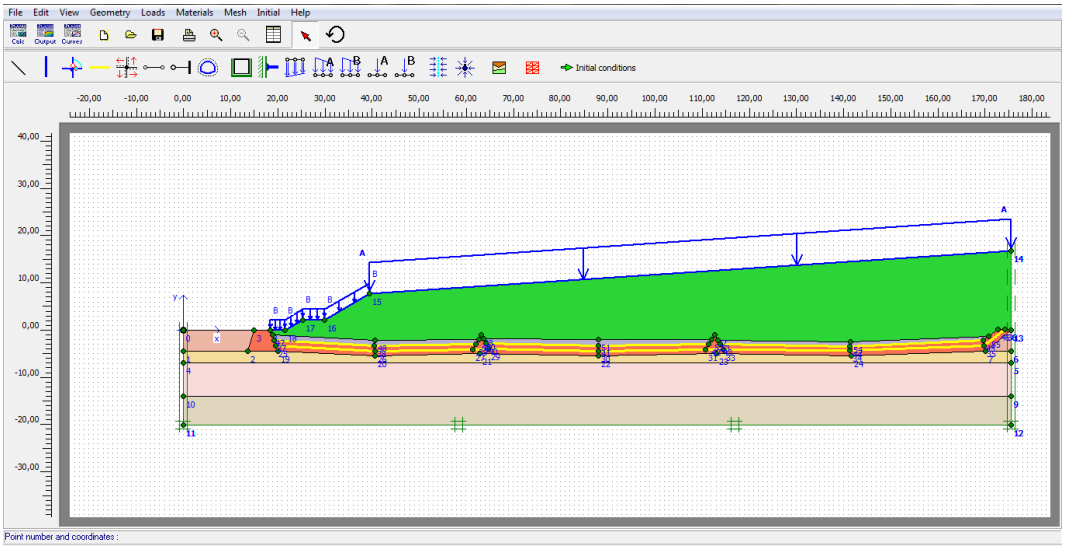

Fig. 7.6 – Section A-A

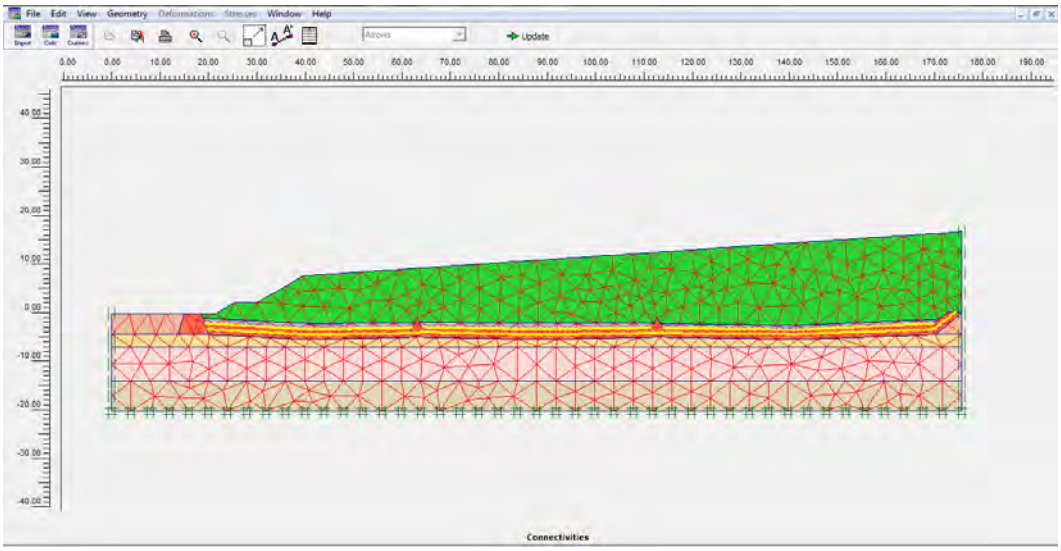

Fig. 7.7 – Generated mesh of section A-A

8. Discussion of the results

This Chapter analyzes more deeply the results obtained by the calculations with SLOPE/W and PLAXIS softwares: the Monte Carlo approach used with SLOPE/W permits to evaluate the results with a probabilistic point of view, while the PLAXIS program allows to observe which are the most critical zones (top cover, bottom barrier, waste body) of the sections for the slope stability.

Regarding the SLOPE/W program, considering the different case studied varying the input parameters, it's possible to obtain a probability density function for the different factors of safety and the related probability of failure and reliability index, that are two useful indices to evaluate the stability or the risk level of the slope. Moreover, a sensibility analysis has been done to establish which are the most influential parameters for such possible cases.

The probability of failure is defined as the probability to obtain a safety factor less than 1.0 and is determined by counting the number of FOS below 1.0 and then taking this number as a percentage of the total number of converged Monte Carlo trials; it's helpful to show the level of risk of instability for the slope under investigation.

The reliability index β is defined as:

$$\beta = \frac{(\mu - 1.0)}{\sigma}$$

where:

- μ = mean of the trial factors of safety;
- σ = standard deviation of the trial factors of safety.

This index defines the stability by the number of standard deviations separating the mean factor of safety from its defined value of 1.0 and can be interpreted as a method to normalize the FOS with respect to its uncertainty level. Once that the probability distribution is known, the reliability index can be related directly to the failure probability (Fig. 8.1).

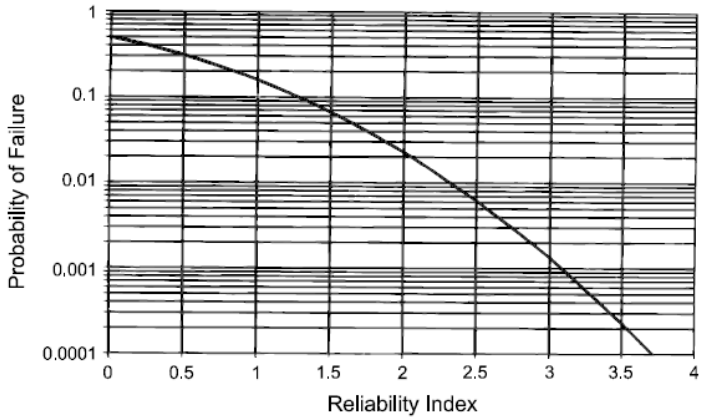

Fig. 8.1 – Relationship between the reliability index and the probability of failure (example taken from SLOPE/W manual)

The sensitivity analysis avails to understand which parameters have the major influence of the slope stability. The parameters are normalized to a value ranging between 0.0 and 1.0: 0.0 means the lowest value and 1.0 means the highest value for the studied parameter; the sensitivity range is then plot with the factor of safety to evaluate the influence on it.

This analysis is defined by the mean, the Delta factor (i.e. the range between the values of the parameters) and the steps from mean (the number of increments to both sides of the mean); for example, to define values [10, 12, 14, 16, 18, 20, 22], the mean is 16, the delta factor is 2 and 3 is the number of steps from the mean. The Delta factor has been assumed as the 5% of the mean value of input material and 5 steps are been considered on both sides of the mean value. This study has been conducted on the worst conditions related to the studies on the lower safety factor with the higher probability of failure.

As described in the previous paragraphs, varying input parameters the worst cases are those presenting the lower waste shear strength values; these particular cases are analyzed more deeply in order to establish their probability of failure and reliability indices. Also for these cases a sensitivity analysis has been conducted in order to evaluate the influence of the input parameters (both for materials and waste) on the factor of safety.

8.1 Section 4-4

Table 8.1 reports the probability of failure and reliability indices for all of the analyzed cases for section 4-4 of the old landfill sector.

Table 8.1. Probability of failure and reliability indices for section 4-4.

Case studies	Circular failure surface passing…								
	at the slope toe			through the base			through the landfill bottom		
	FOS	P. of failure	Reliab. index	FOS	P. of failure	Reliab. index	FOS	P. of failure	Reliab. index
Initial case	2.02	0%	16.07	1.88	0%	13.15	2.24	0%	16.79
Type 1 (γ = 10 kN/m^3, c = 0 kPa, ϕ = 20 °)	1.14	0.25%	2.64	1.16	0.1%	3.01	1.71	0%	7.87
Type 2 (γ = 10 kN/m^3, c = 0 kPa, ϕ = 25 °)	1.43	0%	5.36	1.45	0%	5.68	2.14	0%	9.49
Type 3 (γ = 10 kN/m^3, c = 0 kPa, ϕ = 30 °)	1.76	0%	7.11	1.77	0%	7.35	2.51	0%	11.92
Type 4 (γ = 10 kN/m^3, c = 5 kPa, ϕ = 20 °)	1.49	0%	8.19	1.49	0%	5.61	1.97	0%	10.57
Type 5 (γ = 10 kN/m^3, c = 5 kPa, ϕ = 25 °)	1.79	0%	9.81	1.79	0%	7.47	2.35	0%	13.48
Type 6 (γ = 10 kN/m^3, c = 5 kPa, ϕ = 30 °)	2.11	0%	10.55	2.10	0%	8.81	2.72	0%	13.38
Type 7 (γ = 10 kN/m^3, c = 10 kPa, ϕ = 20 °)	1.80	0%	10.99	1.79	0%	11.04	2.22	0%	14.79
Type 8 (γ = 10 kN/m^3, c = 10 kPa, ϕ = 25 °)	2.11	0%	12.06	2.05	0%	14.51	2.56	0%	14.97
Type 9 (γ = 10 kN/m^3, c = 10 kPa, ϕ = 30 °)	2.45	0%	15.99	2.24	0%	14.72	2.93	0%	14.63

As can be seen from the above Table, the most critical cases for section 4-4 are those presenting a probability of failure major than 0 %, i.e. the “Type 1” cases for circular failure surfaces passing at the toe of the slope and through the ground surface; the first case has a FOS lower than the other case and has a higher probability of failure equal to the 0.25 %.

Fig. 8.2 shows the relationship between the probability of failure and the factor of safety for the most critical case (FOS = 1.14, P. of failure = 0.25 % and reliability index = 2.64). This circumstance is for a “Type 1” material properties for circular failure surface passing through the toe of the slope.

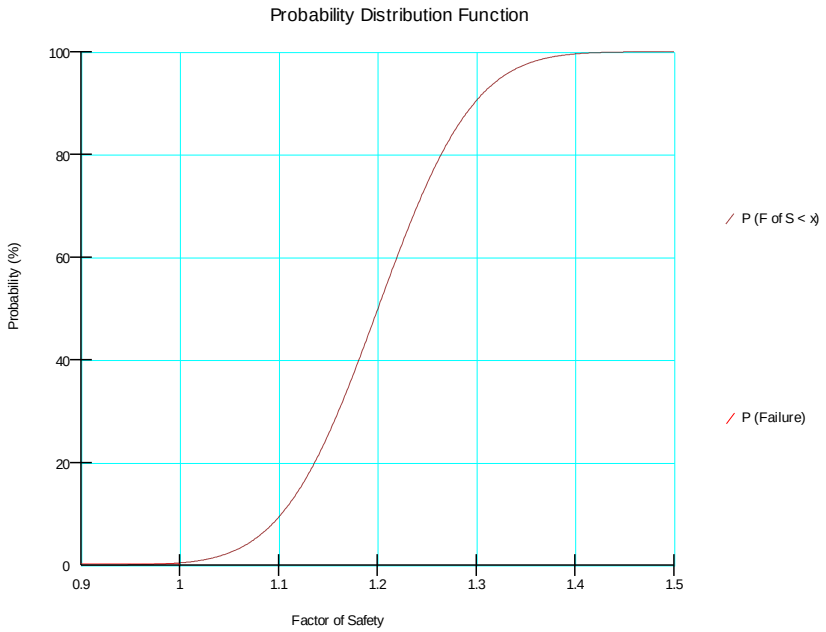

Fig. 8.2 – Probability distribution function of the 2000 Monte Carlo factors of safety showing probability of failure

The graph shows the probability of the factor of safety to be less than a certain value on the x-axis. For this situation the maximum obtainable FOS is 1.49 and the probability to obtain a factor of safety minor than 1.5 is equal to 100 %. The probability to obtain failure conditions remain very low (0.25%) but to evaluate which are the most sensitive input parameters on the factor of safety a sensitivity analysis has been conducted.

A sensitivity analysis has been done on the material properties (Fig. 8.3) and on the waste properties (Fig. 8.4). The only subsoil layers interested in possible failure surfaces are the two shallowest layers (clay with silty layers and fine silty sand).

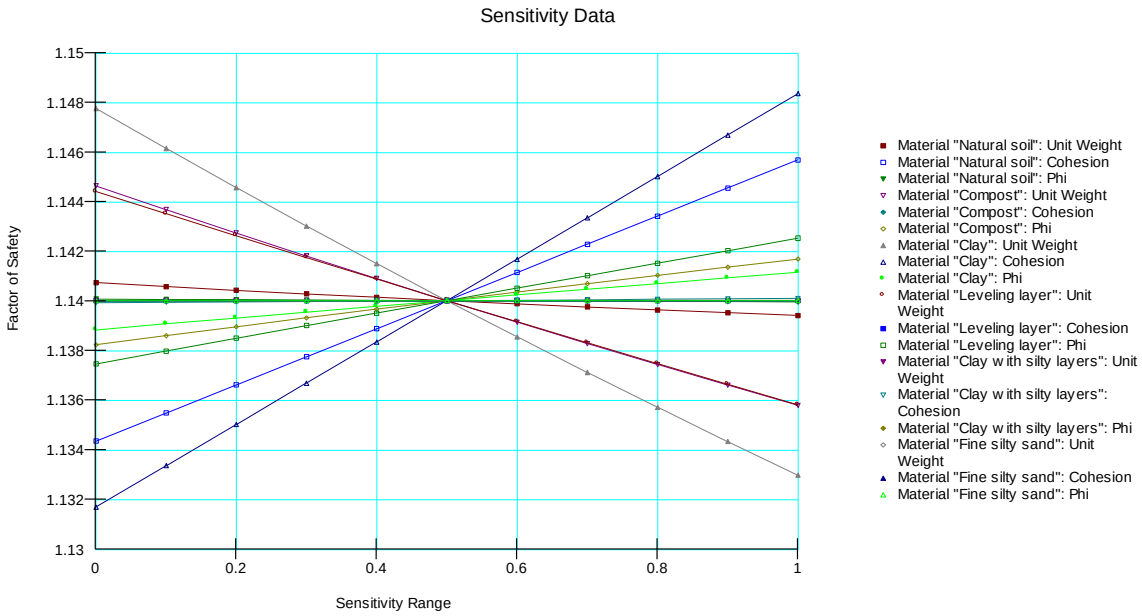

Fig. 8.3 – Sensitivity analysis for material properties

From the above Figure, it's possible to say that the compacted clay cohesion and the natural soil cohesion have the higher positive influence on the safety factor (an increase of their values lead to an increase of the FOS); the unit weight of compacted clay and compost have the higher negative influence on the compute of the factor of safety.

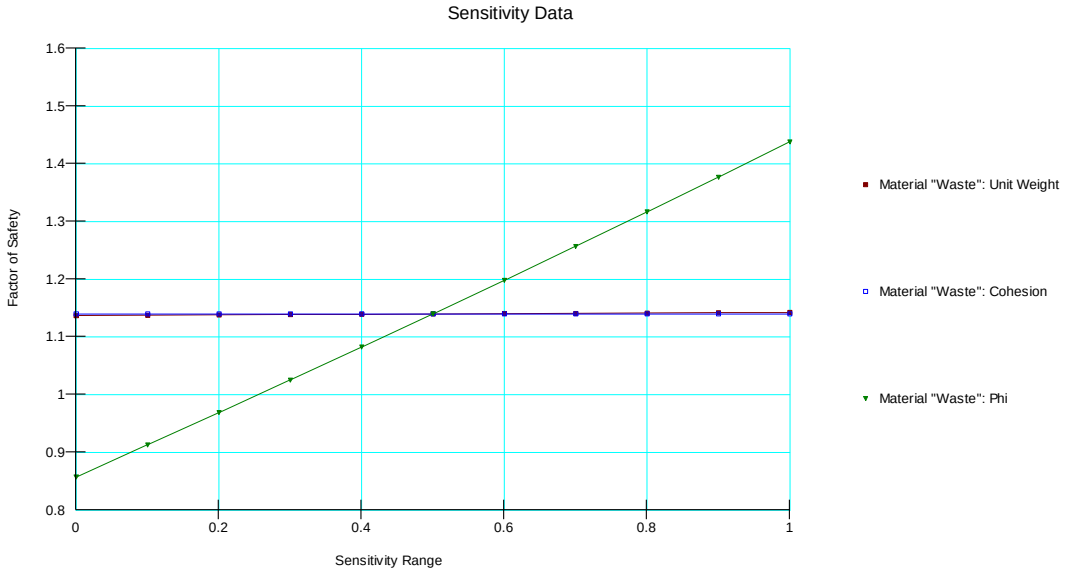

Fig. 8.4 – Sensitivity analysis for waste properties

Figure 8.4 shows that the waste angle of internal friction presents the only positive effect on the stability (a value of 1.0 means that for the higher values of internal friction angle the

factor of safety results to have the higher values). The cohesion is set fix to 0 that is the most precautionary value, while the variation of the unit weight doesn't present any influence on the FOS value.

A sensitivity analysis has been done also for the critical case of the stability of the first slope, where a FOS = 0.99 identified a critical slip surface involving a small movement only for soil and compost layers (Fig. 6.9a). For this particular case (the only one for this analysis with a FOS < 1.0) the probability of failure is equal to 17.4 %. The sensitivity analysis for top barrier materials of old landfill is shown in Fig. 8.5.

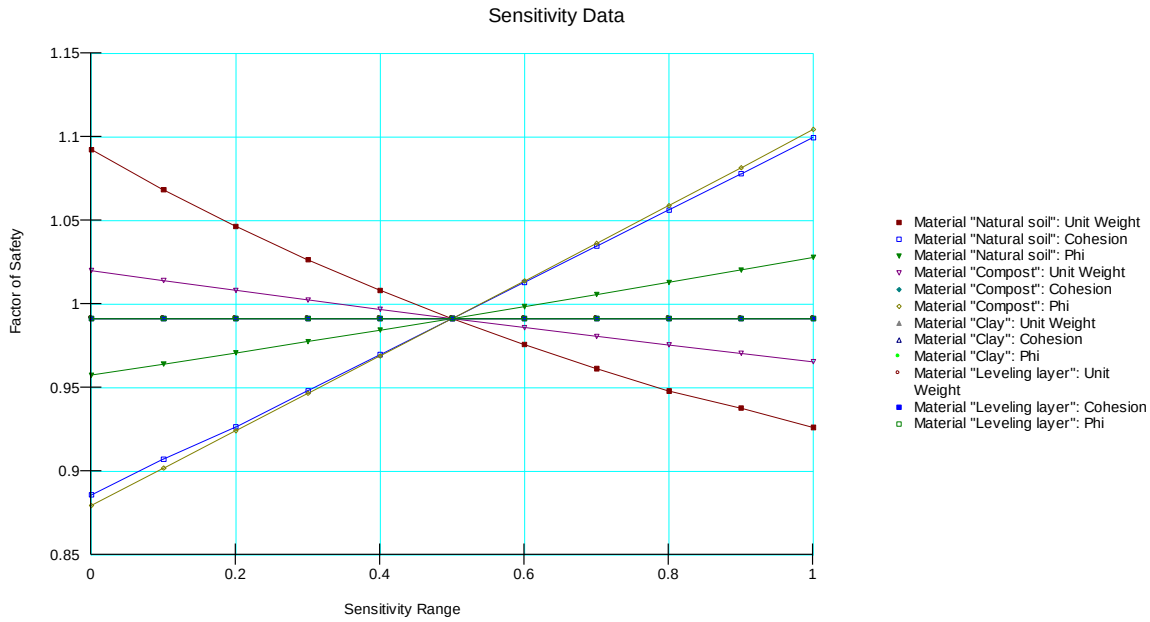

Fig. 8.5 – Sensitivity analysis for top barrier material properties

Cohesion of natural soil and angle of internal friction of compost have the higher positive influence on the FOS values, while unit weights of natural soil and compost have the higher negative influence.

The PLAXIS program permits to identified the most critical zones of the section, considering both initial waste parameters (FOS = 1.27, Fig 8.6) and modified waste parameters (FOS = 1.11, Fig. 8.7).

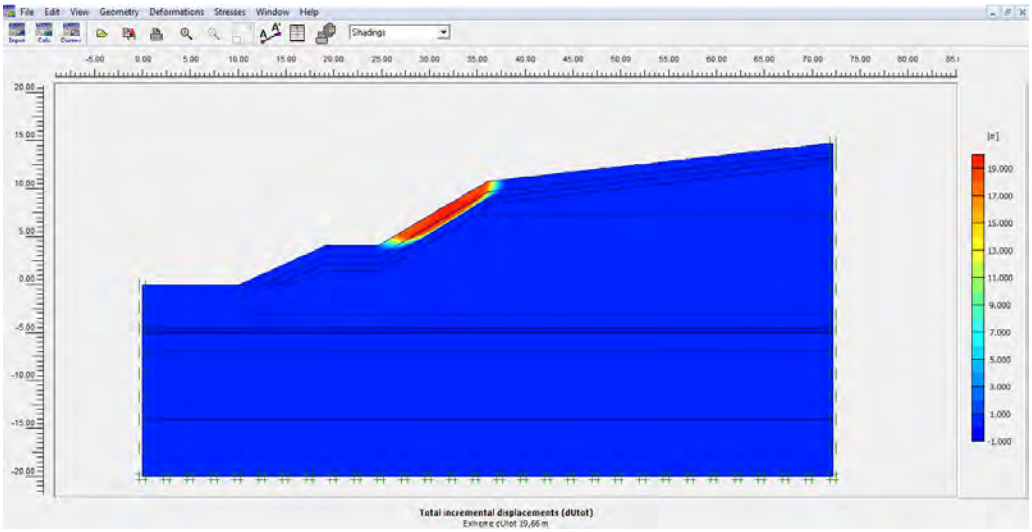

Fig. 8.6 – Zones of influence for section 4-4

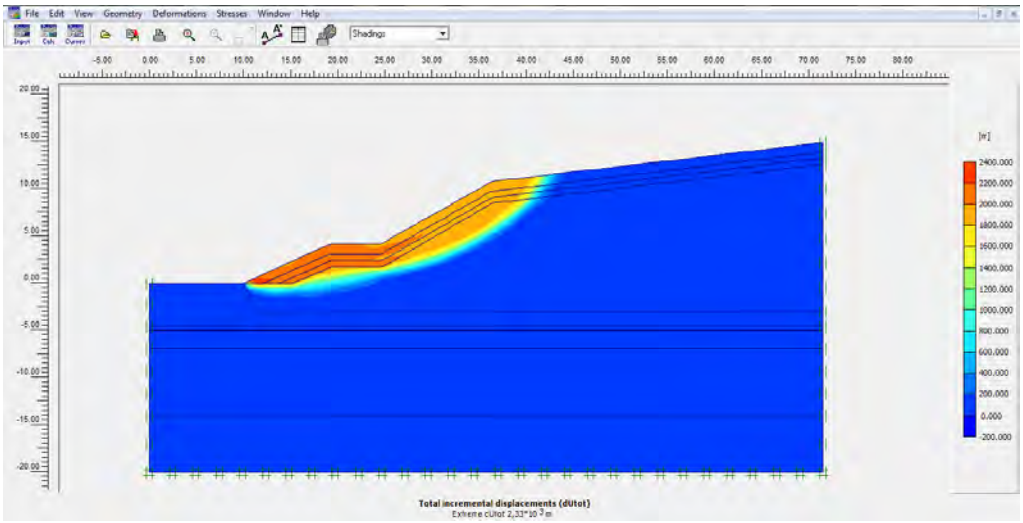

Fig. 8.7 – Zones of influence for section 4-4 varying waste parameters

Figure 8.6 shown that for this section the most critical zone for the slope stability is the top cover barrier system along the first steepest slope, similarly to the result obtained with SLOPE/W where a critical situation was seen in this part of the section (Fig. 6.9a).

Modifying waste input parameters to a situation close to "Type 1" waste shear strength properties, the stability is always satisfied (FOS = 1.11) but for this extreme situation the failure surface found with PLAXIS is a nearly circular failure surface passing at the toe of the slope and involving the entire top barrier system and also a part of the upper waste close to the barrier (Fig. 8.7).

8.2 Section 2-2

Table 8.2 reports the probability of failure and reliability indices for all of the analyzed cases for section 2-2.

Table 8.2. Probability of failure and reliability indices for section 2-2.

Case studies	Circular failure surface passing…								
	at the slope toe			through the base			through the landfill bottom		
	FOS	P. of failure	Reliab. index	FOS	P. of failure	Reliab. index	FOS	P. of failure	Reliab. index
Initial case	1.75	0%	11.61	1.81	0%	13.34	3.05	0%	17.27
Type 1 (γ = 10 kN/m^3, c = 0 kPa, ϕ = 20 °)	1.02	10.55%	1.19	1.24	0%	5.06	1.95	0%	11.65
Type 2 (γ = 10 kN/m^3, c = 0 kPa, ϕ = 25 °)	1.28	0%	4.40	1.48	0%	7.49	2.33	0%	12.62
Type 3 (γ = 10 kN/m^3, c = 0 kPa, ϕ = 30 °)	1.56	0%	6.50	1.74	0%	8.93	2.74	0%	12.88
Type 4 (γ = 10 kN/m^3, c = 5 kPa, ϕ = 20 °)	1.31	0%	5.97	1.46	0%	8.84	2.13	0%	13.85
Type 5 (γ = 10 kN/m^3, c = 5 kPa, ϕ = 25 °)	1.57	0%	8.32	1.72	0%	10.48	2.51	0%	14.30
Type 6 (γ = 10 kN/m^3, c = 5 kPa, ϕ = 30 °)	1.85	0%	9.57	1.99	0%	11.76	2.92	0%	14.99
Type 7 (γ = 10 kN/m^3, c = 10 kPa, ϕ = 20 °)	1.56	0%	9.35	1.67	0%	11.77	2.31	0%	15.65
Type 8 (γ = 10 kN/m^3, c = 10 kPa, ϕ = 25 °)	1.84	0%	10.95	1.93	0%	12.84	2.69	0%	15.77
Type 9 (γ = 10 kN/m^3, c = 10 kPa, ϕ = 30 °)	2.14	0%	12.16	2.21	0%	13.14	3.09	0%	16.15

Waste parameters are been changed also for cases of possible sliding movements on geosynthetic liners, but already in the worst possible case (Type 1 condition) the stability is well respected (FOS = 1.60, P. of failure = 0% and R. index = 8.72 for sliding on geotextile liner; FOS = 1.64, P. of failure = 0% and R. index = 9.06 for sliding on geomembrane liner).

The most critical case among those studied is related to Type 1 waste parameters conditions for circular failure surface passing at the toe of the slope: in this case the safety factor is equal to 1.02 presenting a probability of failure of 10.55% (Fig. 8.8).

A sensitivity analysis on soil and waste properties has been made in order to assess which are the materials and parameters that have the higher (positive or negative) influence on the factor of safety. Fig. 8.9 shows the sensitivity analysis graph for materials involved in the failure surface (not the subsoil materials). Sensitivity analysis for waste parameters is reported in Fig. 8.10.

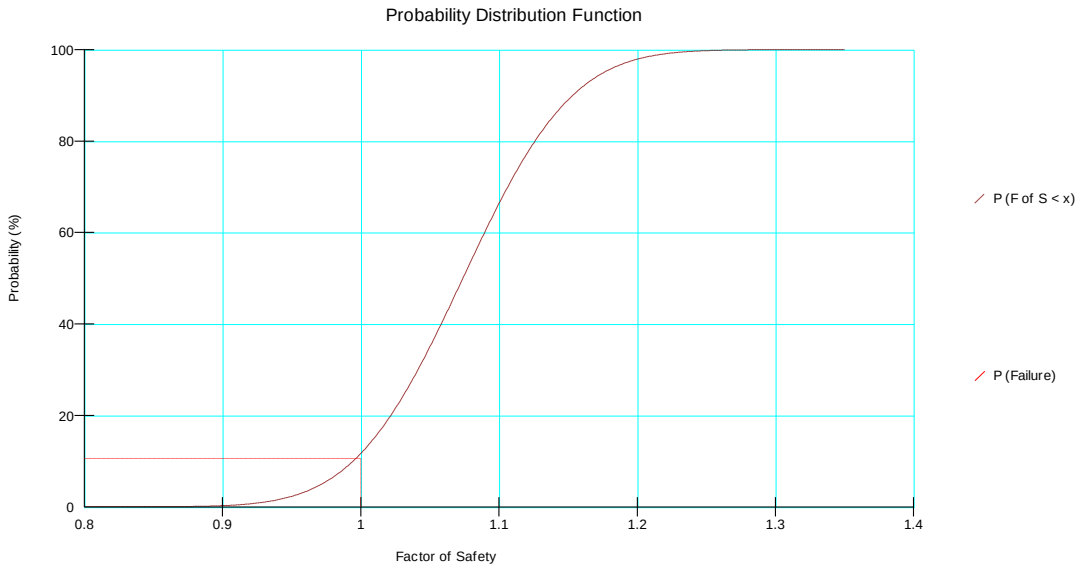

Fig. 8.8 - Probability distribution function of the 2000 Monte Carlo factors of safety showing probability of failure

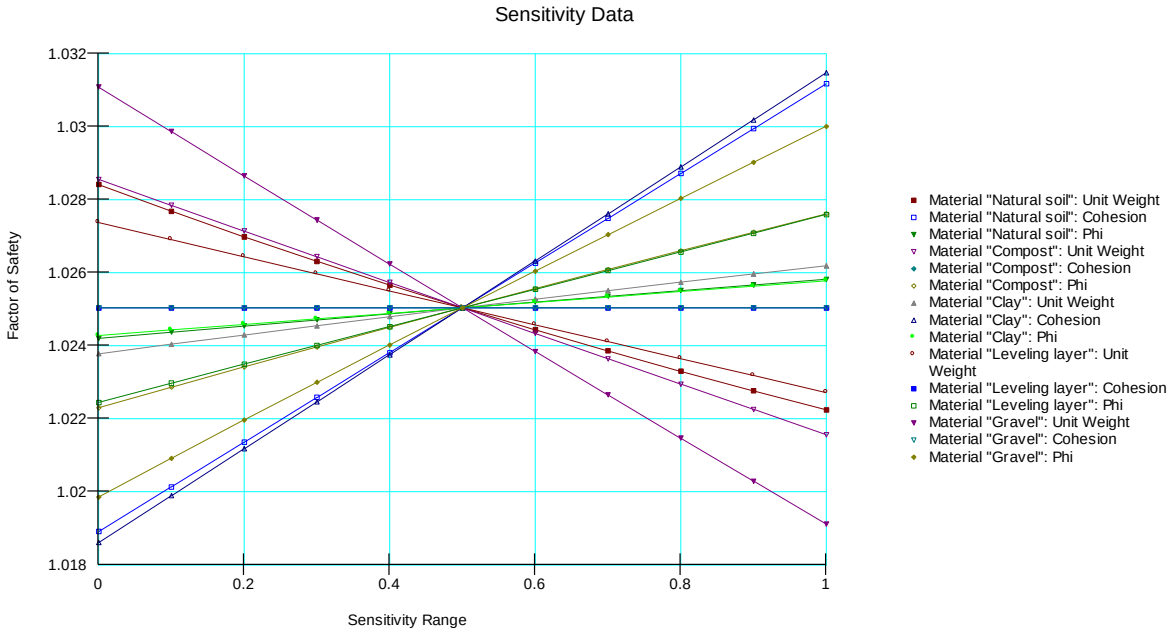

Fig. 8.9 – Sensitivity analysis for material properties

Cohesion of natural soil and clay and angle of internal friction of gravel have the higher positive influence on the safety factor, while unit weights of gravel, compost and soil present the higher negative influence on the calculation of the FOS.

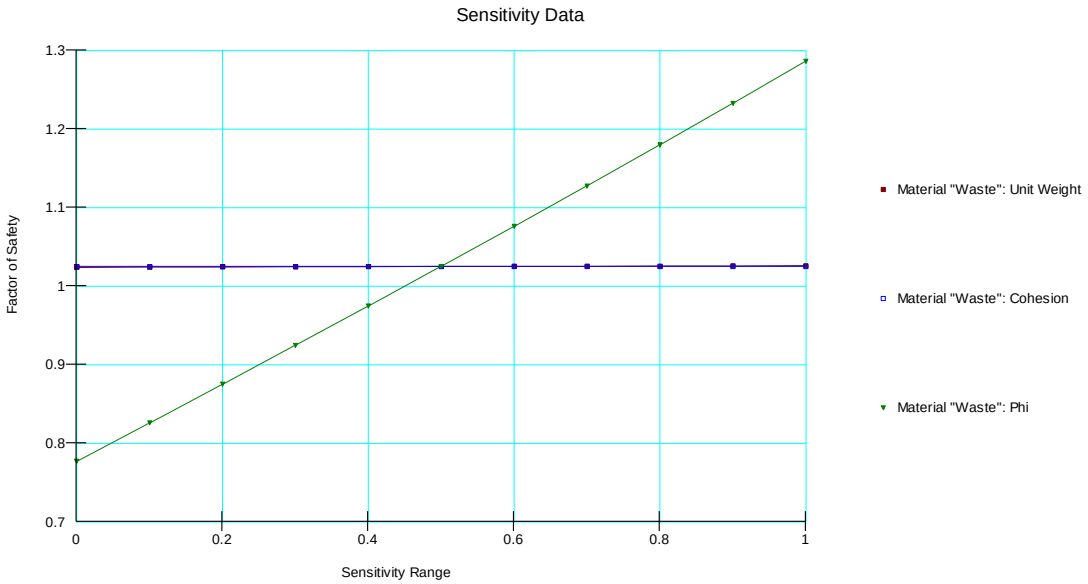

Fig. 8.10 – Sensitivity analysis for waste properties

As expectable, also for section 2-2 the only parameter with a positive influence on the factor of safety is the angle of internal friction of waste, but in this case the maximum obtainable

safety factor is equal to less than 1.3. Figures 8.11 and 8.12 show the most critical zones for the stability implementing PLAXIS procedure. The first case presents a FOS = 2.57, indicating a good stability and pointing out a circular failure surface passing nearly the landfill bottom involving a consistent part of the waste mass.

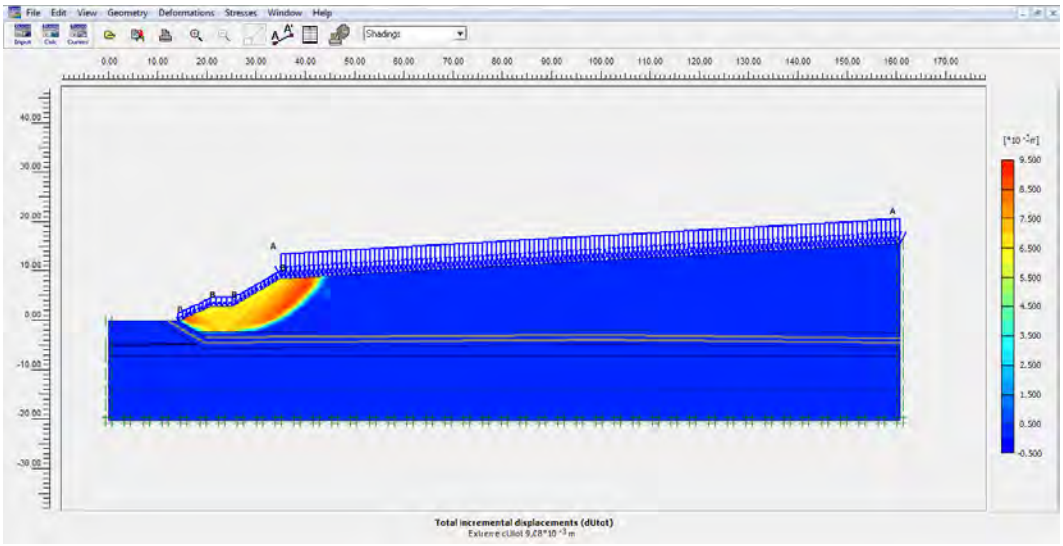

Fig. 8.11 – Zones of influence for section 2-2

Figure 8.12 shows the circular failure surface for the most critical case, varying waste characteristics: also in this case the stability is respected (FOS = 1.6) but yet again the most crucial zone is the part related to the first steepest slope of the section.

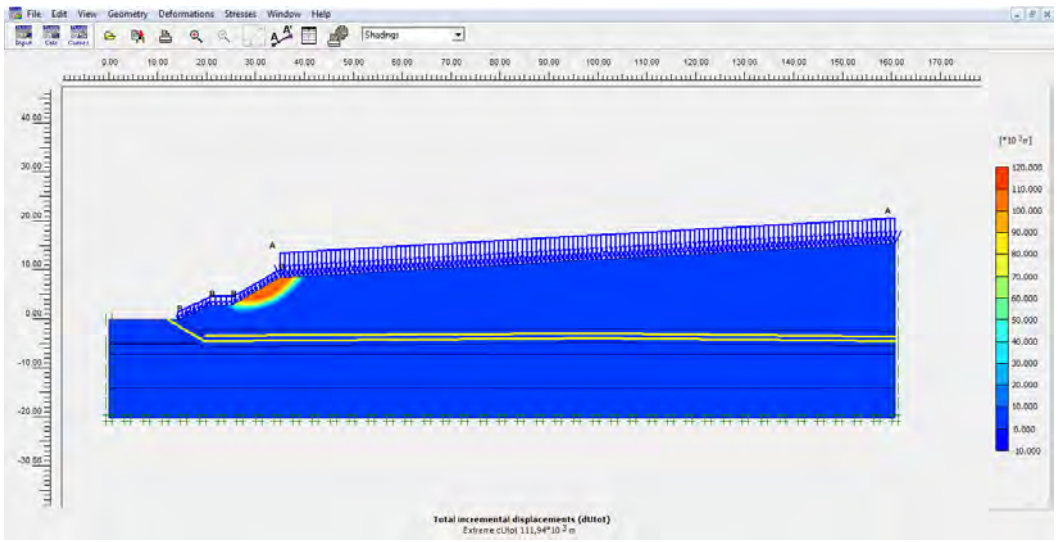

Fig. 8.12 – Zones of influence for section 2-2 varying waste parameters

8.3 Section A-A

Table 8.3 reports the probability of failure and reliability indices for all of the analyzed cases for section A-A.

Table 8.3. Probability of failure and reliability indices for section A-A.

Case studies	Circular failure surface passing…								
	at the slope toe			through the base			through the landfill bottom		
	FOS	P. of failure	Reliab. index	FOS	P. of failure	Reliab. index	FOS	P. of failure	Reliab. index
Initial case	1.75	0%	11.72	1.81	0%	12.71	2.54	0%	12.49
Type 1 (γ = 10 kN/m^3, c = 0 kPa, ϕ = 20 °)	1.03	6.4%	1.41	1.16	0.05%	3.51	1.34	0%	4.99
Type 2 (γ = 10 kN/m^3, c = 0 kPa, ϕ = 25 °)	1.28	0%	4.51	1.42	0%	6.28	1.71	0%	7.55
Type 3 (γ = 10 kN/m^3, c = 0 kPa, ϕ = 30 °)	1.55	0%	6.58	1.68	0%	8.09	2.11	0%	8.97
Type 4 (γ = 10 kN/m^3, c = 5 kPa, ϕ = 20 °)	1.31	0%	5.99	1.41	0%	7.62	1.57	0%	7.95
Type 5 (γ = 10 kN/m^3, c = 5 kPa, ϕ = 25 °)	1.57	0%	8.35	1.68	0%	9.89	1.94	0%	9.80
Type 6 (γ = 10 kN/m^3, c = 5 kPa, ϕ = 30 °)	1.86	0%	9.59	1.95	0%	10.78	2.33	0%	12.85
Type 7 (γ = 10 kN/m^3, c = 10 kPa, ϕ = 20 °)	1.57	0%	9.54	1.65	0%	10.91	1.80	0%	10.62
Type 8 (γ = 10 kN/m^3, c = 10 kPa, ϕ = 25 °)	1.84	0%	11.42	1.92	0%	12.17	2.16	0%	11.87
Type 9 (γ = 10 kN/m^3, c = 10 kPa, ϕ = 30 °)	2.12	0%	12.06	2.21	0%	13.10	2.51	0%	14.36

Type 1 waste parameters condition has been applied also to the cases of possible sliding movements along the geosynthetic liners placed in the landfill bottom. The stability is well respected for the case of a possible sliding both on the geotextile (FOS = 1.70, P. of failure = 0%) and on the geomembrane (FOS = 2.12, P. of failure = 0%).

Similarly to the other sections, the most critical case is related to Type 1 condition for circular failure surface passing at the toe of the slope: in this case, FOS = 1.03 with a P. of

failure of 6.4 % (Fig. 8.13). A sensitivity analysis (Fig. 8.14) has been done to study which cover materials and waste parameters have the higher influence of the calculation of the safety factor.

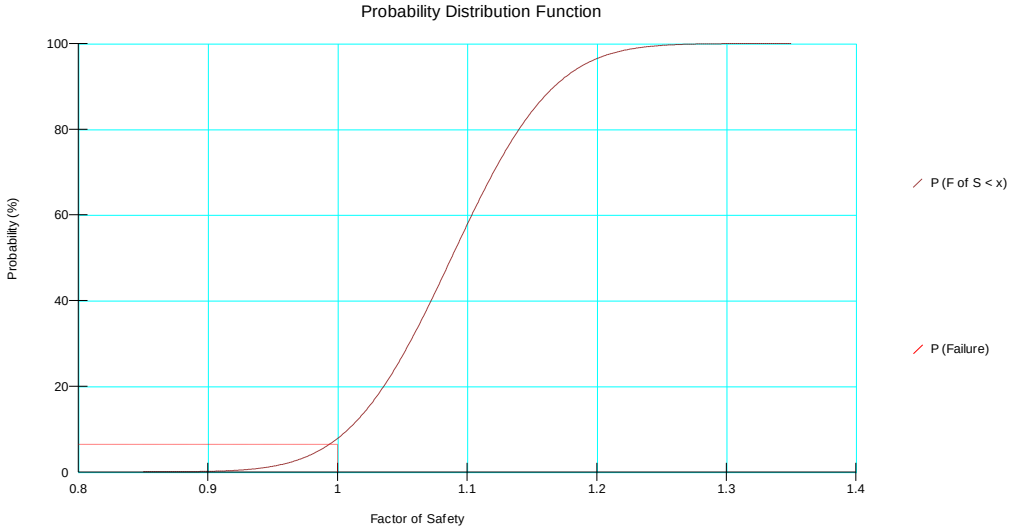

Fig. 8.13 - Probability distribution function of the 2000 Monte Carlo factors of safety showing probability of failure

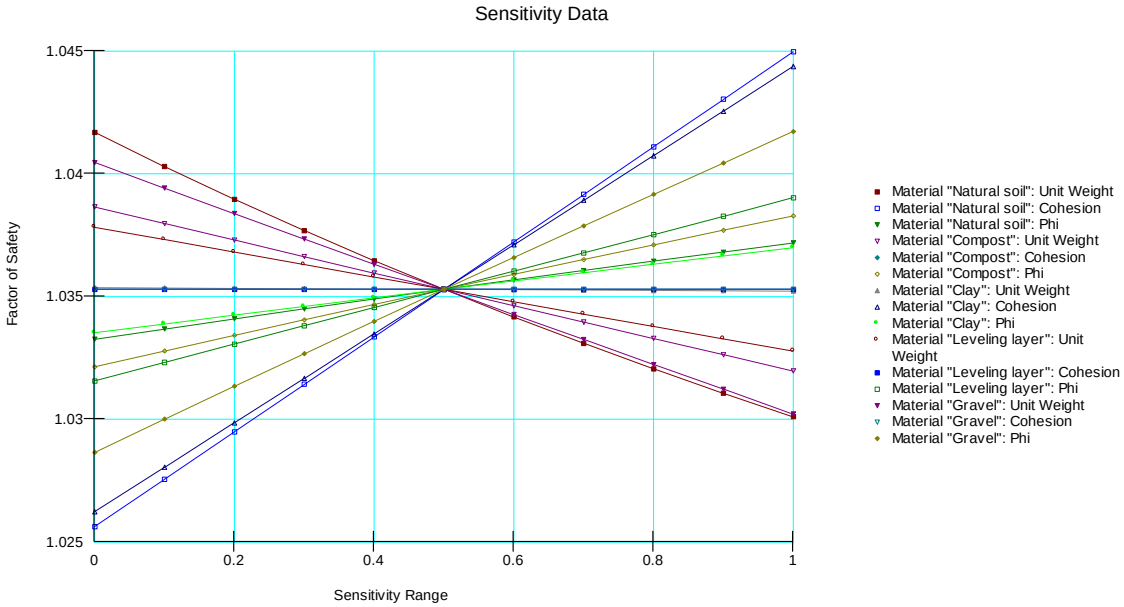

Fig. 8.14 – Sensitivity analysis for material properties

Cohesion of natural soil and clay and angle of shear strength of gravel have the higher positive effect on the FOS, while unit weight of soil, gravel and compost present the higher negative effect on the FOS. These considerations are the same of those made for section 2-2, due to the similar section geometry and top cover barrier system of the previous analyzed

section. As for the two other sections, the only waste parameter which has a positive effect on the factor of safety is the angle of internal friction: for this section FOS augments from 0.8 until about 1.3 (Fig. 8.15).

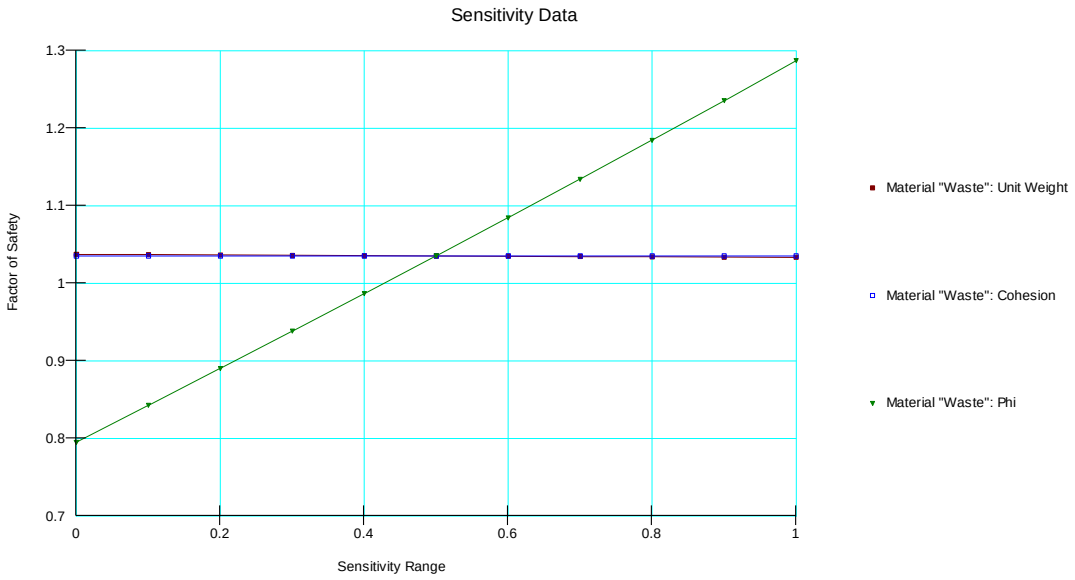

Fig. 8.15 - Sensitivity analysis for waste properties

PLAXIS software confirms the slope stability both considering initial conditions (FOS = 2.38) and modified waste parameters (FOS = 1.35). Fig. 8.16 shows a critical zone around the toe of the slope and near the clay berm that will separate “Lotto 3” from the future sector named “Lotto Ovest”. Fig. 8.17 is related to the most critical waste input properties condition; the stability is reached but the crucial region is, also for this case, the one nearly the higher steepest slope.

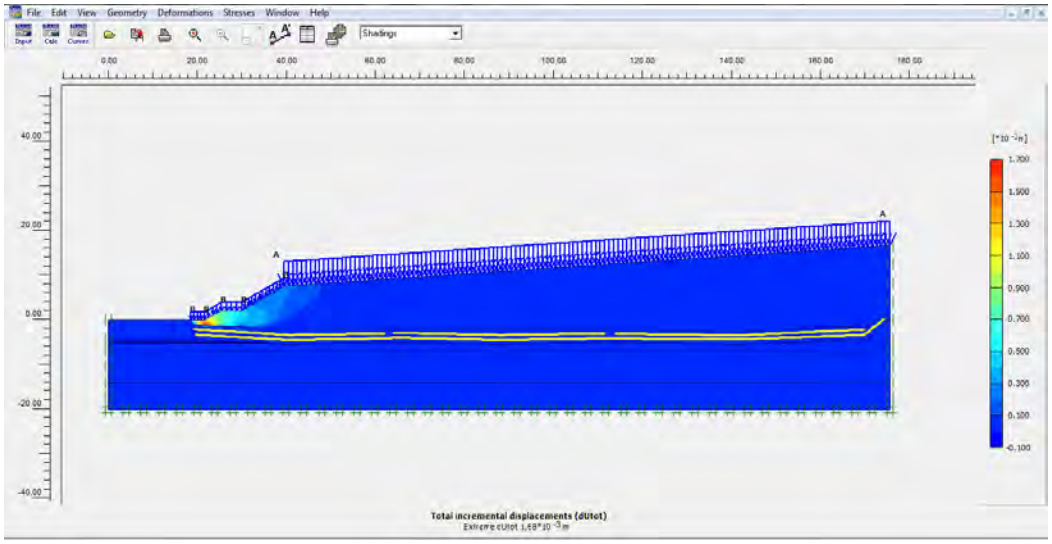

Fig. 8.16 – Zones of influence for section A-A

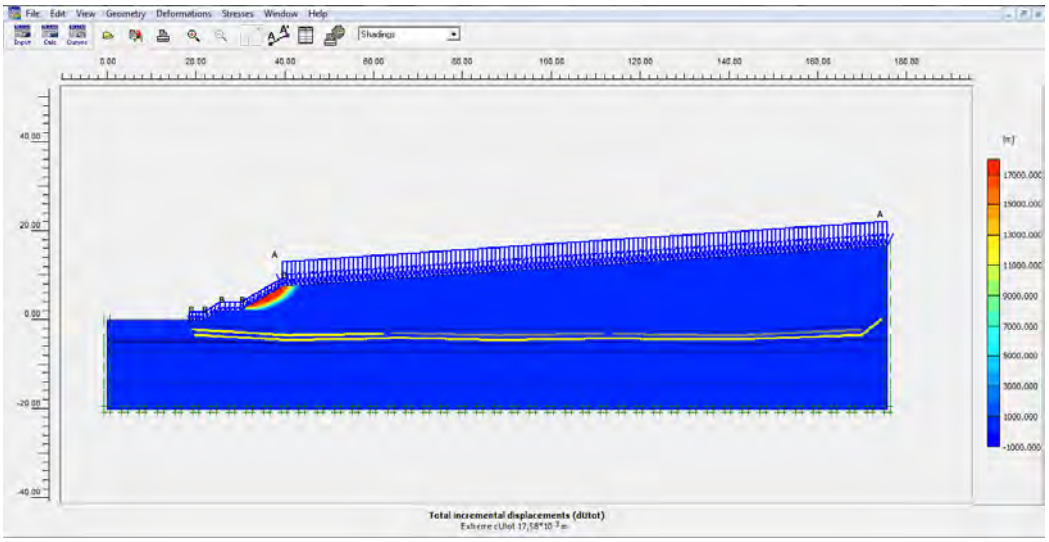

Fig. 8.17 – Zones of influence for section A-A varying waste parameters

9. Conclusions

The study on the evaluation of the slope stability analysis of Este S.E.S.A. landfill has been conducted in order to assess which are the most critical zones of the profile of the chosen studied sections and to estimate which material and waste characteristics have the most positive or negative influence on the stability. These goals have been reached thanks to the use of two-dimensional computer programs which are based on two different approaches of analysis methods: SLOPE/W applies the considerations of the limit equilibrium methods while PLAXIS executes a finite elements analysis.

The three chosen landfill sections present profiles with the steepest slopes among those of the entire site: one section (4-4) refers to the oldest landfill sector whilst the other two (2-2, A-A) are very similar and refer to the newest landfill sectors. In order to consider the spatial variability of the physical properties of materials, the input parameters for SLOPE/W software are been assumed to be normally distributed, and decreased by some specific corrective factors as provided by Italian legislation; moreover, a distinction between the estimation on the waste properties for the different landfill sectors (the one related to the old landfill and the other two representing the more recently dumped waste) has been done in order to consider the difference between waste dumped when a separated collection system was completely absent and the nowadays situation where the waste are landfilled after an appropriate primary selection and separated collection system (that started at the end of the 90s) made by the S.E.S.A. plant and municipalities. In addition, due to the not complete reliability of these estimations for the difficulty to obtain precise waste parameters that varying continuously in time and space, waste physical properties are been modified in order to consider different physical waste properties implementing also extreme situations with very low values. Finally, it's important to underline that for both methods also the seismic contribution has been considered as required by the recent Italian normative (Norme Tecniche di Costruzione, 2008).

SLOPE/W allowed the implementation of different possible circular failure surfaces among the landfill sections, giving safety factors related to the limit equilibrium method of Morgenstern-Price, one of the most used approach that satisfy both force and moment

equilibriums. Then, a sensitivity analysis along with the calculation of the probability of failure and reliability index has been done for all of the case studied.

PLAXIS program has been used to estimate the stability to confirm if the most critical cases and zones of the analyzed sections are the same of those found with the SLOPE/W software.

One of the two most critical cases found is the one related to possible circular failure surface passing through the top cover barrier of the first steepest slope of the 4-4 section profile: this situation presents the lower safety factors and the higher probability of failure, and, even if for only one case among the 216 possible cases studied with SLOPE/W, a FOS = 0.99 has been computed, with a failure surface involving a quantity only for natural soil and compost. A situation for the same part of the slope that involves the entire movement of the top barrier (soil and compost but also clay and leveling layer) presents a higher safety factor equal to 2.00. Also PLAXIS program computes a low safety factor (FOS = 1.27) for 4-4 section of the old landfill, identifying the first steepest slope of the profile as the most critical zone (Fig. 8.6). The sensitivity analysis shows that the material parameters presenting the higher positive influence on the safety factor are the cohesion of natural soil and the friction angle of compost, while the ones that negatively influence the FOS computation are the unit weights of soil and compost. A solution to improve the stability of this part of landfill could be the planting of more vegetations or trees.

The other critical case is the one associated to the circular failure surface that could pass at the toe and the base of the slope: these situations present low computed factors of safety (around 1.7 – 1.8) for all the sections if compared to the other situations studied (like failure surface passing through the landfill bottom or tangent to the geosynthetic liners). This is confirm also in two cases of the analysis made with PLAXIS. Material parameters that seems to have a positive effect on the FOS calculation are the cohesions of soil and clay and the friction angle of the gravel, while material physical properties that show a negative influence on the safety factor are the unit weights of soil, compost and gravel. A solution to augment the safety on this part of the landfill could be the installation of a berm of length equal to the involved part of the base on the instability in order to improve the resisting forces.

A suggestion to increase the reliability of the obtained results could be the investigations with cone penetration test as method to estimate the properties of shear strength of waste, that seems to have no negative effects on the FOS estimation; anyway, the continuous

variation in time and space of waste physical parameters is well known due to the different steps of degradation processes that interested a municipal solid waste landfill.

10. Bibliography

[1] Abramson, Lee W., Lee, Thomas S., Sharma, Sunil, Boyce, Glenn M., 2002. *Slope Stability and Stabilization Methods* (2nd ed.), New York, USA: John Wiley & Sons.

[2] Carrubba, P., 2013. *Aspetti geotecnici nella realizzazione delle discariche di RSU.* Commissione di ingegneria geotecnica – Ordine degli ingegneri della provincia di Bolzano.

[3] Cheng, Y.M., Lau, C. K., 2008. *Slope Stability Analysis and Stabilization: New Methods and Insight.* CRC Press, p. 15-36.

[4] Dal Prà, M., 2008. *Relazione geologica e idrogeologica per il Progetto di ampliamento della discarica SESA di RSU-RSA di Este.*

[5] De Battisti, L., Drago, P., Maggio 2012. *Relazione geologica (Elaborato B24) – Elaborato adeguato alle prescrizioni approvate con la Conferenza dei Serivizi del 02/11/2011. P.A.T.I. Comuni dell'Estense. Provincia di Padova.*

[6] De Marco, C., 2005. *Prova Penetrometrica Statica-Prova Proctor per il terreno di Monselice-Località Schiavonia d'Este (PD).* Geodata S.a.s.

[7] Dixon, N., Russell, D., Jones, V., 2004. *Engineering properties of municipal solid waste*. Department of Civil and Building Engineering, Loughborough University, Leicestershire, UK.

[8] Duncan, J.M., 1996. *State of art: limit equilibrium and finite-element analysis of slopes*. J. Geotech. Eng. 122 (7), p. 577–596.

[9] Fassett, J.B., Leonardo, G.A., Repetto, P.C., 1994. *Geotechnical properties of municipal solid waste and their use in landfill design*. Waste Tech '94, Landfill Technology Technical Proceedings, Charleston, SC (USA).

[10] Favaretti, M., 2010. *Environmental Geotechnics course – MSW Shear Strength.* University of Padua A.Y. 2010-2011. I.M.A.G.E. Department.

[11] Favaretti, M., 2010. *Environmental Geotechnics course – Natural and artificial slopes and general slopes stability concepts.* University of Padua A.Y. 2010-2011. I.M.A.G.E. Department.

[12] Fredlund, D. G., Krahn, J., Pufahl, D.E., 1981. *The Relationship between Limit Equilibrium Slope Stability Methods.* Vol. 3, p. 409 – 416.

[13] Gharabaghi, B., Singh, M.K., Inkratas, C., Fleming, I.R., McBean, E., 2007. *Comparison of slope stability in two Brazilian municipal landfills.* Waste Management 28 (2008) p. 1509-1517, Elsevier.

[14] Grisolia, M., Napoleoni, Q., Tancredi, G., 1995. *The use of the triaxial tests for the mechanical characterization of MSW*. Sardinia 1995.

[15] Landva, A., Clarke, J., 1990. Geotechnics of Waste fill. *Proc Symposium on Geotechnics of Waste* fills, p. 86-103.

[16] Landva, A.O., Valsangkar, A.J., Pelkey, S.G., 2000. Lateral earth pressure at rest and compressibility of municipal solid waste. Canadian Geotechnical Journal 37, p. 1157–1165.

[17] Look, B.G., 2007. *Handbook of Geotechnical Investigation and Design Tables*. Taylor&Francis Group, London, UK.

[18] Manassero, M., Van Impe, W.F., Bouazza, A., 1996. Waste disposal and containment. Second International Congress on Environmental Geotechnics, Osaka.

[19] Matasovic, N., Kavazanjian, E. Jr., and Anderson, R., 1998. *Performance of solid waste landfills in earthquakes,* Earthquake Spectra, Issue #2, Vol. 14, p. 319-334.

[20] Mandato, A., Carraro, G., Avanzi, E.U., 2003. *Piano di adeguamento per la discarica di Este in base all'art. 17 del Dlgs 13 Gennaio 2003 n.36 – Verifiche geotecniche di stabilità. S.E.S.A. S.p.a.*

[21] Mandato, A., Feffin, N., Bagno, I., Piazza, E., 2008. *Discarica in ampliamento. Planimetrie stato di fatto, quote significative e destinazioni funzionali. Piano quotato area interessata discarica (Dis. N° 5) - Nuovo impianto di selezione e valorizzazione rifiuti urbani da raccolta differenziata con adeguamento impianto di smaltimento rifiuti urbani non pericolosi e opere accessorie. S.E.S.A. S.p.a.*

[22] Mandato, A., Feffin, N., Bagno, I., Piazza, E., 2008. *Discarica in ampliamento. Planimetria di insieme, quote significative e destinazioni funzionali delle aree (Dis. N° 7) - Nuovo impianto di selezione e valorizzazione rifiuti urbani da raccolta differenziata con adeguamento impianto di smaltimento rifiuti urbani non pericolosi e opere accessorie. S.E.S.A. S.p.a.*

[23] Mandato, A., Feffin, N., Bagno, I., Piazza, E., 2008. *Discarica esistente. Sezioni significative stato di fatto con stratigrafia e dettagli (Dis. N° 8a – 8b) - Nuovo impianto di selezione e valorizzazione rifiuti urbani da raccolta differenziata con adeguamento impianto di smaltimento rifiuti urbani non pericolosi e opere accessorie. S.E.S.A. S.p.a.*

[24] Mandato, A., Feffin, N., Bagno, I., Piazza, E., 2008. *Discarica in ampliamento. Sezioni significative stato di fatto con stratigrafia e dettagli (Dis. N° 8c – 8d) - Nuovo impianto di selezione e valorizzazione rifiuti urbani da raccolta differenziata con adeguamento impianto di smaltimento rifiuti urbani non pericolosi e opere accessorie. S.E.S.A. S.p.a.*

[25] Mandato, A., Feffin, N., Bagno, I., Piazza, E., 2008. *Relazione tecnico descrittiva di progetto (Allegato 1) – Nuovo impianto di selezione e valorizzazione rifiuti urbani da raccolta differenziata con adeguamento impianto di smaltimento rifiuti urbani non pericolosi e opere accessorie. S.E.S.A. S.p.a.*

[26] Norme Tecniche delle Costruzioni (NTC), 2008.

[27] Omari, A., Bobbula, R., 2012. *Slope Stability Analysis of Industrial Solid Waste Landfills*. Luleå University of Technology. Department of Civil, Environmental and Natural Resources Engineering.

[28] Oweis, I., Khera, R., 1990. *Geotechnology of Waste Management.* Sevenoak, Kent, England. Butterworth and Company Ltd.

[29] Palombi, S., 2005. *Caratterizzazione geostrutturale di una discarica RSU: Analisi di stabilità e dinamica bidimensionale – Problematiche e limitazioni connesse*. Università degli Studi di Roma "La Sapienza".

[30] Pistolato, S., 2013. *Settlement modeling of the Ca' Rossa landfill in a post-closure prospective.* Master Thesis, ICEA Department, University of Padua.

[31] Polimeno. G., 2010. *Dichiarazione ambientale EMAS – S.E.S.A. S.p.a. Impianto di Este (Pd).*

[32] Powrie, W., Beaven, R.P., 1999. Hydraulic properties of household waste and implications for landfills. Institution of Civil Engineers Geotechnical Engineering Journal 137, p. 235–247.

[33] Quian, X., Koerner, R.M., Gray, D.H., 2002. *Geotechnical aspects of landfill design and construction.*

[34] Ranjan, G., Rao, A., 2007. *Basic and applied soil mechanics.* Revised Second Edition. New Age International Publishers, p. 374-376.

[35] S.E.S.A. S.p.a. *Nuovo impianto di selezione e valorizzazione rifiuti urbani da raccolta differenziata con adeguamento impianto di smaltimento rifiuti urbani non pericolosi e opere accessorie - Piano di Sorveglianza e Controllo (P.S.C.)*.

[36] Shafer, A. L., Hargrove, J.Q., Harris, J.M., 2000. *Stability analysis for Bioreactor Landfill Operations.*

[37] Stark, T.D., Eid, H.T., 1998. *Performance of three-dimensional slope stability methods in practice*. J. Geotech. Geoenviron. Eng. 124 (11), p. 1049–1060.

[38] Vajirkar, M.M., 2000. *Slope Stability Analysis of Class I landfills with co-disposal of biosolids using field test data.* University of Central Florida. Department of Civil and Environmental Engineering.

[39] Van Impe, W.F., Squeglia, N., 2002. *Proprietà geotecniche dei rifiuti solidi urbani.* Hevelius Editore.

[40] Yu, L., Batlle, F., 2011. *A hybrid method for quasi-three dimensional slope stability analysis in a municipal solid waste landfill.* Waste Management 31 (2011), p. 2484-2496, Elsevier.

[41] Zekkos, D.P., 2005. *Evaluation of Static and Dynamic Properties of Municipal Solid-Waste.* University of California, Berkeley. Department of Civil and Environmental Engineering.

[42] Zekkos, D., Bray, J.D., Kavazanjian, E., Matasovic, N., Rathje, E.M., Riemer, M.F., Stokoe II, K.H., 2006. *Unit Weight of Municipal Solid Waste*. Journal of Geotechnical and Geoenvironmental Engineering. P. 1250 – 1260.

[43] PLAXIS Version 8 – http://www.plaxis.nl (Delft, The Netherlands).

[44] SLOPE/W – Slope Stability Analysis - http://www.geo-slope.com (Calgary, Canada: Geo-Slope International).